

12-2009

EXPLORING T. BRUCEI HEXOKINASE BIOLOGY: LOCALIZATION AND INHIBITION STUDIES

Todd Lyda

Clemson University, thefoxrdm@gmail.com

Follow this and additional works at: https://tigerprints.clemson.edu/all_dissertations



Part of the [Parasitology Commons](#)

Recommended Citation

Lyda, Todd, "EXPLORING T. BRUCEI HEXOKINASE BIOLOGY: LOCALIZATION AND INHIBITION STUDIES" (2009). *All Dissertations*. 449.

https://tigerprints.clemson.edu/all_dissertations/449

This Dissertation is brought to you for free and open access by the Dissertations at TigerPrints. It has been accepted for inclusion in All Dissertations by an authorized administrator of TigerPrints. For more information, please contact kokeefe@clemson.edu.

EXPLORING T. BRUCEI HEXOKINASE BIOLOGY: LOCALIZATION AND
INHIBITION STUDIES

A Thesis
Presented to
the Graduate School of
Clemson University

In Partial Fulfillment
of the Requirements for the Degree
Doctor of Philosophy
Genetics

by
Todd Andrew Lyda
December 2009

Accepted by:
James Morris, Committee Chair
William Marcotte, Jr.
Kimberly Paul
Kerry Smith

ABSTRACT

Trypanosoma brucei, the causative agent of the disease African sleeping sickness in humans and nagana in animals, is a scourge of sub-Saharan Africa. There is a desperate need for more efficacious therapies for the disease; here we describe research validating *T. brucei* hexokinase 1 (TbHK1) as a drug therapeutic target for *T. brucei* infection and the identification and characterization of novel inhibitors of the enzyme by both low throughput and high throughput means. Additionally this thesis introduces efforts at characterizing a second *T. brucei* hexokinase, focusing mostly on cell biology and the determination of localization.

The small molecule quercetin (QCN) was tested and found to inhibit recombinant TbHK1 and spectroscopic study revealed that quercetin binds to TbHK1 proximal to the active site. Genetic experiments revealed that QCN may be cytotoxic to parasites as a result of TbHK inhibition. QCN localized to punctate bodies and the flagellum of *T. brucei* (consistent with the localization of TbHKs) and over expression of TbHK1 was partially protective.

In order to identify additional TbHK1 inhibitors, high through-put screening (HTS) techniques were implemented. HTS of >220,000 compounds yielded 239 primary inhibitors of TbHK1. Of the 239 hits, 15 were confirmed in validation assays as TbHK1 inhibitors; these compounds had a spectrum of activity against trypanosomes, suggesting possible therapeutic leads.

In order to initiate characterization of the unknown function of TbHK2, localization studies of TbHK2 were performed. Immunofluorescence assays were

employed and TbHK2 was found to localize to the parasite's flagellum, a novel finding that suggests that glycolysis in the parasite may not be limited to glycosomes, organelles related to peroxisomes that heretofore were considered the cellular compartments of glycolysis. Immunofluorescence signal was not exclusive to the flagellum but was observed in the cytosol and glycosomes. To understand the mode of localization, the TbHK sequences were aligned with known and predicted flagellum proteins and a conserved flagellum localization peptide signal was identified in the C-termini of TbHK1 and TbHK2. The peptide signal (RAVLAK) was further explored as a flagellum targeting sequence using fusions to a reporter. These experiments, along with expression and localization of HA-tagged TbHK2 revealed that TbHK2 associates with the flagellum and basal body. This unusual localization suggested that TbHK2 may act as an environmental glucose sensor or perhaps in energy production for the active flagellum.

The appendix is comprised of three chapters. The first appendix section is a published paper that focuses on AMP dependent protein kinase from *T. brucei*. I contributed microscopic expertise (and intellectual input) and am an author on this work. The second appendix section is a summary of research performed to characterize a library of lonidamine analogs against TbHK1 and trypanosomes. And lastly, the third appendix section is the developed assay for testing the viability of *T. brucei* cells and adaptation for high throughput screening.

DEDICATION

For Dr. Morris

ACKNOWLEDGMENTS

I would like to thank the members of the Morris lab, my friends and my family for their support during my time in graduate school.

TABLE OF CONTENTS

	Page
TITLE PAGE	i
ABSTRACT	ii
DEDICATION	iv
ACKNOWLEDGMENTS	v
CHAPTER	
I. LITERATURE REVIEW	1
Introduction.....	1
<i>Trypanosoma brucei</i> : a model organism.....	3
Glycolysis as a drug target.....	4
TbHKs.....	5
Lonidamine	6
LND as an anticancer therapeutic agent	6
LND as a male contraception agent.....	7
LND as an inhibitor of TbHK1	7
Quercetin.....	8
Quercetin fluorescence experiments.....	9
Quercetin as a drug therapy for HAT	9
High-Throughput Screening	10
Chapter Summary	11
References.....	12
II. QUERCETIN, A FLUORESCENT BIOFLAVANOID, INHIBITS <i>TRYPANOSOMA BRUCEI</i> HEXOKINASE 1.....	17
Abstract.....	19
Introduction.....	21
Materials and Methods.....	23
Results.....	26
Discussion.....	31
Acknowledgements.....	33
References.....	34
Figure Legends.....	36
Figure 1	38

Table of Contents (Continued)

	Page
Figure 2	39
Figure 3	40
Figure 4	41
Figure 5	42
Figure 6	43
III. A TARGET-BASED HIGH THROUGHPUT SCREEN YIELDS <i>TRYPANOSOMA BRUCEI</i> HEXOKINASE SMALL MOLECULE INHIBITORS WITH ANTIPARASITIC ACTIVITY	44
Abstract	45
Introduction	46
Results	47
Discussion	53
Materials and Methods	55
Acknowledgements	60
References	61
Figure Legend	63
Figure 1	64
Table 1	65
Table 2	66
Table 3	67
IV. EXTRA-GLYCOSOMAL LOCALIZATION OF <i>TRYPANOSOMA BRUCEI</i> HEXOKINASE 2	68
Abstract	70
Introduction	71
Materials and Methods	72
Results	77
Discussion	83
Acknowledgements	86
References	86
Figure Legends	89
Figure 1	92
Figure 2	93
Figure 3	94
Figure 4	95
Figure 5	96
Figure 6	97

Table of Contents (Continued)

	Page
V. CHAPTER SUMMARY.....	98
APPENDICES	100
A: <i>TRYPANOSOMA BRUCEI</i> AMP-ACTIVATED KINASE SUBUNIT HOMOLOGS INFLUENCE SURFACE MOLECULE EXPRESSION	101
B: IMPROVING AN ANTI-TRYPANOSOMAL COMPOUND: LONIDAMINE ANALOGS INHIBIT <i>T. BRUCEI</i> HEXOKINASE ACTIVITY AND CELL GROWTH	136
C: CELL TITRE BLUE ASSAY DEVELOPMENT FOR <i>TRYPANOSOMA BRUCEI</i> VIABILITY TESTS USING HIGH THROUGHPUT SCREENING TECHNIQUES	145

CHAPTER ONE

LITERATURE REVIEW

Introduction

Trypanosoma brucei is the causative agent of African sleeping sickness in humans and nagana in cattle. Both diseases are endemic to the sub-Saharan regions of Africa where the insect vector, the tsetse fly, is found. Approximately 500,000 people in sub-Saharan Africa are infected per year with 50,000-70,000 deaths per year [Stich 2002]. The defining feature of the disease is the complete exhaustion experienced by the infected host [Dauvilliers, 2008]. Eventually, if untreated, the host will slip into a coma and die. There are two main progressions of the disease in which the parasite is either only localized to the host blood stream or the parasite has crossed the blood-brain barrier [Amin, 2008].

However, even with treatment the host may still die, as current drug therapies can be deadly in their own right [Enserink, 2007]. Most of the available approved drugs are arsenic derivatives that are noxious with side effects including blindness [Barrett, 2003], encephalopathy and death [Pepin 1991]. Approximately 10% of patients die when taking the drug melarsoprol to treat human African trypanosomiasis (HAT) [Docampo 2003]. Drugs are required in part because a vaccine is not available for treating *T. brucei* infections. Future vaccine development is unlikely because this ancient eukaryotic cell can evade the host immune system as a population through a process known as antigenic variation [Hartley, 2008]. In this process the parasite population presents a single surface molecule that the host will recognize and produce antibodies against. However, within

the population, a small percentage changes the single surface protein and evades the antibody-mediated immune response. This causes a constant flux in parasitemia in which the host kills a majority of the parasites but a few survive to multiply and elicit another immune response when the parasite number reaches a threshold.

A vaccine would be possible if the number of surface molecules was finite.

Unfortunately, the gene responsible for the surface molecule, variant surface glycoprotein (VSG) has multiple copies of multiple alleles that can recombine through homologous recombination [Hartley, 2008; Hutchinson, 2007]. Control of the single expression of one allele is based on the location of the VSG allele. There are 20 telomeric expression sites for VSG alleles. Each allele can be exchanged through homologous recombination but only one expression site is active [Dreesen, 2007]. Therefore, a useful vaccine would have to contain every probable combination of VSGs that could be produced. This is not likely to be obtainable because there are over 1000 alleles contained on microchromosomes in the genome [Taylor, 2006].

The effect of African sleeping sickness on human health is a problem for the sub-Saharan regions of Africa but the effect on the economy is also important. The cattle industry suffers to the point where large herds cannot be sustained. In fact, European breeds of cattle are devastated by nagana. For this reason the sub-Saharan region of Africa has what are known as green deserts [Enserink, 2007]. In the green deserts ~4.5 billion dollars are lost each year as a result of the unused land [Enserink, 2007]. Not only would this money be beneficial to struggling economies in this region but it would also bring food to the starving. Therefore, combating *T. brucei* will not only alleviate a human

health hazard but also increase the wealth of the region and potentially combat world hunger.

***Trypanosoma brucei*: a model organism**

T. brucei is a flagellated unicellular parasitic eukaryote. *T. brucei* also has some characteristics that make it a model organism for genetic studies. One such characteristic is the fact that most *T. brucei* genes do not contain introns – an example of an exception is poly(A) polymerase which has been shown to contain a single intron of 653 nucleotides [Mair, 2000]. The lack of introns makes it easier to predict open reading frames, clone full length genes, and recombinantly express genes in prokaryotic cells. Also, the parasite undergoes the biological phenomenon known as RNA interference [Balaña-Fouce, 2007]. With RNA interference, gene expression can be reduced without producing a knockout. Homologous recombination is another characteristic that makes *T. brucei* amenable genetic system, allowing knock ins and knock outs to assess gene function [Barnes, 2007]. These facts make *T. brucei* very attractive as a genetic model organism.

The life cycle of the parasite is composed of two major stages: the insect procyclic form and the bloodstream form. From both environments *T. brucei* can be cultured and studied. Curiously, the two stages have different metabolisms. In the insect form the primary metabolism used by the parasite is through the TCA cycle and the metabolism of proline [van Hellemond, 2005]. Within the tsetse fly amino acids are at high concentrations and thus readily available [Schneider, 2008]. However, the environment is

different within the bloodstream of mammalian hosts. The bloodstream is rich with glucose when compared to the fly and upon differentiation from insect to bloodstream form *T. brucei* shifts its metabolism to rely exclusively on glycolysis [Besteiro, 2005].

Glycolysis as a drug target

Glycolysis is an exploitable pathway for therapy development. This metabolic shift is the weakness that can be exploited to kill the parasite. The BSF parasite cannot survive disruption of glycolysis [Verlinde, 2001]. When the parasites differentiate to the bloodstream form they change not only their metabolic pathway to that of glycolysis but also lose most functionality of the singular mitochondrion through the repressed expression of mitochondrial targeted proteins [Williams, 2008]. Therefore, without a completely functional mitochondrion, inhibition of the glycolytic pathway is toxic.

Glycolysis in the African trypanosome occurs in the specialized organelles known as glycosomes [Opperdoes, 2006]. This is distinct from most organisms in which glycolysis is cytosolic. Targeting of proteins to the glycosome is mediated by two peptide sequences known as peroxisomal targeting sequence 1 (PTS 1) [Gould, 1989] and peroxisomal targeting sequence 2 (PTS 2) [Blattner, 1995]. PTS1 sequences are found on the C-terminus of proteins while PTS2 sequences are found on the N-terminus of proteins. Both PTS sequences mediate the incorporation of glycosomal proteins.

However, all glycolytic and metabolic enzymes are not exclusive to the glycosome. The metabolic enzyme adenylate kinase has been shown to be found in the flagellum of

T. brucei [Pullen 2004]. In *Leishmania*, a HK has been found to moonlight as a heme-binding protein in the flagellar pocket [Krishnamurthy 2005].

Flagellum localization in *T. brucei* is also accomplished by peptide targeting sequences [Ersfeld 2000]. One such targeting sequence is found near the C-terminus of proteins and was described for the flagellum protein paraflagellar rod A (PFRA) [Bastin 1999]. For TbHKs to localize to the flagellum a peptide sequence would be expected. Mitochondrial HKs have also been described and these are physically associated with the mitochondrial membrane [Crane 1952]. In *Chlamydomonas* and mammalian sperm, glycolytic enzymes have been found in the flagellum [Mitchell 2005; Lardy 1941].

TbHKs

Two hexokinases named TbHK1 and TbHK2 are expressed in BSF and PF parasites [Colasante, 2006]. Arranged in tandem on chromosome 10, the two polypeptides are 98% identical, with 7 of 10 differences in the C-terminus region of the protein. These changes are influential in ATP binding [Chambers, 2008 BBRC]. TbHKs have previously been localized to the glycosome where *T. brucei* undergoes glycolysis [Opperdoes, 2006].

Biochemical studies have revealed that authentic and recombinant TbHKs multimerize in to hexamers [Opperdoes, 2006; Morris 2006]. Notably recombinant TbHK2 (rTbHK2) is not active by itself but in complex with rTbHK1 the enzyme is active [Chambers, 2008 JBC].

Genetic evidence supports the targeting of TbHK1 in therapeutic development. TbHK1 has been shown to be essential through RNAi of the 3' UTR of TbHK1 in

bloodstream form parasites [Morris, 2002]. RNAi of TbHK1 and TbHK2 led to cell death due to a disruption of glycolytic flux [Albert, 2005].

Biochemical validation of TbHKs as therapeutic targets has also been considered. Inhibitors of TbHK1 can be tested easily *in vitro* by using a simple hexokinase assay. Using such an assay TbHKs have been shown to be sensitive to fatty acids [Chambers, 2008 JBC]. Structurally based inhibitors of TbHK have been used in the past but are trypanocidal at high concentrations [Trinquier 1995][Willson 2002].

In an attempt to uncover more efficacious trypanocidal compounds that use TbHK as a target, known HK inhibitors were tested against TbHK1 and trypanosomes. From these inhibitors of hexokinases, two were investigated, lonidamine and quercetin.

Lonidamine

Lonidamine (LND, 1-(2,4-dichlorobenzyl)-1H-indazole-3-carboxylic acid) has been shown to inhibit hexokinases bound to the mitochondrion of mammalian cells [Paggi, 1988]. Thus, LND is described as an inhibitor of aerobic glycolysis. Over the years, LND mediated hexokinase inhibition has been used for two major applications: cancer therapeutics [Silvestrini, 1991] and male contraception [Silvestrini, 1984].

LND as an anticancer therapeutic agent

Cancerous cells and other proliferative cells have a high demand for energy. Therefore, if metabolic pathways are inhibited the cancerous cells are predicted to die. Because LND inhibits hexokinase it inhibits glycolysis and is used as a therapeutic

treatment for cancer. Currently, LND is used in Europe against cancers such as lung and breast cancers [Pasquale, 2005]. However, LND is mostly used in the treatment of benign prostatic hyperplasia (BPH) [Pasquale, 2005]. BPH is a disease that is becoming more frequent due to increased male life expectancy. The prostate is an ideal target for LND because the area depends solely on glycolysis for energy [Guzman, 1994]. This is due to a zinc-mediated enzyme block in the citric acid cycle of prostate gland cells because the prostate secretes abnormally high levels of citrate and zinc [Costello, 2000]. Therefore, replication of the cells of the prostate is inhibited by LND. In fact patients with BPH have seen a reduction in prostate volume when taking LND [Pasquale, 2005].

LND as a male contraception agent

LND works as a male contraception drug because it inhibits the growth of fertile spermatigotes, preventing maturation of spermastigotes [Yan Cheng, 2002]. Because new spermatigotes are produced constantly in males this contraception drug is reversible when LND treatment is stopped [Maranghi, 2005]. However, LND has not yet been approved for use as a male contraceptive in humans.

LND as an inhibitor of TbHK1

Recently, LND has been found to inhibit rTBHK1 *in vitro* [Chambers, 2008 LND]. The inhibitory concentration (IC₅₀) for LND is 850 µM. But when the drug is tested against bloodstream form parasites it has a lethal dose (LD₅₀) of 50 µM [Chambers, 2008 LND]. The increase may be due to the fact that the inhibition of TbHK1 does not have to

be complete to be toxic to the parasite or off target effects. Another factor could be the relative concentration of LND within the glycosome. LND may be concentrated within the glycosome while in the culture it is at a lower concentration or LND may be affecting other pathways besides glycolysis. In either case LND is a promising drug for *T. brucei* infection.

Quercetin

Quercetin, 3,5,7,3',4' pentahydroxyflavone (QCN), is a bioflavonoid isolated from plants such as apples, onions, and capers [Cerhauser, 2008, Slimestad, 2007, Sharaf, 2000]. QCN has been shown to exhibit antioxidant properties [Bischoff 2008] as well as play a role in the signaling between plants and microbes for nodulation [Novak 2002]. Over the years, QCN has been used as a probe because of the fluorescent nature of the molecule [Guharay 2001]. The fluorescent property is also useful for determining protein binding because QCN fluoresces differently when bound to protein such as bovine serum albumin [Sengupta 2002]. But the key feature of QCN is that it inhibits enzymes such as tyrosine protein kinase, a phosphorylase kinase [Srivastava 1985], a phosphatidyl 3-kinase [Matter 1992], and a DNA topoisomerase [Boege 1996]. The proposed mode of inhibition has been suggested to be the formation of a hydrogen-bonded complex with ATP [Granot 2002]. This complex may mimic the transition state of ATP and the tyrosyl residue on the inhibited enzyme [Granot 2002].

Quercetin fluorescence experiments

As previously mentioned, QCN is used in protein binding experiments. Proteins like human serum albumin (HSA) have been used in these experiments. When QCN binds to HSA, the nature of QCN emission changes such that it exhibits a second major emission wavelength [Sengupta 2002]. The phenomenon known as fluorescence resonance energy transfer (FRET) can be used to indicate the proximal location of QCN binding to the protein when exciting tryptophan at 280 nm. If FRET occurs between the protein and QCN then the relative location of QCN binding is near a tryptophan residue. For protein molecules with a singular tryptophan, the location of QCN binding can then be assumed to be within 5 nm of the tryptophan due to the maximum distance limitation of FRET [Lakowicz 1983].

Quercetin as a drug therapy for HAT

QCN has been shown to inhibit the growth of cancer cell lines such as Ehrlich ascites tumors and NK/Ly ascites tumor cells [Suolinna 1975, Molnar 1981]. The target of QCN within the cells is unknown. It has been proposed that the target may be Src protein kinase (pp60^{v-src}) [Graziani 1983] or HKs [Graziani 1977].

QCN not only affects cancer cells. QCN appears to affect any rapidly dividing cell, even BSF parasites [Mamani-Matsuda 2004]. QCN is toxic and induces apoptosis at a relatively low level with an LD₅₀ of 10 μM QCN [Mamani-Matsuda 2004]. While the connection between QCN and apoptosis is not resolved, apoptosis is linked in mammalian cells with mitochondrial associated hexokinase activity [Gottlob 2001]. In

fact, an increase in hexokinase activity can prevent apoptosis induced by oxidative stress [Bryson 2002].

High-Throughput Screening

The creation and discovery of novel chemical compounds and drugs has been an on-going goal of pharmaceutical companies and chemical labs. Now there are a tremendous number of compounds that have been produced. In order to take advantage of these created compounds, libraries have been constructed with these compounds and drugs in order to accommodate their use in screens.

One approach to discovering therapies for HAT is to use chemical libraries in high-throughput screens (HTS). HTS can be used to assess the viability of *T. brucei* cells [Mackey 2006]. The drawback of using a HTS to identify inhibitors of cell growth is that the target of the drug will remain unknown and identifying the target may be extremely difficult. Additionally, target-based screens allow for refinement of lists *in silico* based on the structures and activities of the target.

In order to circumvent such problems, target based HTS has been used. In such an approach the HTS is put to test against an *in vitro* assay. Then hits from the enzyme assay are tested against cells. This approach allows the investigators to assume at least one of the targets of the inhibitor within the cell. Enzyme assays such as UDP-Glc 4'-epimerase and trypanothione reductase have been used with success to identify inhibitors of trypanosome viability [Ubaniak 2006; Martyn 2007].

The TbHK1 assay is a coupled reaction with the production of glucose-6-phosphate linked to the conversion of glucose-6-phosphate to 6-phosphogluconolactone in the presence of the enzyme glucose-6-phosphate dehydrogenase [Parry 1966]. The reduction of NADP^+ to NADPH from the last step is observed spectrophotometrically and can be formatted to fit a 384 well plate design. In order for the TbHK1 assay to be used in a HTS the assay must have an appropriate Z-factor score. The Z-factor score is a mathematically calculated value that approximates the efficiency of a HTS. Basically, the Z-factor score is a measurement of the maximum and minimum values of the assay. A value above 0.5 is considered a good score while any value below 0.5 is an undesirable assay for HTS [Zhang 1999].

Chapter Summary

The literature review is a supplemental for the following three chapters. The next two chapters comprise research using TbHK1 as a drug target. The first is on the research performed using QCN as a TbHK1 inhibitor, trypanocidal compound and a molecular probe for TbHK binding. The next chapter is the high throughput screen in which additional compounds were found to inhibit TbHK1 and kill *T. brucei*.

The last chapter is focused on the localization of TbHK2. Localization studies have revealed that TbHK2 is found in the flagellum and cell bodies including glycosomes and basal bodies. The flagellum localization appears to be mediated through a similar flagellum targeting sequence as that found and described in this chapter. The function of TbHK2 is still unknown but the location of the enzyme is now understood.

References

- Stich A., Abel P.M., Krishna S. (2002) *BMJ* **325**, 203-6
- Dauvilliers Y., Bisser S., Chapotot F., Vatunga G., Cespuglio R., Josenando T., Buguet A. (2008) *Sleep* **31**, 348-54
- Amin D. N., Masocha W., Ngan'dwe K., Rottenberg M., Kristensson K. (2008) *Acta Trop* **106**, 72-4
- Enserink M. (2007) *Science* **317**, 310-3
- Barrett M. P., Burchmore R. J. S., Stich A., Lazzari J. O., Frasci A. C., Cazzulo J. J., Krishna S. (2003) *Lancet* **362**, 1469–80
- Pepin J., Milord F. (1991) *Trans. R. Soc. Trop. Med. Hyg.* **85**, 222-4
- Docampo R., Moreno S. N. (2003) *Parasitol. Res.* **90**, 10-3
- Hartley C. L., McCulloch R. (2008) *Mol Microbiol* **68**, 1237-51
- Hutchinson O. C., Picozzi K., Jones N. G., Mott H., Sharma R., Welburn S. C., Carrington M. (2007) *BMC Genomics* **13**, 234
- Dreesen O., Cross G. A. (2008) *Exp Parasitol* **118**, 103-10
- Taylor J. E., Rudenko G. (2006) *Trends Genet* **22**, 614-20
- Mair G., Shi H., Li H., Djikeng A., Aviles H. O., Bishop J. R., Falcone F. H., Gavrilescu C., Montgomery J. L., Santori M. I., Stern L. S., Wang Z., Ullu E., Tschudi C. (2000) *RNA* **6**, 163-9
- Balaña-Fouce R., Reguera R. M. (2007) *Trends Parasitol* **23**, 348-51
- Barnes R. L., McCulloch R. (2007) *Nucleic Acids Res* **35**, 3478-93
- van Hellemond J. J., Opperdoes F. R., Tielens A. G. (2005) *Biochem Soc Trans* **33**, 967-71
- Schneider A., Bursac D., Lithgow T. (2008) *Trends Cell Biol* **18**, 12-8
- Besteiro S., Barrett M. P., Rivière L., Bringaud F. (2005) *Trends Parasitol* **21**, 185-91

- Verlinde C. L., Hannaert V., Lonski C., Willson M., Perie J. J., Fothergill-Gilmore L. A., Opperdoes R. R., Gelb M. H., Hol W. G., Michels P. A. (2001) *Drug Resist Updat* **4**, 50-65
- Williams S., Saha L., Singha U. K., Chaudhuri M. (2008) *Exp Parasitol* **118**, 420-33
- Chambers J. W., Fowler M. L., Morris M. T., Morris J. C. (2008) *Mol Biochem Parasitol* **158**, 202-7
- Willson M., Sanejouand Y. H., Perie J., Hannaert V., and Opperdoes F. (2002) *Chemistry and Biology* **9**, 839–847
- Crane R. K., Sols A. (1952) *J. Biol. Chem.* **203**, 273-92
- Mitchell B. F., Pedersen L. B., Freely M., Rosenbaum J. L., Mitchell D. R. (2005) *Mol. Biol. of the Cell* **16**, 4509-18
- Lardy H. A., Phillips P. H. (1941) *Am. J. Pysiol.* **133**, 602-9
- Opperdoes F. R., Szikora J. P. (2006) *MBP* **147**, 193-206
- Gould, S.J., Keller, G.A., Hosken, N., Wilkinson, J. and Subramani, S. (1989) *J Cell Biol* **108**, 1403-1411
- Blattner J., Dorsam H., Clayton C. E. (1995) *FEBS Letters* **360**, 310-14
- Pullen T. J., Ginger M. L., Gaskell S. J., Gull K. (2004) *Mol. Biol. Cell.* **15**, 3257-65
- Krishnamurthy G., Vikram R., Singh S. B., Patel N., Agarwal S., Mukhopadhyay G., Basu S. K., Mukhopadhyay A. (2005) *J. Biol. Chem.* **280**, 5884-91
- Ersfeld K., Gull K. (2000) *J. Cell Science.* **114**, 141-48
- Bastin P., MacRae T. H., Francis S. B., Matthews K. R., Gull K. (1999) *Mol. Cell. Biol.* **19**, 8191-8200
- Colasante C., Ellis M., Ruppert T., and Voncken F. (2006) *Proteomics* **6**, 3275-3293
- Morris M. T., DeBruin C., Yang Z., Chambers J. W., Smith K. S., and Morris J. C. (2006) *Eukaryot Cell* **5**, 2014-2023

- Chambers J. W., Morris M. T., Smith K. S., and Morris J. C. (2008) *Biochem Biophys Res Commun* **365**, 420-425
- Chambers J. W., Kearns M. T., Morris M. T., and Morris J. C. (2008) *J Biol Chem* **283**, 14963-14970
- Morris J. C., Wang Z., Drew M. E., Englund P. T. (2002) *EMBO J* **21**, 4429-38
- Albert M. A., Haanstra J. R., Hannaert V., Joris Van Roy R. V., Opperdoes F. R., Bakker B. M., and Michels P. A. M. (2005) *JBC* **280**, 28306-28315
- Misset O., and Opperdoes F. R. (1984) *Eur J Biochem* **144**, 475-483
- Parry M. J., Walker D. G. (1966) *Biochem J.* **99**, 266-74
- Trinquier M., Perie J., Callens M., Opperdoes F., Willson M. (1995) *Bioorg. Med. Chem.* **3**, 1423-7
- Paggi M. G., Fanciulli M., Perrotti N., et al. (1988) *Ann N Y Acad Sci* **551**, 358-60
- Silvestrini B. (1991) *Semin Oncol* **18**, 2-6
- Silvestrini B., Palazzo G., De Gregorio M. (1984) *Prog Med Chem* **21**, 110-35
- Ditunno P., Battaglia M., Selvaggio O., Garofalo L., Lorusso V., Selvaggi F. P. (2005) *Rev Urology* **7**, 27-33
- Guzman Barron E. S., Huggins C. (1995) *J Urol* **51**, 630-34
- Costello L. C., Franklin R. B. (2000) *Oncology* **59**, 269-82
- Yan Cheng C., Mo M., Grima J., Saso L., Tita B., Mruk D., Silvestrini B. (2002) *Contraception* **65**, 265-68
- Maranghi F., Mantovani A., Macri C., Romeo A., Eleuteri P., Leter G., Rescia M., Spano M., Saso L. (2005) *Contraception* **72**, 268-72
- Gerhauser C. (2008) *Planta Med* **74**, 1608-24
- Slimestad R., Fossen T., Vagen I. M. (2007) *J Agric Food Chem* **55**, 10067-80
- Sharaf M., el-Ansari M. A., Saleh N. A. (2000) *Fitoterapia* **71**, 46-9
- Bischoff S. C. (2008) *Curr. Opin. Clin. Nutr. Metab. Care* **11**, 733-40

- Novák K., Chovanec P., Skrdleta V., Kropáčová M., Lisá L., Nemcová M. (2002) *J. Exp. Bot.* **53**, 1735-45
- Guharay J., Sengupta B., and Sengupta P. K. (2001) *Proteins* **43**, 75-81
- Sengupta B., and Sengupta P. K. (2002) *Biochem Biophys Res Commun* **299**, 400-403
- Srivastava A. K. (1985) *Biochem Biophys Res Commun* **131**, 1-5
- Matter W. F., Brown R. F., and Vlahos C. J. (1992) *Biochem Biophys Res Commun* **186**, 624-631
- Boege F., Straub T., Kehr A., Boesenberg C., Christiansen K., Andersen A., Jakob F., and Kohrle J. (1996) *J Biol Chem* **271**, 2262-2270
- Granot Y. (2002) *Isr Med Assoc J* **4**, 633-635
- Lakowicz J. R. *The Principles of Fluorescence Spectroscopy.* (1983) *Plenum Press.* New York, London.
- Suolinna E. M., Buchsbaum R. N., and Racker E. (1975) *Cancer Res* **35**, 1865-1872
- Molnár J., Béládi I., Domonkos K., Földeák S., Boda K., Veckenstedt A. (1981) *Neoplasma* **28**, 11-8
- Graziani Y., Erikson E., and Erikson R. L. (1983) *Eur J Biochem* **135**, 583-589
- Graziani Y. (1977) *Biochim Biophys Acta* **460**, 364-373
- Mamani-Matsuda M., Rambert J., Malvy D., Lejoly-Boisseau H., Daulouede S., Thiolat D., Coves S., Courtois P., Vincendeau P., and Mossalayi M. D. (2004) *Antimicrob Agents Chemother* **48**, 924-929
- Gottlob K., Majewski N., Kennedy S., Kandel E., Robey R. B., and Hay N. (2001) *Genes Dev* **15**, 1406-1418
- Bryson J. M., Coy P. E., Gottlob K., Hay N., and Robey R. B. (2002) *J Biol Chem* **277**, 11392-11400
- Mackey Z. B., Baca A. M., Mallari J. P., Apsel B., Shelat A., Hansell E. J., Chiang P. K., Wolff B., Guy K. R., Williams J., McKerrow J. H. (2006) *Chem. Biol. Drug Des.* **67**, 355-63

Martyn D. C., Jones D. C., Fairlamb A. H., Clardy J. (2007) *Bioorg. Med. Chem. Lett.* **17**, 1280-3

Urbaniak M. D., Tabudravu J. N., Msaki A., Matera K. M., Brenk R., Jaspars M., Ferguson M. A. (2006) *Bioorg. Med. Chem. Lett.* **16**, 5744-7

Zhang J. H., Chung T. D., Oldenburg D. R. (1999) *J. Biomol. Screen* **4**, 67-73

CHAPTER TWO

QUERCETIN, A FLUORESCENT BIOFLAVANOID, INHIBITS *TRYPANOSOMA*

BRUCEI HEXOKINASE 1

Todd L. Lyda¹, Jeremy W. Chambers^{1,3}, Meredith T. Morris¹, Kenneth A. Christensen²,
and James C. Morris^{1*}

¹Department of Genetics and Biochemistry

²Department of Chemistry

Clemson University

Clemson, SC 29634

Running Title: Spectroscopic characterization of quercetin binding

To be submitted

*Corresponding author:

Dept. of Genetics and Biochemistry

Clemson University

214 BRC

51 New Cherry Street

Clemson SC 39634

Tel. (864) 656-0293

FAX (864) 656-0393

Email: jmorri2@clermson.edu

³Current address:

Department of Molecular Therapeutics

The Scripps Research Institute, Scripps Florida

130 Scripps Way, #A2A

Jupiter, Florida 33458

Abstract

Hexokinases from the African trypanosome, *Trypanosoma brucei*, are attractive targets for the development of anti-parasitic drugs, in part because the parasite utilizes glycolysis exclusively for energy production during the mammalian infection. Here, we have found that both recombinant *Trypanosoma brucei* hexokinase 1 (TbHK1, $IC_{50} = 86 \mu\text{M}$) and authentic TbHK activity from cell lysates were inhibited by the trypanocidal bioflavanoid quercetin (QCN). Spectroscopic analysis of QCN binding to TbHK1, taking advantage of the intrinsically fluorescent single tryptophan (Trp177) in TbHK1 revealed that QCN quenches Trp177 emission. ATP similarly quenched Trp177 emission, while glucose had no impact on fluorescence. QCN interaction with TbHK1 led to the production of a distinct fluorescence emission at 460 nm. This fluorescence, characteristic of flavanols bound to proteins, was inhibited by glucose but unaffected by ATP. These spectroscopic studies suggested that ATP and QCN bind TbHK1 at a similar location near Trp177 while glucose binding altered the TbHK1 conformation sufficiently to prevent dual fluorescence from the flavanol.

QCN was toxic to bloodstream and procyclic form parasites (LD_{50} s of $7.5 \mu\text{M}$ and $35 \mu\text{M}$, respectively) possibly as a result of inhibition of the essential TbHKs. Supporting this idea, RNAi-mediated silencing of TbHK expression in procyclic form parasites expedited QCN-induced death, while over-expressing TbHK protected parasites from the compound. Additionally, QCN fluorescence suggested a cellular distribution similar to that of TbHKs. In summary, these observations support the suggestion that QCN toxicity is a result of interaction with, and inhibition of, TbHKs.

Keywords: *Trypanosoma brucei*, hexokinase, quercetin

Introduction

Trypanosoma brucei is the causative agent of human African trypanosomiasis (HAT) and nagana, a wasting disease, in livestock. The World Health Organization classifies *T. brucei* as a re-emerging/uncontrollable human pathogen, partly due to a lack of a vaccine and suitable treatments for the disease. Current therapeutics for HAT may have serious side effects, including blindness and death (1).

T. brucei relies exclusively on glycolysis for energy generation in the mammalian bloodstream. Hexokinases (HK¹) catalyze the first step in glycolysis facilitating the transfer of the γ -phosphoryl group of ATP to the C6 of glucose. The parasite expresses two HKs, TbHK1 and TbHK2, with proteomic studies revealing that both are found in the mammalian bloodstream (BSF) and insect (PF) forms of the parasites (2).

TbHK1 and TbHK2 are 98% identical at the amino acid level (3). RNA interference (RNAi) has been used to demonstrate that both enzymes are essential to the BSF parasites, as silencing of either *TbHK1* or *TbHK2* results in the loss of HK activity and cell death (4,5). In addition to this genetic evidence validating TbHKs as potential therapeutic targets, we have found that chemicals that inhibit HKs from other systems also inhibit TbHKs and are toxic to the trypanosome. For example, the anticancer drug lonidamine (LND) inhibits recombinant TbHK1 and HKs from parasite lysate and is toxic to both BSF and PF parasites (5). LND trypanocidal activity likely results in part from inhibition of TbHKs. Parasites were partially protected from LND-induced cell death by ectopic over-expression of TbHK1.

Quercetin (3,5,7,3',4' pentahydroxyflavone, QCN) is an abundant naturally occurring flavanol found in plants such as apples, onions, and capers. QCN and related flavanols are of interest as potential anti-cancer therapies, because they inhibit the growth of several types of cancer cell lines (6,7). Potential *in vivo* QCN targets include a number of enzymes that are inhibited *in vitro*, ranging from the Src protein kinase (pp60^{v-src}) to HKs (8,9).

Biophysically, QCN has several unusual fluorescence properties, including intramolecular excited-state proton transfer and dual fluorescence behavior that have been exploited in the use of flavanols as environmental probes (10). Additionally, QCN binding to bovine serum albumin has been studied using these spectral properties (11). These efforts suggest that QCN could be a useful tool in the study of target enzyme mechanisms if the target enzyme has a single tryptophan residue proximal to a site of interest.

Here, we have characterized the impact of QCN on recombinant TbHK1 and transgenic parasites. Our work builds on the observation that QCN is toxic to trypanosomes (12), revealing that TbHK1 may be a molecular target of the flavanoid. We have found that over-expression of TbHK1 provides protection from QCN, while RNAi depletion of TbHKs expedites parasite death. Additional spectroscopic investigations taking advantage of the intrinsic fluorescence of QCN suggest that QCN toxicity may be due in part to binding near the TbHK1 active site, causing enzyme inactivation.

Materials and Methods

Reagents

Quercetin dihydrate (QCN, 3,3',4',5,7-pentahydroxyflavone) was purchased from Spectrum Chemical Manufacturing Corporation (Gardena, CA).

Trypanosome cell culture and transfection

BSF parasites (cell line 90-13, a 427 strain) were grown in HMI-9 supplemented with 10% fetal bovine serum and 10% Serum Plus (Sigma-Aldrich, St. Louis, MO). PF parasites (29-13, a 427 strain) were grown in SDM-79. The T7 RNA polymerase and the tetracycline repressor constructs were maintained by the addition of 2.5 $\mu\text{g/ml}$ G418 and 5 $\mu\text{g/ml}$ hygromycin to the medium. PF parasites were transfected and selected as described (13). RNAi specific for TbHK1 was performed by targeting the unique 3'UTR of the transcript. Briefly, RNAi of TbHK1 was achieved using pZJM harboring a 341 bp fragment previously identified as a 3' untranslated region sequence (14). Parasite growth was monitored on a Becton-Dickinson FACScan flow cytometer.

For studies exploring the impact of over-expression of TbHK1 in PF cells, parental cells (PF 29-13) were transformed with linearized pLew111(2T7)GFP β (15) harboring the TbHK1 gene in the multicloning site. This vector fuses the green fluorescent protein (GFP) to the carboxyl termini of expressed proteins. After selection for stable transformants, TbHK1 expression was induced by addition of tetracycline (1 $\mu\text{g/ml}$) to the media.

Assays of recombinant and lysate-derived HK

Recombinant TbHK1 was expressed and purified as described previously (3). Parasite lysates were prepared by hypotonic lysis of 1×10^7 cells in the presence of 1 mM PMSF, 20 mg/ml leupeptin, and 100 mg/ml TLCK. The mixture was added to lysis buffer (for a final concentration of 0.1 M triethanolamine (TEA) pH 7.4 and 0.1% Triton X-100) and lysates used in HK assays.

HK assays were performed in triplicate using a coupled reaction. Briefly, assays used glucose 6-phosphate dehydrogenase (1 unit/assay, EMD Biosciences, Inc, San Diego, CA) as a coupling enzyme to reduce NADP^+ to NADPH during the oxidation of glucose-6-P to 6-phosphogluconic acid (3), a reaction that can be monitored spectrophotometrically. Final conditions were 0.1M TEA, pH 7.9 containing 1.0 mM ATP, 33 mM MgCl_2 , 20 mM glucose, and 0.75 mM NAD^+ . Assays were performed in 96-well microtiter plate format in a GENios spectrophotometer (Phenix Research Products, Hayward, CA).

Tryptophan Quenching Assay of TbHK1

Glucose, ATP, and QCN were added at varying concentrations individually and in combination to a solution (3 ml) of 0.1M TEA, pH 7.4. A scanning spectrofluorometer (Photon Technology International, Birmingham, NJ) was used to monitor emission from

300-550 nm after excitation of the lone Trp on TbHK1 (W177) at 280 nm. After acquiring background emission, TbHK1 (~1 µg) was added to the cuvette, mixed by inversion, and an emission scan performed. Using the PTI software, the area under the emission curves from 370-380 nm was integrated. Values were converted into the percent of Trp emission lost and plotted versus concentration of substrate/inhibitor using KaliedaGraph software version 4.03. Sigmoidal curves were fit to the plots and IC₅₀ values were determined for the substrate/inhibitor by setting y equal to 50 and solving for x using the sigmoidal equation.

Spectroscopic Binding Assay of TbHKs and QCN

To explore QCN binding to TbHK1 or TbHK2, QCN (100 µM), ATP (1 mM) and/or glucose (20 mM), and TbHK1 or TbHK2 (16 nM) were mixed in a 100 mM TEA (pH 7.4) solution. The sample was excited at 280 nm and excitation monitored from 300-550 nm. Spectra were gathered from 3 independent samples, with representative data presented.

QCN Localization in T. brucei by Fluorescence Microscopy

For microscopic examination of QCN localization, *T. brucei* were grown to 1×10^6 /ml (BSF 90-13) or 1×10^7 /ml (PF 29-13), harvested (800 x g, 10 min) and washed twice in modified PBS (5 mM KCl, 8 mM NaCl, 1 mM MgSO₄, 20 mM Na₂HPO₄, 2 mM NaH₂PO₄, 20 mM glucose). QCN (100 µM) was then added to cells in the modified PBS. After incubation (15 min, at growth conditions), cells were pelleted, washed twice,

and applied to slides after the addition of VectaShield mounting medium with DAPI (Vector Laboratories, Inc., Burlingame, CA). Images were captured by epifluorescence microscopy (Axiovert 200M, Carl Zeiss MicroImaging, Inc., Thornwood, NY).

For glycosome labeling, the aldolase peroxisomal targeting sequence (PTS2) (16) was introduced into a yellow fluorescent protein (YFP) modified pXS (17) expression vector to yield an N-terminal fusion with YFP. Briefly, two primers FPTS2 (5'AGCTTATGAGTAAGCGTGTGGAGGTGCTTCTTACACAGCTTG 3') and RPTS2 (5'CTAGCAAGCTGTGTAAGAAGCACCTCCACACGCTTACT CATA 3') were annealed and the resulting product cloned into pXS. PF parasites were then stably transfected with 10 µg of the pXS_{AldoPTS}YFP construct and selected by supplementing the growth media with 15µg/mL blasticidin. Live cells were visualized after resuspension in mounting medium (with DAPI) diluted 1:1 in PBS. Alternatively, fixed PF cells were stained with a rabbit anti-*T. brucei* glycosomal antibody (2841D, (18)), raised primarily against the glycosomal proteins pyruvate phosphate dikinase, aldolase, and glyceraldehyde phosphate dehydrogenase (18) (the kind gift of Dr. Marilyn Parsons (Seattle Biomedical Research Institute, Seattle WA)). Primary antibodies were detected with texas red-conjugated goat anti-rabbit (Rockland, Gilbertsville PA) secondary antibodies.

Results

QCN inhibits TbHK1, interacting with the enzyme near the active site - QCN has been shown to inhibit HK in cancer cells (9), suggesting that it might similarly inhibit rTbHK1. Incubation of TbHK1 with QCN inhibits the enzyme ($IC_{50} = 86 \mu\text{M}$) (Fig. 1). Of note, QCN has does not cause dissociation of TbHK hexamers (a previously characterized mechanism for regulation of activity (19)) indicating that the inhibition that we observed are not related to dissociation of the hexamer (data not shown).

To determine if endogenous HK activity from parasite lysates was also sensitive to QCN inhibition, cell lysates from either BSF or PF parasites were incubated with QCN and then assayed for HK activity. QCN inhibited both BSF and PF HK activity similarly (with IC_{50} s = $24 \mu\text{M}$ and $30 \mu\text{M}$, respectively) (Not shown).

TbHK1 inhibition coincides with changes in Trp fluorescence. TbHK1 harbors a single Trp (residue 177) that is modeled to lie on the face of the enzyme near the hinge region (Fig. 2A) (3). When this residue is excited with an excitation wavelength (λ_{ex}) of 280 nm, TbHK1 yields an emission band with a λ_{em} at ~ 370 nm (Fig. 2B, inset). QCN is intrinsically fluorescent with a maximum emission wavelength of 550 nm. When excited at 280 nm, it yields little fluorescence at 370 nm. Addition of increasing amounts of QCN to TbHK1, however, quenched the Trp177 emission (Fig. 2B, inset), yielding an IC_{50} for quenching of $\sim 35 \mu\text{M}$ (Fig. 2B).

Addition of glucose had minimal impact on Trp177 emission at 370 nm (not shown). However, ATP quenched the Trp177 emission nearly completely at 5 mM and $\sim 20\%$ at 0.05 mM (Fig. 2C). Addition of glucose and ATP did not alter quenching, yielding emission loss similar to ATP alone.

QCN excitation and emission as a result of intramoleccular energy transfer - Incubation of QCN with TbHK1 alters the emission profile acquired with a λ_{ex} of 280 nm. First, inclusion of TbHK1 in the analysis causes an alteration in fluorescence emission intensity at 540 nm (Fig. 3A), suggesting interacting with TbHK1 improves the fluorescent qualities of QCN. Second, the mixture of QCN and TbHK1 yields a second λ_{em} at \sim 460 nm. This peak is characteristic of QCN bound to protein and results from typical dual fluorescence behavior common to flavanoids (11).

Glucose and ATP have different impact on the 460 nm peak observed when QCN and TbHK1 are spectrally analyzed. Addition of glucose inhibits the generation of the 460 nm peak but does not alter the 540 nm emission peak; this observation is true whether glucose is added before or after QCN (Fig. 3B). ATP, on the other hand, does not impact the λ_{em} at 460 nm but instead reduces QCN emission at 540 nm, suggesting that ATP binding enhance the QCN-TbHK1 interaction (Fig. 3C). Last, inclusion of both glucose and ATP leads to a loss of both the λ_{em} at 540 nm and 460 nm (Fig. 3D). Note that the spectra of glucose and ATP are equivalent to the background signal, while inclusion of either glucose or ATP with QCN had yielded traces indistinguishable from QCN alone (data not shown).

While differing from TbHK1 by a total of 10 residues (out of 471), rTbHK2 does not interact with QCN to yield emission at 460 nm in the presence or absence of the two co-substrates glucose and ATP (Fig. 4). This finding indicates either a lack of QCN binding or a difference in binding that leads to a failure to coordinate QCN for productive

dual fluorescence. (ATP and QCN, however, quench the 540 nm emission, as seen above.)

QCN is toxic to T. brucei - Previous research has demonstrated that QCN is toxic to *T. b. gambiense* ($LD_{50} = 10 \mu\text{M}$) (12). To determine if the 427 *T. b. brucei* lab strain was susceptible to QCN, BSF 90-13 parasites were incubated for 24 hr in the presence of compound and growth monitored by cell counting. QCN was found to be toxic to BSF parasites, with an $LD_{50} = 7.5 \mu\text{M}$ (Fig. 5A). QCN is also toxic to *T. b. brucei* PF 29-13 trypanosomes, with an LD_{50} of $35 \mu\text{M}$, nearly 5-fold higher than the LD_{50} for BSF parasites (Not shown).

Exploring potential in vivo targets of QCN - Glycolysis is essential to both BSF and PF parasites grown in standard culture medium. Unlike BSF parasites (which rely exclusively on glycolysis for energy), genetic manipulation of glycolytic enzymes can be tolerated in PF parasites if the trypanosomes are first provided an opportunity to down-regulate hexose metabolism. Manipulations that are inducible, including over-expression and RNAi-based silencing of glycolytic enzymes, are examples that can be tolerated (3,14).

If QCN is toxic as a result of its inhibition of glycolysis, increased cellular HK polypeptide could temper the toxicity of the compound. Cells over-expressing TbHK1 from the inducible ectopic expression vector pLew111(2T7) were incubated with $50 \mu\text{M}$ QCN and cell growth monitored. After 24 hrs, QCN-treated control parasites growth was

repressed 58%. Cells over-expressing TbHK1, which displayed cellular HK activity 2.1 greater than control cells (data not shown), were more resistant to QCN with growth reduced only 10% (Fig. 5B).

The incomplete penetrance of RNAi (and the slowly developing phenotypes associated with the silencing) can allow manipulation of glycolytic enzyme abundance without cell toxicity in PF parasites (14). Therefore, we have explored the sensitivity of the RNAi of TbHK1 using pZJM(TbHK1), which targets the distinct 3'UTR of *TbHK1* (14). RNAi was induced for 24 hours before cells were passed into medium containing QCN and cell growth compared to parental PF 29-13 parasites after an additional 24 hours. Silencing TbHK1 led to enhanced sensitivity to QCN, with cells induced to silence TbHK1 reduced in number to 17% of the corresponding untreated cell lines (Fig. 5B).

Glycosomal localization of QCN in BSF parasites - QCN is taken up by *T. brucei* through an unknown mechanism. To explore cellular localization of QCN, parasites were incubated with the compound and the inherent fluorescence of QCN scored by microscopy (Fig. 6). Both PF and BSF parasites yielded punctate patterns of staining similar to that seen with either fluorescence localized by PTS2 to glycosomes in live parasites (Fig. 6) or using an antibody to label glycosomes in fixed parasites (3). (The broad emission spectra of QCN limited immunofluorescence experiments, though similar signals were seen using glycosome-targeted YFP.)

Discussion

BSF *T. brucei* generate energy exclusively by glycolysis, suggesting that inhibitors of enzymes in the pathway could be therapeutic lead compounds. The trypanosome glycolytic enzymes, TbHK1 and TbHK2, are potential drug targets. These proteins, which are 30-33% identical to those from yeast, plants, and mammals, have a number of unique biochemical features (in addition to amino acid composition) that suggest that identification of trypanosome-specific HK inhibitors may be possible. These differences include multimerization of the enzyme into hexamers, localization of the protein to the glycosome, and sensitivity of the TbHKs to fatty acids (3,19,20).

Genetic studies using RNAi have shown that both TbHKs are essential to the parasite (4,5), and chemical inhibitors of the enzyme have demonstrated anti-parasitic activity *in vitro* (5,21). In an effort to identify and characterize new TbHK1 inhibitors, we have scanned the literature for HK inhibitors from different systems. These efforts have yielded a number of small molecules, including QCN.

Here, we report that QCN, a previously recognized anti-trypanosomal flavanoid (12), inhibits recombinant TbHK1. Many of the other enzymes that have been reported to be sensitive to QCN including a tyrosine protein kinase, a phosphorylase kinase (22), a phosphatidyl 3-kinase (23), and a DNA topoisomerase (24) share the feature of binding nucleotides or nucleotide triphosphates. It has been suggested that QCN inhibits Tyr kinases (like pp60^{v-src}) by forming a hydrogen-bonded complex with ATP, which would mimic the transition state of ATP and the tyrosyl residue of the enzyme (25). A similar mechanism is unlikely in TbHK1, as QCN alone can quench Trp177 fluorescence and

QCN interacts with TbHK1 to yield a λ_{em} at 460 nm in the absence of ATP (Figs. 2 and 3).

We have reported previously that ATP binding is influenced by the unusual C-termini of TbHK1 and TbHK2, which lies proximal to the hinge domain and Trp177 (Fig. 2A) (26). The majority of the differences between TbHK1 and TbHK2 (7 of the 10 total residue differences) are found in the terminal 18 amino acids of the polypeptide, and these differences yield catalytic differences between the proteins (3). Two different TbHK1 variants harboring difference in the C-termini (I458V, V468A) had altered affinity for ATP, suggesting that the tail influences ATP binding (26). Here, TbHK1 QCN binding yields a 460 nm emission peak, while TbHK2 does not, suggesting again that the C-termini of the proteins influences small molecule binding. The surprising difference in QCN binding between the two proteins suggests that TbHK1 is an *in vivo* target while TbHK2 may not be; an idea supported by our observation that the TbHK2 knockout parasites share nearly identical LD₅₀s for QCN with the parental PF 29-13 parasites (data not shown).

We have recently completed a screen of a library of 1280 pharmaceutically active compounds for small molecules that alter TbHK1 activity. In this screen, we identified both inhibitors (that reduced activity > 50% at 10 μ M) and activators (increased activity > 150% at 10 μ M) of TbHK1 (data not shown). Notably, we recovered one inhibitor, myricetin, which differs structurally from QCN by a single hydroxyl group. One activator, taxifolin (dihydroquercetin), is also structurally similar to QCN, suggesting that the interaction can also positively influence enzyme activity.

QCN has been shown to trigger *T. brucei* death through apoptosis (12). In mammalian cells, mitochondrial associated HK activity is required to prevent apoptosis (27) and increased HK activity prevents oxidant-induced apoptosis (28). Our observation that QCN inhibits TbHK1 suggests that the apoptosis may result from a mechanism that measures HK activity, similar to that found in mammalian cells. The TbHKs are unusual in a number of ways, including the finding that they oligomerize into hexamers (19) and localize to the peroxisome-like glycosome (20). These characters suggest novel mechanisms connecting TbHK to cell signaling, which remain to be resolved.

Acknowledgements

The authors would like to thank April Coley, Heidi Dodson, and Marcia Wilson for their comments on this manuscript. This work was supported in part by the US National Institutes of Health 1R15AI075326 to JCM.

¹Abbreviations used: BSF, bloodstream form; G6-P, glucose-6-phosphate; G6PDH, glucose-6-phosphate dehydrogenase; HK, hexokinase; LND, lonidamine; PF, procyclic form; TbHK1, recombinant *T. brucei* hexokinase 1; TbHK2, recombinant *T. brucei* hexokinase 2; TbHK, *T. brucei* hexokinase; TEA, triethanolamine; QCN, quercetin.

References

1. Barrett, M. P., Burchmore, R. J., Stich, A., Lazzari, J. O., Frasch, A. C., Cazzulo, J. J., and Krishna, S. (2003) *Lancet* **362**, 1469-1480
2. Colasante, C., Ellis, M., Ruppert, T., and Voncken, F. (2006) *Proteomics* **6**, 3275-3293
3. Morris, M. T., DeBruin, C., Yang, Z., Chambers, J. W., Smith, K. S., and Morris, J. C. (2006) *Eukaryot Cell* **5**, 2014-2023
4. Albert, M. A., Haanstra, J. R., Hannaert, V., Van Roy, J., Opperdoes, F. R., Bakker, B. M., and Michels, P. A. (2005) *J Biol Chem* **280**, 28306-28315
5. Chambers, J. W., Fowler, M. L., Morris, M. T., and Morris, J. C. (2008) *Mol Biochem Parasitol* **158**, 202-207
6. Suolinna, E. M., Buchsbaum, R. N., and Racker, E. (1975) *Cancer Res* **35**, 1865-1872
7. Molnar, J., Beladi, I., Domonkos, K., Foldeak, S., Boda, K., and Veckenstedt, A. (1981) *Neoplasma* **28**, 11-18
8. Graziani, Y., Erikson, E., and Erikson, R. L. (1983) *Eur J Biochem* **135**, 583-589
9. Graziani, Y. (1977) *Biochim Biophys Acta* **460**, 364-373
10. Guharay, J., Sengupta, B., and Sengupta, P. K. (2001) *Proteins* **43**, 75-81
11. Sengupta, B., and Sengupta, P. K. (2002) *Biochem Biophys Res Commun* **299**, 400-403
12. Mamani-Matsuda, M., Rambert, J., Malvy, D., Lejoly-Boisseau, H., Daulouede, S., Thiolat, D., Coves, S., Courtois, P., Vincendeau, P., and Mossalayi, M. D. (2004) *Antimicrob Agents Chemother* **48**, 924-929
13. Wang, Z., Morris, J. C., Drew, M. E., and Englund, P. T. (2000) *J. Biol. Chem.* **275**, 40174-40179.
14. Morris, J. C., Wang, Z., Drew, M. E., and Englund, P. T. (2002) *EMBO J.* **21**, 4429-4438
15. Motyka, S. A., Drew, M. E., Yildirim, G., and Englund, P. T. (2006) *J Biol Chem* **281**, 18499-18506
16. Blattner, J., Dorsam, H., and Clatyon, C. E. (1995) *FEBS Lett* **360**, 310-314
17. Marchetti, M. A., Tschudi, C., Kwon, H., Wolin, S. L., and Ullu, E. (2000) *J. Cell Sci.* **113 (Pt 5)**, 899-906
18. Parker, H. L., Hill, T., Alexander, K., Murphy, N. B., Fish, W. R., and Parsons, M. (1995) *Mol. Biochem. Parasitol.* **69**, 269-279
19. Chambers, J. W., Kearns, M. T., Morris, M. T., and Morris, J. C. (2008) *J Biol Chem* **283**, 14963-14970
20. Misset, O., and Opperdoes, F. R. (1984) *Eur J Biochem* **144**, 475-483
21. Willson, M., Sanejouand, Y. H., Perie, J., Hannaert, V., and Opperdoes, F. (2002) *Chem. Biol.* **9**, 839-847
22. Srivastava, A. K. (1985) *Biochem Biophys Res Commun* **131**, 1-5
23. Matter, W. F., Brown, R. F., and Vlahos, C. J. (1992) *Biochem Biophys Res Commun* **186**, 624-631

24. Boege, F., Straub, T., Kehr, A., Boesenberg, C., Christiansen, K., Andersen, A., Jakob, F., and Kohrle, J. (1996) *J Biol Chem* **271**, 2262-2270
25. Granot, Y. (2002) *Isr Med Assoc J* **4**, 633-635
26. Chambers, J. W., Morris, M. T., Smith, K. S., and Morris, J. C. (2008) *Biochem Biophys Res Commun* **365**, 420-425
27. Gottlob, K., Majewski, N., Kennedy, S., Kandel, E., Robey, R. B., and Hay, N. (2001) *Genes Dev* **15**, 1406-1418
28. Bryson, J. M., Coy, P. E., Gottlob, K., Hay, N., and Robey, R. B. (2002) *J Biol Chem* **277**, 11392-11400

Figure Legends

Figure 1. QCN inhibits TbHK1. (A) Increasing concentrations of QCN were incubated with TbHK1 (150 ng) for 1 hour at room temperature, and then assayed for HK activity as described in the Materials and Methods. All assays were performed in triplicate.

Figure 2. QCN bound to rTbHK1 alters Trp177 fluorescence. (A) TbHK1 was modeled to *S.cerevisiae* hexokinase PII. The active site, D214, and Trp177 are indicated, along with residues that are involved in ATP binding in the C-terminal tail. For clarity, the lower lobe of the protein has been isolated and rotated to position the C-terminal tail perpendicular to the page. (B) Trp177 emission is inhibited by QCN. TbHK1 (1 μ g) was incubated with QCN (100 μ M) in a 100 mM TEA (pH 7.4) solution and, following excitation at 280 nm, emission monitored from 340-550 nm. To assess the percentage of Trp emission lost, the region between 370-380 nm (inset) was calculated and the % reduction in response to QCN determined. (C) ATP and QCN are additive in Trp177 quenching. Spectra were acquired from samples containing different amounts of ATP as described in 2B, and percentage of Trp emission lost calculated.

Figure 3. TbHK1 and QCN interact to yield an emission peak at 460 nm. (A) Emission spectra from 400-550 nm of TbHK1, QCN, and TbHK1 incubated with QCN (A). Spectra were also collected from TbHK1 incubated with substrates, including glucose (B), ATP (C) or both co-substrates (D) added before or after QCN.

Figure 4. TbHK2 and QCN do not interact to yield the 460 nm emission peak. QCN alone or rTbHK2 incubated with QCN have similar emission spectra from 400-450 nm (A), while inclusion of ATP (B) quenches Trp177 emission.

Figure 5. (A) BSF trypanosomes grown in triplicate in HMI-9 medium were incubated for 24 hr with increasing amounts of QCN and densities determined by counting as described. (B.) RNAi of TbHK1 enhances QCN toxicity, while over-expression of TbHK1 tempers it. Parental PF trypanosomes (29-13) or parasites transformed with pLEW111(2T7):TbHK1 or pZJM:TbHK1 were induced with tetracycline (1 μ g/ml) for 24 hours to either express or silence TbHK1, QCN (50 μ M) added, and cell viability scored after an additional 24 hour incubation.

Figure 6. Localization of QCN by microscopy in BSF and PF parasites. BSF and PF parasites incubated with QCN (100 μ M, 10 min and 1 hr for BSF and PF, respectively) were stained with DAPI and imaged. Glycosome localization in live PF cells was visualized by eYFP emission. Fluorescence of the QCN is captured here using a 488 nm filter set.

Fig 1.

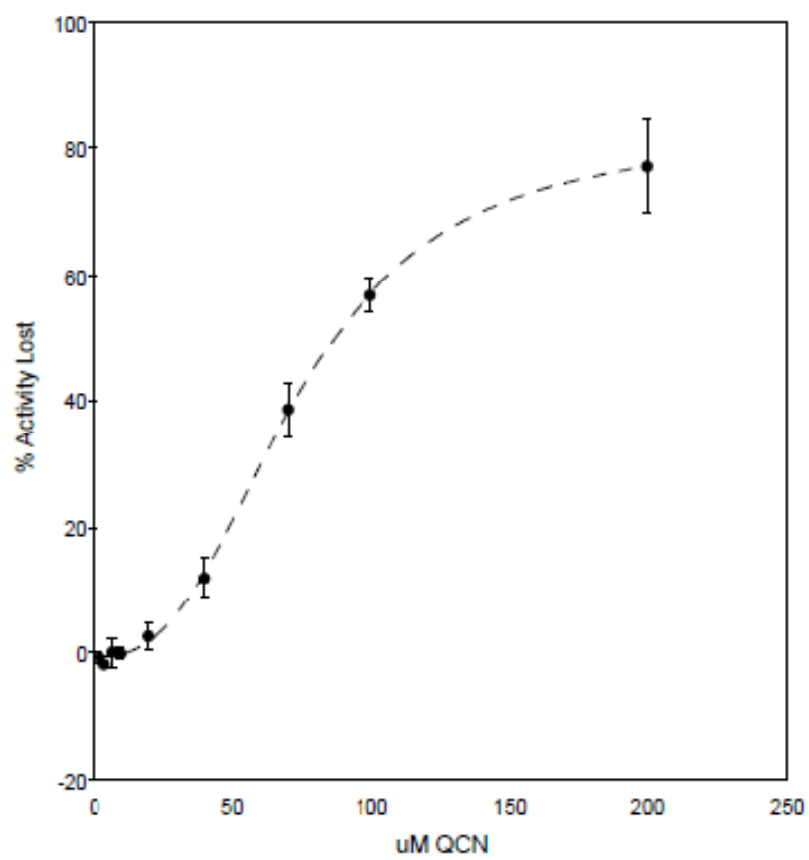
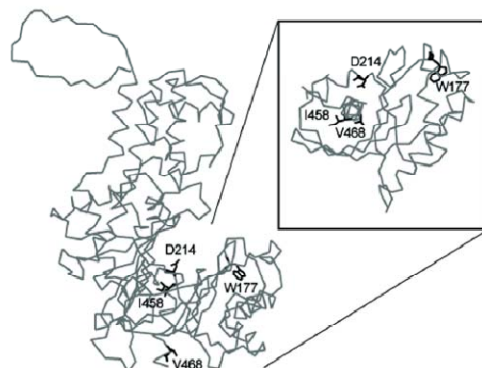
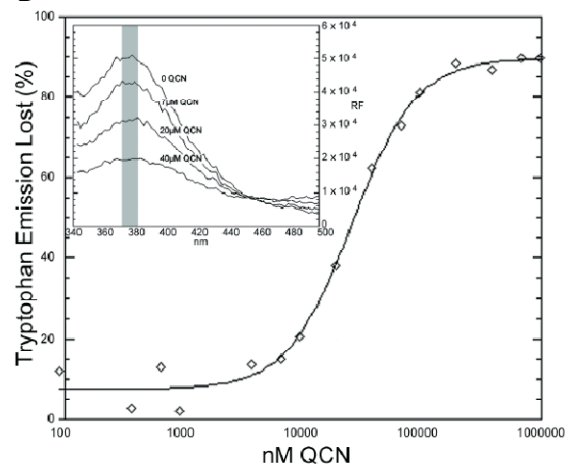


Fig 2.

A



B



C

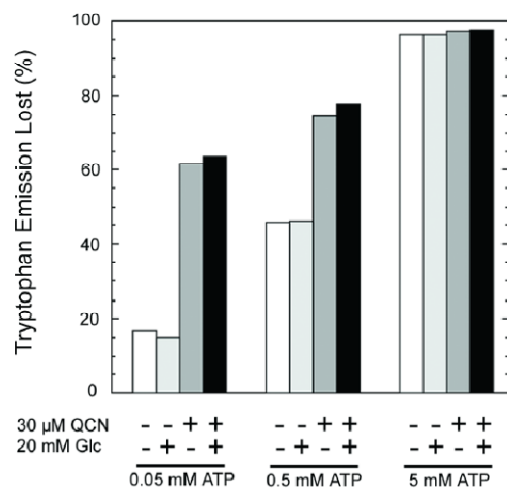


Fig 3.

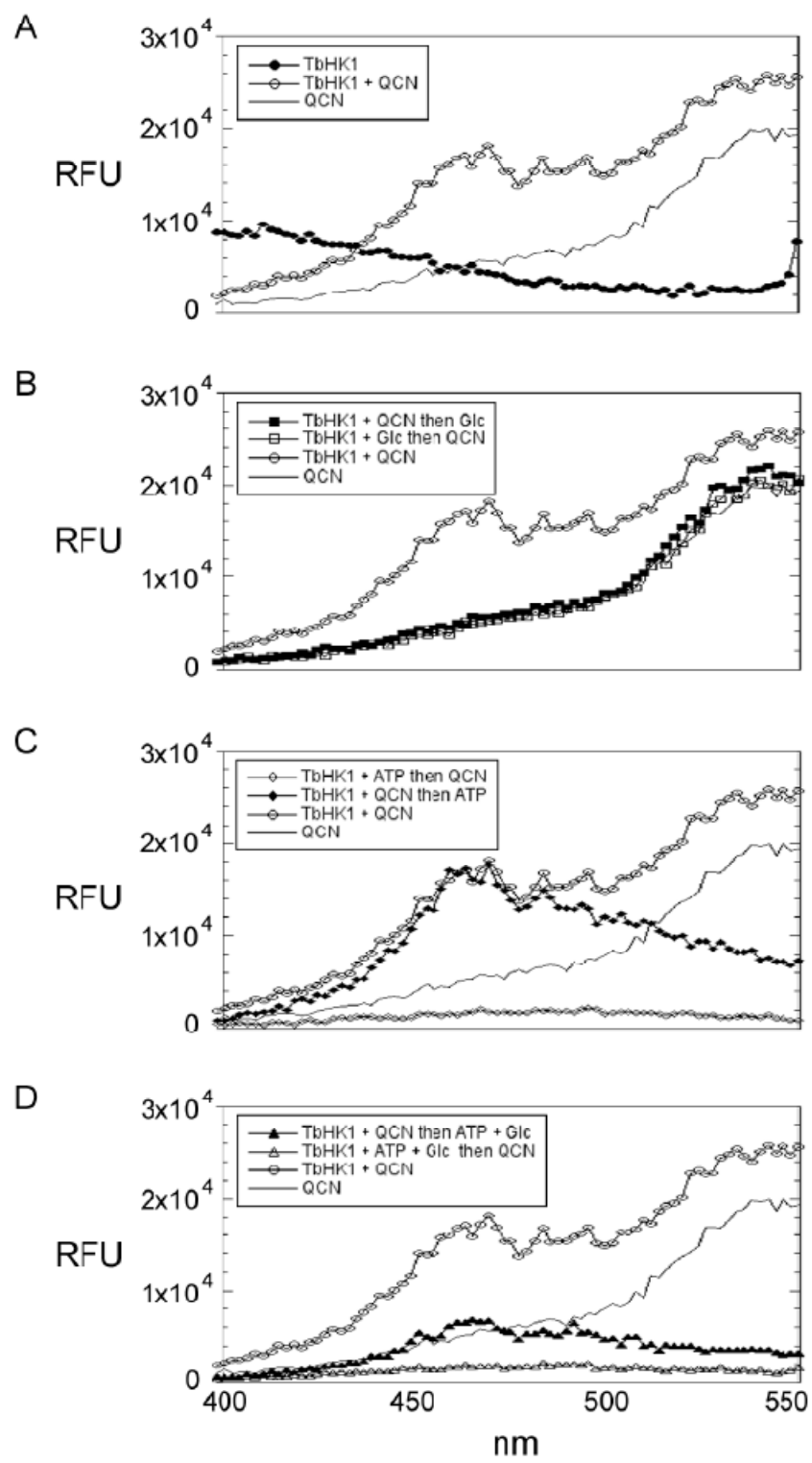


Fig 4.

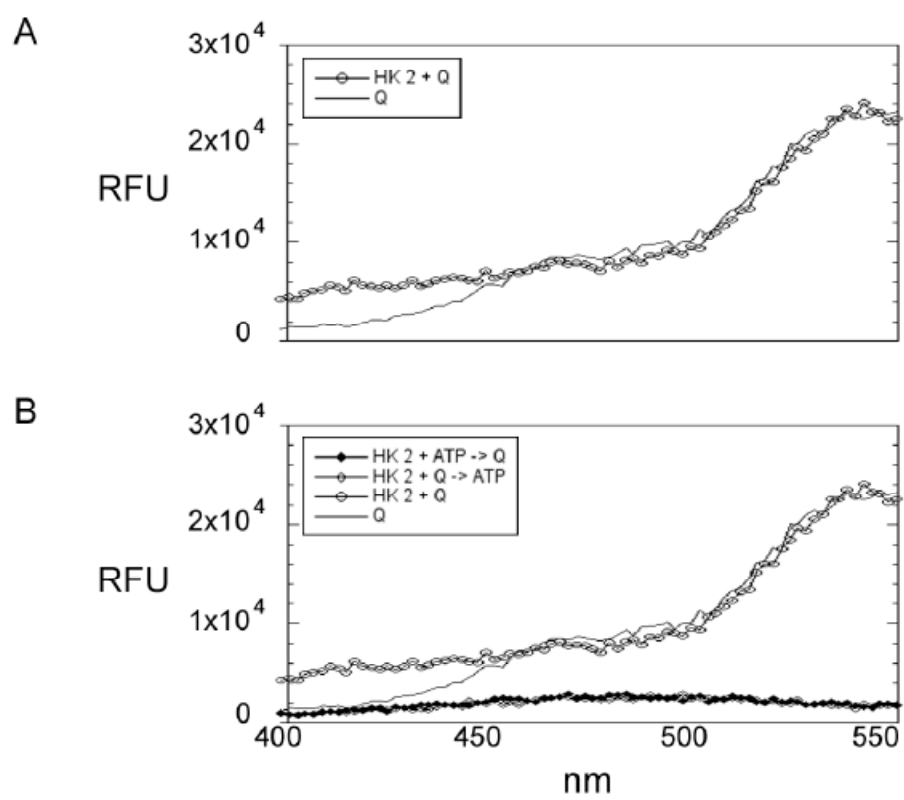
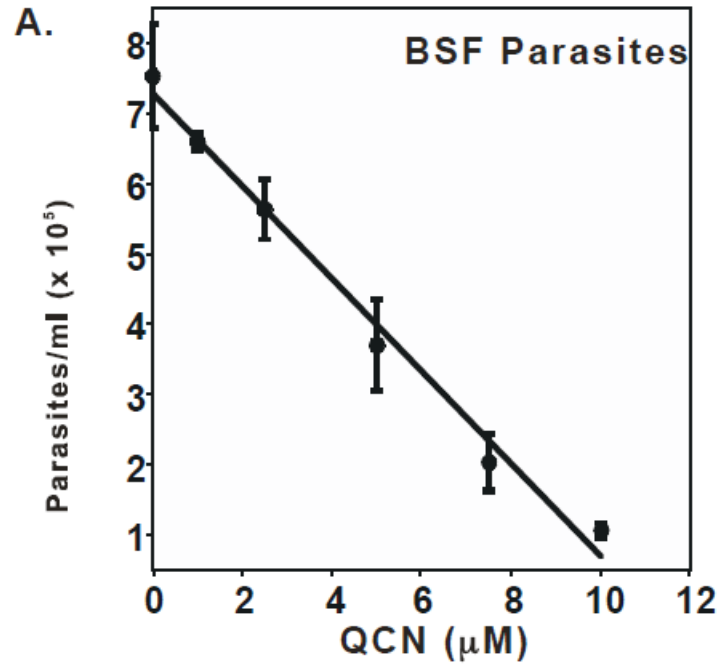


Fig 5.



B.

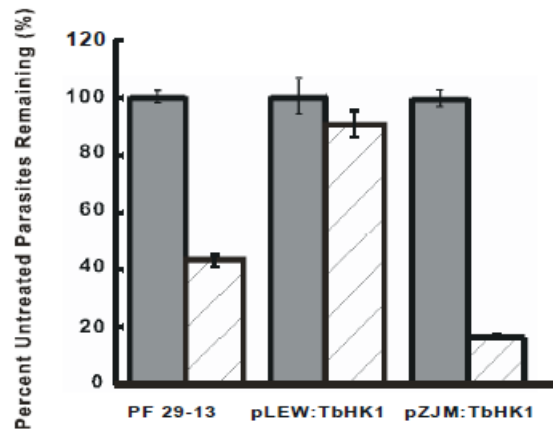
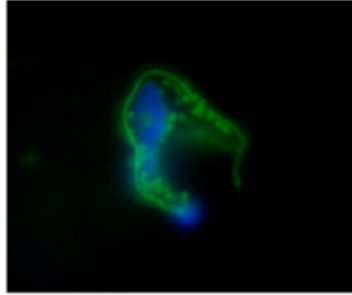
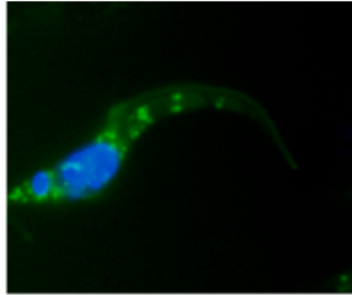


Fig 6.

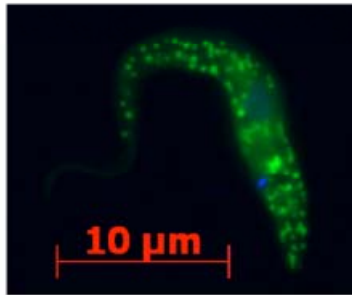
BSF
+QCN



PF
+QCN



PF
PTS
eYFP



CHAPTER THREE

A TARGET-BASED HIGH THROUGHPUT SCREEN YIELDS *TRYPANOSOMA*
BRUCEI HEXOKINASE SMALL MOLECULE INHIBITORS WITH
ANTIPARASITIC ACTIVITY

Abstract

The parasitic protozoan *Trypanosoma brucei* utilizes glycolysis exclusively for energy production during infection of the mammalian host. The first step in this metabolic pathway is mediated by hexokinase (TbHK), an enzyme essential to the parasite that transfers the γ -phosphoryl of ATP to a hexose. Here we describe the identification of novel small molecule inhibitors of TbHK1, which were then assessed for their impact on parasite viability. These compounds were identified using a TbHK1 high throughput screen (HTS) assay format that couples the production of glucose-6-phosphate to a change in absorbance at OD₃₄₀ through the activity of a reporter enzyme, glucose-6-phosphate dehydrogenase. Our HTS assay conditions were optimized and then validated using a pilot screen of a library of 1280 pharmaceutically active compounds. This screen yielded 12 compounds that inhibited TbHK1 >50% at 10 μ M and the resulting average Z-factor of 0.69 ± 0.02 indicated that the *in vitro* assay was sufficiently robust for an HTS campaign. Our interrogation of 220,233 unique compounds yielded 239 compounds as primary actives (>50% inhibition at 10 μ M) for a 0.1% hit rate. The average Z-factor for the screen was 0.80 ± 0.14 and subsequent IC₅₀ value determinations confirmed TbHK1 inhibitory activity for 10 small molecules. Cluster analysis indicated that five compounds were structurally related while the remaining 5 compounds were classified as singletons. Of these, three inhibited parasite growth with EC₅₀ values < 50 nM with EC₅₀s values for mammalian cell lines of >12.5 μ M, suggesting promising target cell specificity. These compounds represent novel leads for future therapeutic development against the African trypanosome.

Introduction

African sleeping sickness conjures images of the past - of disease-induced fatal slumber striking down men, women, and children while the malady decimates villages of colonial Africa. Unfortunately, people living in many countries of sub-Saharan Africa today know that African sleeping sickness is *not* a disease of history but rather is a much-neglected disease of the present, particularly in areas that suffer the additional burdens of war, famine, and other infectious agents. The causative agents of sleeping sickness (or human African trypanosomiasis, HAT) are subspecies of the African trypanosome *Trypanosoma brucei*. Approximately 500,000 people in sub-Saharan Africa are infected annually with the parasite leading to 50,000-70,000 deaths per year (Stich *et al.*, 2002). Few therapeutics are available and of the drugs currently used in the treatment of HAT most have serious adverse side effects, including encephalopathy and death (Pepin *et al.*, 1991). Thus, there is a desperate need for new HAT therapeutics.

Bloodstream form (BSF¹) *T. brucei* parasites generate energy exclusively through glycolysis and *T. brucei hexokinase 1* (TbHK1), the first enzyme in glycolysis, has previously been validated as a target for therapeutic development. In these experiments, BSF parasites were shown to be sensitive to RNA interference (RNAi)-based silencing of TbHKs (Albert *et al.*, 2005; Chambers *et al.*, 2008), with cell toxicity observed after 3-5 days of RNAi exposure. Further, known inhibitors of HKs from other systems have been demonstrated to inhibit TbHK1 and to be toxic to the parasite (Opperdoes *et al.*, 2006). However, while some mammalian HK inhibitors can inhibit TbHK1, TbHK1 is distinct enough from mammalian HKs to suggest that it can be

specifically targeted. For example, TbHK1 shares only 30-33% sequence identity with the mammalian HKs, while differing in a number of ways including the fact that the trypanosome enzymes are found as hexamers (Misset *et al.* 1984). Moreover, the unusual spectrum of known inhibitors of the trypanosome enzymes, including fatty acids and other small molecules (like pyrophosphate, (Chambers *et al.*, 2008), support the idea that this essential parasite protein is sufficiently distinct from any mammalian counterpart to make an ideal target for therapeutic development. Indeed, targeting TbHK using structurally based inhibitors has yielded trypanocidal compounds, albeit at high concentrations (Trinquier *et al.*, 1995; Willson *et al.*, 2002).

Here we describe our target-based approach to identify and confirm specific inhibitors of the essential parasite enzyme, TbHK1. Most of the potent TbHK1 inhibitors are toxic to culture grown BSF *T. brucei* while not exhibiting toxicity towards mammalian cells, suggesting that they may be useful lead compounds in the development of new therapies for African trypanosomiasis.

Results

Validation of optimized HTS assay conditions using the LOPAC set

The TbHK1 coupled assay was optimized and validated for HTS by screening the library of pharmaceutically active compound set (LOPAC). Compounds were assayed in duplicate at a single concentration (10 μ M) and reproducibility between the duplicate screens is represented in Fig. 1A ($R^2 = 0.96$). Average Z-factors were 0.69 ± 0.02 for the two LOPAC assays demonstrating the robustness of the developed assay format (Zhang

et al., 1999). Eighteen compounds inhibited TbHK1 enzymatic activity $\geq 40\%$ at 10 μM including myricetin ($48.9 \pm 0.7\%$), a structural analog of quercetin, which we previously identified as a TbHK1 small molecule inhibitor (Lyda and Morris, unpublished observation) (Fig. 1B). These data confirmed that our automated HTS assay conditions were robust and could be used to identify compounds that inhibited TbHK1 activity.

Interrogation of 220,233 compounds for TbHK1 small molecule inhibitors.

We next screened 220,223 compounds at a single concentration (10 μM) for small molecule inhibitors of TbHK1. The HTS assay performed robustly with average Z-factors of 0.80 ± 0.1 and 239 compounds were identified as primary actives for an overall hit rate of 0.1%. The 239 active compounds were cherry-picked and the initial inhibitory activity confirmed in the primary TbHK1 assay. Additionally, the compounds were tested against the reporter enzyme, glucose-6-phosphate dehydrogenase, to determine if they interfered with the assay format. After initial 20 point IC_{50} value determinations using cherrypicked compounds, 13 small molecules with IC_{50} values $< 50 \mu\text{M}$ were obtained from commercial sources. The activity of the resupplied compounds was empirically determined to control for possible TbHK1 inhibitory effects associated with compound library degradation. Ten small molecules confirmed with TbHK1 IC_{50} values $< 50 \mu\text{M}$ while 3 compounds failed to inhibit TbHK1. Leadscope analysis of the 10 confirmed TbHK1 inhibitors classified 5 compounds into a cluster of structurally related compounds (cluster 1) while the remaining 5 compounds were classified as singletons (Tables 1 and 2). Ebselen (SID 856002) was the most potent compound in cluster 1 with

an $IC_{50}=0.05 \pm 0.03 \mu\text{M}$. For the majority of the compounds IC_{50} values either improved or remained similar to cherry-picked compounds with the exceptions of SID 17386310 and 14728414 (Table 2).

Experiments aimed at exploring specificity of hits for TbHK1 included data mining of the PubChem Bioassay database to determine the frequency with which a compound has been found to be active in other assays. In general, the cluster 1 compounds have been active in other assays more frequently than the singletons, with SID 17387000 the most frequently active (identified in 14.1% of the 226 assays in which it was tested). Singletons, on the other hand, were less frequently active. For example, SID 14728414 was active in 2 of 210 assays (1%) (Table 2).

Additional experiments to assess the *in vitro* specificity included testing the compounds against human glucokinases (hGlcK). This enzyme is similar in size, shares 34% identity with TbHK1, and, like TbHK1, is not inhibited by its product glucose-6-phosphate. The activity against hGlcK was varied, with the cluster 1 compounds yielding a spectrum of potency, from very low inhibition at 10 μM (for example, SID 17387000, with 6.7% inhibition, Table 1) to near complete inhibition by SID 856002 (ebselen, 97.8% inhibition). Singletons also demonstrated a spectrum of activity against hGlcK, with SID 22401406 and 14728414 having minimal impact on the enzyme while 16952891 and 17386310 were more potent inhibitors (Table 2).

TbHK1 inhibitors are toxic to BSF parasites

TbHK1 has previously been shown to be an essential gene for BSF *T. brucei* (REFS), suggesting that inhibitors of the enzyme may be promising lead compounds for therapeutic development. To initially explore this possibility, cultured BSF parasites were grown in the presence of 10 μ M compound (dissolved in 1% DMSO, f.c.) and cell density monitored after 48 hr (Table 3). The DMSO carrier had minimal impact on cell growth, with a ~20% reduction at the highest concentration used (1% f.c.) compared to untreated cells after 48 hr. The 10 resupplied compounds were tested in this assay, with EC₅₀s determined for those that inhibited cell growth >50% at 10 μ M (Table 3). Compounds in cluster 1 included two of the most potent anti-trypanosomal compounds, SID 17387000 and 24785302. Singletons were also toxic, with SID 17386310 being one of the most potent compounds tested to date. Four molecules, including a member of cluster 1 (SID 3716597) and three singletons (SID 22401406, 24797131, 14728414) inhibited TbHK1 but were minimally toxic to BSF.

With the exception of 856002 (ebselen), the resupplied compounds that were anti-parasitic exhibited EC₅₀ values that were 10-1000 fold lower than the IC₅₀ values, suggesting possible off-target effects. This discrepancy could alternatively result from the finding that TbHK1 is localized in a small peroxisome-like organelle, the glycosome, which may effectively concentrate the inhibitors. Additionally, BSF parasites are sensitive to genetic manipulation that leads to decreased but not ablated TbHK1 expression. This suggests that modest inhibition of cellular TbHK1 activity could be toxic to the parasite.

Specificity of TbHK1 inhibitor toxicity

To explore the likelihood of off-target effects, we first assessed the toxicity of the TbHK1 inhibitors against PF parasites. Unlike BSF parasites, PF parasites can utilize both amino acids and glucose for energy generation. This dynamic metabolism suggests that the PF parasites may be less sensitive to TbHK1 inhibitors. Indeed, at 10 μM most of the resupplied compounds had only a modest impact on PF parasite growth, inhibiting growth between 0-51% when compared to control cell lines.

Tests of target specificity also included assaying the HTS hits against other parasites. Compounds toxic to *T. brucei* were assayed against a related kinetoplastid parasite, *Leishmania major*. *L. major* promastigotes were typically less sensitive to the resupplied compounds (with EC_{50} values $>12.5 \mu\text{M}$), with the exception of ebselen, 17387000, 17386310, and 24785302. These compounds had EC_{50} values against *L. major* between 1-5 μM in exponentially growing parasites (Table 3). Moreover, our identified TbHK1 inhibitors have minimal impact on human cells with EC_{50} values $>12.5 \mu\text{M}$ for all tested cell lines, suggesting at least 400-fold greater toxicity toward parasites for the most potent *T. brucei* cytotoxic compounds (data not shown).

In silico analysis of ADME characteristics of the TbHK1 inhibitors

Experimental assessment of the ADME-Tox and physicochemical profile of an entire hit set from an HTS campaign represents a considerable challenge considering that we will end-up with several hundred to several thousand compounds. To rationally break

down these large numbers we performed an *in silico* assessment of ADME/Tox properties.

Further characterization of two structurally related compounds

Ebselen, 2-phenyl-1,2-benzisoselenazol-3(2*H*)-one, was the most potent resupplied TbHK1 inhibitor. Resupply of the structurally related inhibitor 17387000 (2-phenyl-1,2-benzisothiazol-3(2*H*)-one) yielded different IC₅₀ values (0.05 ± 0.03 and 2.0 ± 0.5, for ebselen and 17387000, respectively). In secondary assays, the two compounds behaved differently. Ebselen was less potent against parasite lysate-derived TbHK activity than against the recombinant protein, with an IC₅₀ of 10 μM, suggesting that the compound may be metabolized by cellular components. Compound 17387000 was nearly as potent against lysate activity as against the recombinant protein, with an IC₅₀ value against lysate enzyme of 8.6 μM.

Additional differences include the activity of the compounds in screens against hGlck and parasite cells. Ebselen was a potent inhibitor of hGlck (97.8% inhibition at 10 μM), while 17387000 had relatively little activity (6.7% inhibition) against the kinase (Table 1). Additionally, ebselen was ~100-fold less active against BSF parasites (Table 3), suggesting that the subtle differences between the two compounds yielded remarkable changes in their pharmacological behavior.

Analysis of the nature of inhibition revealed subtle difference between the two molecules. Ebselen inhibition was competitive with respect to ATP, while non-competitive with respect to glucose. This observation suggests that the inhibitor allows

glucose to bind but competes with ATP, leading to the formation of ternary E-I-glucose complexes (Willson *et al.*, 1999). Unlike ebselen, 17387000 was competitive with respect to both ATP and glucose, with K_i values of 0.62 μM and 1.2 μM , respectively.

Discussion

There are currently four drugs approved for treatment of HAT. Suramin and pentamidine, developed in 1921 and 1941, respectively, are not effective against disease caused by *T. b. rhodesiense*. Melarsoprol, which was introduced in 1949, leads to fatal complications in 10% of patients receiving the drug (Docampo *et al.*, 2003). The most recently developed drug, eflornithine, is efficacious against only *T. b. gambiense*, but is curative for both the early blood-borne infection and the late stage of disease that occurs when the parasite crosses the blood-brain barrier; delivery of eflornithine is difficult, as the compound must be administered intravenously four times a day for 14 days (delivering $\sim 360\text{g/patient}$).

A number of screens of chemical libraries have been undertaken to identify therapeutic leads against the African trypanosome. These include a phenotypic screen that interrogated a library of FDA-approved drugs for anti-trypanosomal activity (Mackey *et al.*, 2006), as well as screens developed to identify inhibitors of essential parasite enzymes. A screen for UDP-Glc 4'-epimerase inhibitors using a small natural products library (Urbaniak *et al.*, 2006) and a screen of a commercial 134,500 compound library for trypanothione reductase inhibitors (Martyn *et al.*, 2007) are two examples of target-based screens used to identify lead compounds for therapeutic development.

In the last few years, TbHK inhibitors have been explored as potential anti-parasitic compounds. Previous efforts to identify TbHK inhibitors include the development of compounds based on models of the TbHK structure (predicted from homology studies of the yeast structure), and exploring the activity of HK inhibitors from other systems (Opperdoes *et al.*, 2006). Here we have used a HTS of 220,223 compounds to identify new inhibitors of the parasite enzyme.

In our screens, we have identified several novel inhibitors of TbHK1. One compound, ebselen, was the most potent inhibitor from the LOPAC validation screen and was the second most potent enzyme inhibitor identified in the HTS. Ebselen is a lipid-soluble seleno-organic compound that has been employed in clinical trials to assess its value in prevention of ischemic damage in brain hemorrhage and stroke (Saito *et al.*, 1998; Yamaguchi *et al.*, 1998). Ebselen inhibits lipid peroxidation through a glutathione peroxidase-like action (Muller *et al.*, 1984), but may act through other mechanisms as well. Notably, a single oral dose (100mg/kg) of ebselen yields serum values of 4-5 mM (Salom *et al.*, 2004) and brain levels of the drug reach 21% of plasma levels (Imai *et al.*, 2001), suggesting that the compound (or its derivatives) may be useful for both early and late stage sleeping sickness therapy development.

Ebselen likely has polypharmacological effects on BSF parasites, as the compound is known to inhibit a number of enzymes in addition to TbHK1, including the trypanosome UDP-Glc 4'-epimerase (Urbaniak *et al.*, 2006). The notable discrepancy between the IC₅₀s and EC₅₀s of the TbHK1 inhibitors identified here are also possibly the result of off-target inhibition. Alternatively, differences between the two values could

result from the concentration of the compound within the parasite (perhaps in the glycosome) or metabolism of the inhibitor to a more potent form.

An ideal therapeutic drug for African sleeping sickness would target only the parasite and work at concentrations low enough to limit the severity of side effects. In the search for potential drug targets, we have focused on the trypanosome TbHK1, a protein that the parasite requires to make energy and have identified compounds that may serve as leads in for the development of therapeutics in the continuing fight against the African trypanosome.

Materials and Methods

Chemicals and Reagents. Clear 384-well microtiter plates were purchased from Greiner (Monroe, NC) and used for all experiments. Glucose-6-phosphate dehydrogenase, β -nicotinamide adenine dinucleotide (NAD⁺), adenosine triphosphate (ATP), lipoic acid (Pubchem SID 11532893) and glucose were purchased from Sigma (St. Louis, MO). Phosphoenol pyruvate (PEP), ebselen (PubChem SID 856002) and glucosamine were obtained through VWR (West Chester, PA) and dimethyl sulfoxide (DMSO) was purchased from Fisher (Pittsburgh, PA). The following PubChem SID compounds were obtained from commercial vendors: 3715577, 3716597, 24830882, 17386310, and 16952891 (Enamine/Kiev, Ukraine); 24797131 and 14746394 (Chembridge/San Diego, CA); 14728414 and 17387000 (Specs/Delft, The Netherlands); 24785302, 24790923, and 24814083 (University of Kansas Specialty Chemistry Center/Lawrence, KS); 17507245

(Asinex/Moscow, Russia) and 22401406 (Dr. K.H. Lee/University of North Carolina, Chapel hill, NC).

Compound Libraries. The library of pharmacologically active compounds (LOPAC) (1,280 compounds) was purchased from Sigma-Aldrich. The Pittsburgh Molecular Libraries Screening Center (PMLSC) provided the 220,233 compound library screened for *T. brucei* hexokinase 1 small molecule inhibitor, which was made available as part of the NIH Molecular Libraries. Cherry-picked compounds from the PMLSC library were supplied by BiofocusDPI (San Francisco, CA).

Purification of Recombinant TbHK1. For purification of recombinant TbHK1 (rTbHK1), a previously described protocol (Morris *et al.*, 2006) was modified to increase yield. Briefly, a starter culture of *E. coli* M15(pREP) harboring pQE30 (Qiagen, Valencia, CA) with TbHK1 cloned in frame of a 6-His tagging sequence was grown in ECPM1 {Wigelsworth, 2004 #1772} and then inoculated into a 5 L a bioreactor (Biostat B, B. Braun Biotech International, Allentown, PA) and grown at 37°C. At OD₆₀₀ between 3-5, the culture was induced with IPTG (0.8 mM), grown without supplement O₂ (37°C, 16 hr), and cells collected by centrifugation (5000 x g, 20 min, 4°C). The pellet was resuspended in lysis buffer (50 mM NaPO₄, pH 8.1, 5 mM glucose, 150 mM NaCl, and 0.1% Tween) and lysed by using a cell disruptor (Constant Cell Disruption Systems, Sanford, NC). The resulting supernatant was applied (5 ml/min) to a 50 ml ProBind column (Invitrogen, Eugene, OR) on a FPLC (GE Lifesciences, Piscataway, NJ) and

protein eluted by step gradient (5 to 250 mM imidazole) in lysis buffer. Fractions were screened using HK activity assays and Western blotting and those containing rTbHK1 were pooled, concentrated, and applied to a HiTrap SP HP column (GE Lifesciences, Piscataway, NJ). Following elution, fractions harboring rTbHK1 were analyzed and determined to be ~95% pure based on coomassie stained SDS polyacrylamide gels.

Automated primary TbHK1 HTS and glucose-6-phosphate dehydrogenase coupled

assays. TbHK1 assays were an adaptation of a coupled enzyme HK assay to a 384-well format (Morris *et al.*, 2006; Parry and Walker, 1966). Briefly, test and control compounds (30 μ M in 15 μ L volume) were added to a 384 well black, opaque microtiter plate using a Velocity 11 V-prep (Santa Clara, CA) for a final test compound concentration of 10 μ M. Negative (vehicle) controls contained 1% DMSO, positive controls contained 133 mM glucosamine and IC₅₀ controls contained 1.3 mM glucosamine (final well concentrations). A mixture containing glucose (1.5 mM), ATP (1.05 mM), MgCl₂ (4.5 mM), NAD⁺ (9 mM), and G6PDH (0.018 mUnits/ μ L) in a 15 μ L volume was then added to each well of the assay plate using a Perkin Elmer FlexDrop (Waltham, MA) followed by addition of rTbHK1 (1.5 ng/ μ l in 15 μ L volume). The 45 μ L reaction mixture was incubated at RT for 2 hours and then quenched with 5 μ L EDTA (500 mM). The resulting signal, which remains stable for up to 5 hr after addition of stop reagent, was collected on a Molecular Devices SpectraMax M5 (Absorbance_{340nm})(Sunnyvale, CA).

To account for possible inhibition of the reporter enzyme in the primary coupled reaction, putative inhibitors were screened to assess their activity against a G6PDH coupled assay. Briefly, test and controls compounds were added to the wells of a 384 well assay plates as described above. Negative (vehicle) controls contained 1% DMSO, positive controls contained 100 mM PEP and IC₅₀ controls contained 8.6 mM PEP (final well concentrations). A mixture containing glucose-6-phosphate (0.6 mM) and NAD⁺ (9 mM) in a volume of 15 μ L was then added to each assay plate well. The reaction was initiated by addition of 15 μ L G6PDH (0.018 mUnits/ μ L) and change in absorbance at OD₃₄₀ was monitored as above.

Additional specificity assays were performed using human HK 4 (human glucokinase, hGlk, GenBank accession no. BC001890) that was expressed from a cloned cDNA (OPEN Biosystems, Huntsville, AL) in pQE30. After sequencing, the plasmid was transformed into *E. coli* M15 (pREP) and cultures were grown to an OD₆₀₀ of 0.9 in terrific broth and protein expression induced (3 hr, 37°C) with 1 mM IPTG. Nickel-affinity chromatography was used to purify soluble proteins, and purity was determined to be >95% by commassie standard SDS-PAGE gel (not shown).

T. brucei blood stream form (BSF) viability assay. To determine the impact of TbHK1 inhibitors on cell growth, 5 x 10³ BSF parasites (cell line 90-13, a 427 strain) were seeded into 96-well clear-bottomed polystyrene plates in HMI-9 supplemented with 10% fetal bovine serum and 10% Serum Plus (Sigma-Aldrich, St. Louis, MO) and grown for 3 days in 5% CO₂ at 37°C grown. CellTiter Blue (Promega, Madison WI) was added to a final

concentration of 16% (v/v) and the plates incubated an additional 3 hours under standard culture conditions. Fluorescence emission at 585nm was then measured after excitation at 546nm in a GENios microtiter plate reader (Phenix Research Products, Hayward CA). DMSO is tolerated by BSF parasites and has minimal impact on the assay described here, with 1% DMSO (f.c.) causing a 16% reduction in cell number at the end of the three day assay.

PF parasites (29-13, a 427 strain, 5×10^4 /well) were grown in 96-well clear-bottomed polystyrene plates in grown in SDM-79 for 2 days (5% CO₂, 25°C) and then CellTiter Blue added. Plates were then incubated for 1 hour under standard culture conditions. Fluorescence of samples was then characterized as above.

Mammalian cell-line and Leishmania major promastigote specificity assays. Cell-based specificity assays were performed as previously described (Sharlow *et al.*, 2009). Briefly, mammalian cell line and *L. major* promastigote assays were performed in final volumes of 25 μ L using our previously described 384-well microtiter format (Sharlow *et al.*, 2008). All mammalian cell lines were cultured and maintained in complete growth medium preparations according to ATCC specifications (ATCC, Manassas, VA). *L. major* promastigotes were cultured as previously described (Sharlow *et al.*, 2009). A549 (1,000 cells/22 μ L), IMR-90 (1,000 cells/22 μ L), HeLa (1,000 cells/22 μ L), MDA-MB-231 (3,000 cells/22 μ L), *L. major* promastigotes (5,000 parasites/22 μ L) were seeded into each well of 384-well microtiter plates and test and control compounds were added to individual wells. Vehicle and positive controls were 1% and 10% DMSO, respectively.

For mammalian cells, assay plates were incubated for 44-46 h at 37°C in the presence of 5% CO₂.and for the *L. major* promastigotes, assay plates were incubated for 44 h at 28°C with 5% CO₂. Five µL alamar blue reagent were added to each assay plate well and incubated for 2-4 h at 37°C with 5% CO₂. Data were captured on a Molecular Devices SpectraMax M5 (excitation A₅₆₀; emission A₅₉₀).

HTS data analysis and statistical analysis. Primary HTS data analysis and subsequent compound IC₅₀ calculations were performed using ActivityBase (IDBS, Guilford, UK) and Cytominer (University of Pittsburgh drug Discovery Institute, Pittsburgh, PA). Structural similarity of the confirmed inhibitors was determined using Leadscope software (Columbus, OH). Additional visualization and statistical analysis were performed using GraphPad Prism software 5.0 and Spotfire (Somerville, MA). The PubChem database (<http://PubChem.ncbi.nlm.nih.gov>) was datamined to determine if the confirmed TbHK1 small molecule inhibitors exhibited bioactivity in other assays.

Acknowledgements

Marcia Hesser, Robyn Reed, Tongying Shun

References

- Stich A., Abel P.M., Krishna S. (2002) *BMJ* **325**, 203-6
- Pepin J., Milord F. (1991) *Trans. R. Soc. Trop. Med. Hyg.* **85**, 222-4
- Albert M. A., Haanstra J. R., Hannaert V., Joris Van Roy R. V., Opperdoes F. R., Bakker B. M., and Michels P. A. M. (2005) *JBC* **280**, 28306-28315
- Chambers J. W., Fowler M. L., Morris M. T., Morris J. C. (2008) *Mol Biochem Parasitol* **158**, 202-7
- Opperdoes F. R., Szikora J. P. (2006) *MBP* **147**, 193-206
- Misset O., and Opperdoes F. R. (1984) *Eur J Biochem* **144**, 475-483
- Chambers J. W., Kearns M. T., Morris M. T., and Morris J. C. (2008) *J Biol Chem* **283**, 14963-14970
- Trinquier M., Perie J., Callens M., Opperdoes F., Willson M. (1995) *Bioorg. Med. Chem.* **3**, 1423-7
- Willson M., Sanejouand Y. H., Perie J., Hannaert V., and Opperdoes F. (2002) *Chemistry and Biology* **9**, 839-847
- Morris J. C., Wang Z., Drew M. E., Englund P. T. (2002) *EMBO J* **21**, 4429-38
- Willson M., Perie J. (1999) *Spectrochimica acta Part A* **55**, 911-7
- Docampo R., Moreno S. N. (2003) *Parasitol. Res.* **90**, 10-3
- Mackey Z. B., Baca A. M., Mallari J. P., Apse B., Shelat A., Hansell E. J., Chiang P. K., Wolff B., Guy K. R., Williams J., McKerrow J. H. (2006) *Chem. Biol. Drug Des.* **67**, 355-63
- Urbaniak M. D., Tabudravu J. N., Msaki A., Matera K. M., Brenk R., Jaspars M., Ferguson M. A. (2006) *Bioorg. Med. Chem. Lett.* **16**, 5744-7
- Martyn D. C., Jones D. C., Fairlamb A. H., Clardy J. (2007) *Bioorg. Med. Chem. Lett.* **17**, 1280-3
- Saito I., Asano T., Sano K., Takakura K., Abe H., Yoshimoto T., Kikuchi H., Ohta T., Ishibashi S. (1998) *Neurosurgery* **42**, 269-78

Yamaguchi T., Sano K., Takakura K., Saito I., Shinohara Y., Asano T., Yasuhara H. (1998) *Stroke* **29**, 12-7

Müller A., Cadenas E., Graf P., Sies H. (1984) *Biochem. Pharmacol.* **33**, 3235-9

Salom J. B., Pérez-Asensio F. J., Burguete M. C., Marín N., Pitarch C., Torregrosa G., Romero F. J., Alborch E. (2004) *Eur. J. Pharmacol.* **495**, 55-62

Imai H., Masayasu H., Dewar D., Graham D. I., Macrae I. M. (2001) *Stroke* **32**, 2149-54

Morris M. T., DeBruin C., Yang Z., Chambers J. W., Smith K. S., and Morris J. C. (2006) *Eukaryot Cell* **5**, 2014-2023

Wigelsworth D. J., Krantz B. A., Christensen K. A., Lacy D. B., Juris S. J., Collier R. J. (2004) *J. Biol. Chem.* **279**, 23349-56

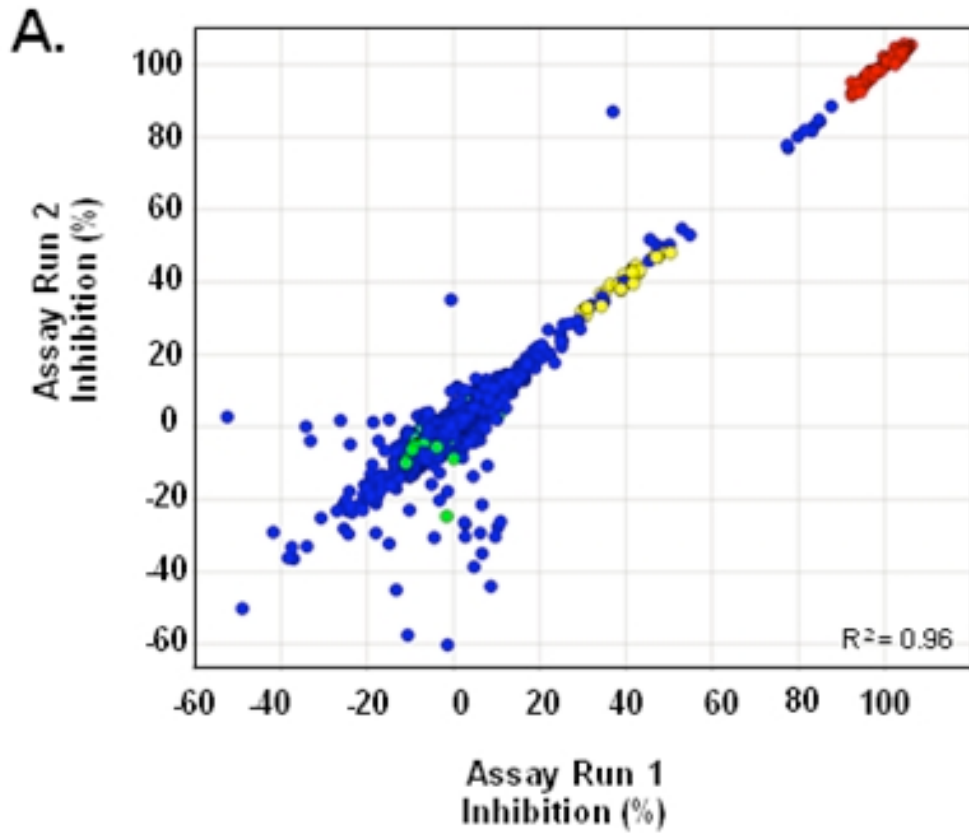
Parry M. J., Walker D. G. (1966) *Biochem J.* **99**, 266-74

Wang Z., Morris J. C., Drew M. E., and Englund P. T. (2000) *J. Biol. Chem.* **275**, 40174-40179

Figure Legend

Fig. 1. Validation of the HTS by LOPAC screening. (A.) Plot of % inhibition for duplicate screen of the 1280 LOPAC compounds. (B.) The LOPAC screen yielded a compound similar to a known inhibitor. Quercetin, a flavonol that inhibits mammalian HKs (REF), also inhibits TbHK1 (Lyda and Morris, unpublished). A structural relative, myricetin, was identified in the LOPAC set as an inhibitor of TbHK1.

Figure 1



B.

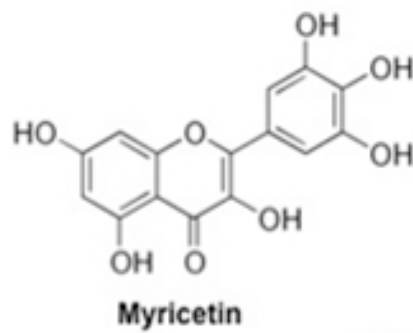
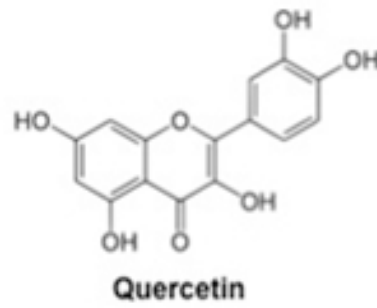
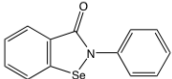
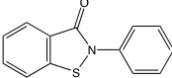
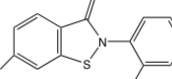
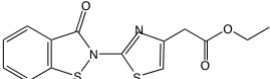
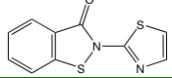
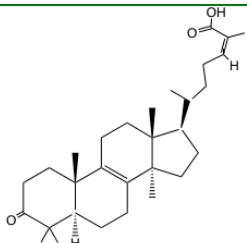
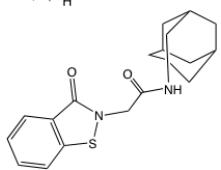
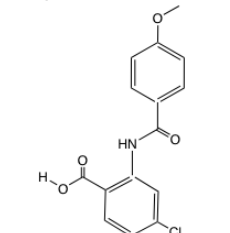
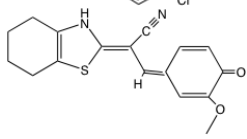
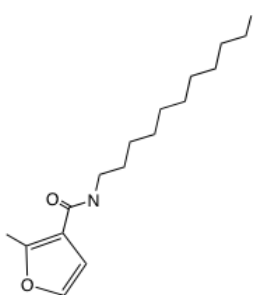


Table 1. Cluster 1 HTS Hits

PubChem SID	Structure	PubChem Bioassay Activity ¹	IC ₅₀ (μM) Cherry Pick	IC ₅₀ (μM) Resupply	%Inhibition of hGlcK (10 μM)
856002		336/43 ²	0.9 ± 0.1	0.05 ± 0.03	97.8 ± 0.1
17387000		226/32	6.8 ± 1.7	2.0 ± 0.5	6.7 ± 9.4
24785302		164/18	4.6 ± 0.9	4.2 ± 1.0	6.9 ± 4.2
3716597		312/28	36.7 ± 6.6	9.3 ± 0.3	7.8 ± 7.1
24830882		167/11	11.03	16.9 ± 0.1	88.8 ± 4.9

¹As of 06/21/09²Number of assays in which the compound was tested/number of assays in which the compound was active.

Table 2. Singleton HTS Hits

PubChem SID	Structure	PubChem Bioassay Activity ¹	IC ₅₀ (μM) Cherry Pick	IC ₅₀ (μM) Resupply	% Inhibition of hGlc (10 μM)
22401406		178/5	5.8	2.3 ± 0.3	0.0
16952891		207/20	10.7 ± 1.2	2.6 ± 0.2	44.9 ± 9.9
24797131		169/6	15.8 ± 0.03	11.4 ± 3.2	6.3 ± 8.8
17386310		205/10	4.5 ± 1.1	33.6 ± 10.2	70.3 ± 3.6
14728414		210/2	6.4 ± 0.3	41.7 ± 3.0	1.9 ± 7.0

¹As of 07/22/09

Table 3. Anti-parasitic activity of HTS compounds

PubChem SID	BSF EC ₅₀ (μM)	% PF Growth Inhibition (10 μM)	<i>L. major</i> EC ₅₀ (μM)
<i>Cluster 1</i>			
856002	2.9 ± 0.28	51 ± 0.16	4.1
17387000	0.030 ± 0.067	48 ± 0.15	1.9
24785302	0.042 ± 0.0028	47 ± 0.15	1.9
3716597	n.d. ¹	27 ± 0.080	>12.5
24830882	0.83 ± 0.20	8.6 ± 0.030	>12.5
<i>Singletons</i>			
22401406	n.d.	0.0	>12.5
16952891	0.30 ± 0.079	47 ± 0.15	>12.5
24797131	n.d.	0.0	>12.5
17386310	0.038 ± 0.0038	50 ± 0.15	2.6
14728414	n.d. ¹	0.0	>12.5

¹n.d., not determined. These compounds inhibited TbHK1 < 50% at 10 μM.

CHAPTER FOUR
EXTRA-GLYCOSOMAL LOCALIZATION OF *TRYPANOSOMA BRUCEI*
HEXOKINASE 2

Todd L. Lyda¹, Emilie Verplaetse², Heidi C. Dodson¹, Meredith T. Morris¹, Paul A. M. Michels², Derrick R. Robinson³, and James C. Morris^{1*}

¹Department of Genetics and Biochemistry, Clemson University, Clemson, SC

²Research Unit for Tropical Diseases, de Duve Institute and Laboratory of Biochemistry, Universite catholique de Louvain, Brussels, Belgium

³CNRS- University of Bordeaux 2, Bordeaux, France

Running Title: Targeting of *T. brucei* Hexokinase 2 to the flagellum is influenced by a conserved motif

To be submitted to “The Journal of Cell Science”

Corresponding author:

Dept. of Genetics and Biochemistry

Clemson University

214 BRC

51 New Cherry Street

Clemson SC 39634

Tel. (864) 656-0293

FAX (864) 656-0393

Email: jmorri2@clermson.edu

Abstract

The majority of the glycolytic enzymes in the African trypanosome are associated with peroxisome-like organelles, the glycosomes. Polypeptides harboring peroxisomal targeting sequences (PTS type 1 or 2) are targeted to these organelles. Here, we have found that a trypanosomal hexokinase, TbHK2, which has a PTS2, localized to both glycosomes and to the flagellum. Evidence included fractionation studies and immunofluorescence assays of both cells and cytoskeletal preparations using antibodies generated to the C-terminal tail of TbHK2. In addition to flagellar localization, the protein co-localized with basal bodies as revealed by localization of an HA epitope-tagged version of TbHK2. Comparison of the sequences of several known and predicted flagellar proteins with the sequence of TbHK2 revealed a shared hexameric amino acid sequence (RAVLAK in the TbHK2) that can direct GFP to the flagellum. These findings suggest that TbHK2 is positioned in the flagellum to perform a task distinct from glycosomally-compartmentalized glycolysis.

Key Words: *Trypanosoma brucei*, hexokinase, flagellum, glycosome, glycolysis

Introduction

In the African trypanosome, *Trypanosoma brucei*, glycolytic enzymes have been localized to peroxisome-like organelles called glycosomes (Opperdoes and Borst, 1977). This organization, which is thought to serve as a means of regulation of the pathway (Haanstra et al., 2008), is unusual as glycolysis is a cytosolic event in most cells. Even in systems with cytosolic glycolysis, glycolytic enzymes have been found in subcellular compartments distinct from the cytoplasm. These include such diverse compartments as the sarcoplasmic reticulum in rabbit muscle tissue (Xu and Becker, 1998) and the *Toxoplasma gondii* apicoplast (Fleige et al., 2007).

A number of species also localize glycolytic and other metabolic enzymes near the flagella. *Chlamydomonas reinhardtii* has three glycolytic enzymes (phosphoglycerate mutase, enolase, and pyruvate kinase) associated with flagellum to produce ATP (Mitchell et al., 2005). In mammals, a hexokinase (HK) has been found attached to the fibrous sheath that surrounds the axoneme and outer dense fibers of sperm flagellum, suggesting a role in extramitochondrial energy production (Miki et al., 2004; Nakamura et al., 2008; Travis et al., 1998).

Kinetoplastid metabolic enzymes have also been found proximal to the flagellum. For example, three isoforms of adenylate kinase localize to either the flagellar axoneme or paraflagellar rod (PFR) via an N-terminal extension in the proteins (Ginger et al., 2005). Additionally, a *Leishmania* HK (which was characterized as a hemoglobin receptor) has been localized to the flagellar pocket, suggesting that proteins may serve multiple functions depending upon localization (Krishnamurthy et al., 2005).

The *T. brucei* genome encodes two 98 % identical HKs (TbHK1 and TbHK2) that are expressed in both bloodstream form (BSF) and procyclic form (PF) parasites. These polypeptides form hexamers that *in vitro* have distinct biochemical properties depending on the ratio of TbHK1 and TbHK2 included in the oligomers (Chambers et al., 2008b). Proteomic analysis of purified glycosomes has revealed that both proteins are detectable in BSF and PF glycosomes, a finding that supports the observation that over-expression of TbHK2 tagged with a C-terminal GFP localizes to the glycosome (Colasante et al., 2006; Morris et al., 2006). While the function of these polypeptides is currently unclear, genetics-based studies have confirmed that both are essential to BSF parasites (Albert et al., 2005; Chambers et al., 2008a).

The glycosomal localization of the TbHKs has been attributed to the presence of N-terminal peroxisomal targeting sequences (PTS2) in both proteins. This sequence has been shown to be responsible for the import of other glycosomally-targeted proteins (Blattner et al., 1995), so glycosomal localization of TbHKs was anticipated. Here, however, we report the unexpected dual localization of TbHK2 to both the glycosome and flagellum. The flagellar localization is the result, in part, of a C-terminal targeting sequence, found in both TbHK1 and 2, that is conserved in both described flagellar resident proteins and hypothetical proteins thought to have flagellar localization.

Materials and Methods

Subcellular Fractionation and cytoskeletal extraction of trypanosomes – Subcellular fractionations were performed using BSF and PF *T. brucei* (cell line 449 (Biebinger et

al., 1997)), that were constitutively expressing the tetracycline repressor gene (Tet) from the chromosomally integrated plasmid pHD449, which also endows phleomycin resistance. This cell line is metabolically indistinguishable from the wild type. BSF parasites were cultured in HMI-9 medium containing 10% heat-inactivated foetal calf serum (Invitrogen) and $0.18 \mu\text{g}\cdot\text{mL}^{-1}$ phleomycin (Cayla) at 37°C under water-saturated air with 5% CO_2 . Procyclic trypanosomes were grown in SDM-79 medium (Brun and Shonenberger, 1979) supplemented with 15% foetal calf serum and $0.5 \mu\text{g}\cdot\text{mL}^{-1}$ phleomycin at 28°C under water-saturated air with 5% CO_2 . Cultures were always harvested in the exponential growth phase, *i.e.*, at densities lower than $2\cdot 10^6$ cells $\cdot\text{mL}^{-1}$ for bloodstream forms and $2\cdot 10^7$ cells $\cdot\text{mL}^{-1}$ for procyclic cells, by centrifugation at $700 \times g$ for 10 min.

Localization of glycosomal enzymes was studied by subcellular fractionation of cells by treatment with increasing concentrations of digitonin. Bloodstream (10^8 cells) and procyclic trypanosomes (2×10^8 cells) were washed twice in ice-cold buffer (25 mM HEPES, pH 7.4, 250 mM sucrose and 1 mM EDTA), and then resuspended in 0.5 mL of the same buffer. The cell suspension was divided in aliquots each containing 100 μg of protein and HBSS buffer (Invitrogen) was added to adjust each volume to 100 μL . Digitonin, dissolved in dimethylformamide, was then added followed by incubation for 4 min at room temperature. Untreated cells and those completely lysed (total release, generated by incubation in 0.5% Triton X-100) were used for comparison. After centrifugation of the suspensions ($12,000 \times g$ for 2 min), the supernatant (released fraction) was probed by western blotting for glycosomal resident proteins. For detection

of the proteins, rabbit polyclonal antisera raised against *T. brucei* pyruvate kinase (PYK, antiserum used at a dilution of 1:100,000), hexokinase (HK, at 1: 100,000), enolase (ENO, at 1:150,000) and glycerol kinase (GK, at 1:100,000) were used and detected with anti-(rabbit IgG) conjugated to horseradish peroxidase (Rockland Immunochemicals) that was visualized using the ECL Western Blotting System (Pierce).

Cytoskeleton preparations were produced from the addition of Voorheis's modified PBS (vPBS; 137 mM NaCl, 3 mM KCl, 16 mM Na₂HPO₄, 3 mM KH₂PO₄, 46 mM sucrose, 10 mM glucose, pH 7.6) washed cells with either 0.25% NP 40 in 100 mM PIPES, pH 6.8 with 1mM MgCl₂ or 0.5% Triton X-100 in MME (10 mM MOPS, 2 mM EGTA and 1 mM MgSO₄) buffer as described (Robinson et al., 1991). After 5 min, cytoskeleton preparations were washed with buffer without detergent. Cytoskeleton preparations were then visualized after adhering to poly-lysine coated slides or left in solution for hexokinase assays.

Immunolocalization and western blotting of TbHK2 - Immunofluorescence assays were performed using a protocol modified from (Field et al., 2004). In short, parasites were harvested by centrifugation at 800 x g, washed with vPBS, and then fixed (10 min on ice (BSF) or 1 hr on ice (PF)) in an equal volume of 6% paraformaldehyde and vPBS. Cells were washed with vPBS, allowed to settle on poly-lysine slides for 20 minutes, and then permeabilized with 0.1% Triton X-100 in PBS (137 mM NaCl, 3 mM KCl, 16 mM Na₂HPO₄, 3 mM KH₂PO₄) for 10 minutes. After washing in PBS, block (1% BSA and .25% Tween in PBS) was added (1 hr, RT), followed by addition of primary affinity-

purified TbHK2 polyclonal antibodies (1:1 or 1:10), which were raised against a peptide corresponding to the C-terminal end of TbHK2 (CGVGAALISAIIVADGK) (Morris et al., 2006). Basal bodies were detected using a monoclonal antibody raised against the tripartite attachment complex (MAB 22), which lies very close to basal bodies (Bonhivers et al., 2008). This antibody stains both the mature and pro-basal body. The monoclonal antibody MAB 25 was used to detect the axoneme (Absalon et al., 2007). GFP was detected using a mouse monoclonal antibody (3E6 GFP, Molecular Probes, Eugene, OR, 1:200) and glycosomes localized using a rabbit anti-*T. brucei* glycosomal antibody (2841D, (Parker et al., 1995)) raised primarily against the glycosomal proteins pyruvate phosphate dikinase, aldolase, and glyceraldehyde phosphate dehydrogenase (Parker et al., 1995) (the kind gift of Dr. Marilyn Parsons (Seattle Biomedical Research Institute, Seattle WA)). Primary antibodies were detected with FITC-conjugated goat anti-mouse antibodies or TexasRed-conjugated goat anti-rabbit (1:100, Rockland, Gilbertsville PA) secondary antibodies and visualized on a Zeiss Axiovert 200M using Axiovision software version 4.6.3 for image analysis. Live PF parasites expressing GFP were harvested by centrifugation (800 x g, 5 min), washed with vPBS, and then resuspended in an equal volume of vPBS and mounting media with DAPI.

Western blotting was performed on proteins resolved by 10% SDS-PAGE followed by transfer to a nitrocellulose support. The membrane was incubated in block (1% non-fat milk, 10 mM Tris-Cl, pH 8.0, 150 mM NaCl, 0.05% Tween-20) and either mouse anti-RGS-His₆ antibody (Qiagen, Valencia, CA) or TbHK2 antibody added (1:2000 or 1:20) in block. After washes, primary antibody was detected with horseradish

peroxidase-conjugated secondary antibody (1:10,000) in block. Membranes were developed using SuperSignal West Pico chemiluminescent substrate (Pierce Biotechnology, Inc., Rockford, IL).

DNA constructs for fusion protein expression - In order to explore the role of putative flagellar targeting sequences that impact localization, pXSGFP (Marchetti et al., 2000) was modified. First, the primers FAlDoPTS (AGCTTATGAGTAAGCGTGTGGAGGTGCTTCTTACACAGCTTG) and RAlDoPTS (CTAGCAAGCTGTGTAAGAAGCACCTCCACACGCTTACTCATA) were annealed and ligated into pXSGFP to produce pXSAlDoPTSGFP. This construct fuses the *T. brucei* aldolase gene PTS2 upstream of GFP. To engineer putative flagellar targeting sequences downstream of the GFP in pXSAlDoPTSGFP, the C-terminal 34 residues of TbHK1 or TbHK2 (including 10 amino acids upstream of the RAVLAK sequence through the end of TbHK1 or TbHK2) was amplified using the primer set FHKCTermFsigSphI (GATCGCATGCAACCGTATCCTTGGCC) and RHK1CTermFsigEcoRI (GATCGAATTCTTACTTGTCGTTACC) or RHK2CTermFsigEcoRI (GATCGAATTCTCACTTCCCGTCAGCA). After ligation to GFP lacking a stop codon (generated using FGFPNheI (GATCGCTAGCGTGAGCAAGGGCGAGGAGC) and RGFPnostopSphI (GATCGCATGCCTTGTACAGCTCGTCC)), the construct was introduced into pXSAlDoPTSGFP that lacked GFP as a result of restriction digestion to yield pXSAlDoPTSGFPHKCTerm.

Mutagenesis of the RAVLAK sequence to RAGGGK was performed with a Quickchange II site directed mutagenesis kit (Stratagene, Cedar Creek TX) using a primer set for TbHK1 (GATGTCAGGGCCGGTGGCGGAAAGGATGGCAGT and ACTGCCATCCTTTCCGCCACCGGCCCTGACATC) and TbHK2 (GATGTCAGGGCCGGTGGCGGAAAGGGTGGCAGT and ACTGCCACCCTTTCCGCCACCGGCCCTGACATC). The mutagenesis was used on pXSAl_{do}PTS_GFPHK_Cterm, pLewHK2HA, and pQE30TbHK1 to produce pXSAl_{do}PTS_GFPHK_CtermGGGmut, pLewHK2HAGGGmut, and pQE30TbHK1GGG respectively.

Expression of HA tagged TbHK2 was performed by fusing the HA tag to the C-terminus of TbHK2 followed by cloning into pLew111(2T7)GFPb (the generous gift of Drs. Shawn Motyka and Paul Englund, Johns Hopkins School of Medicine). PF 29-13 strain trypanosomes were transformed with linearized DNA and selected as described (Wang et al., 2000). Recombinant TbHK2 expression was induced in PF 29-13 cells harboring pLew111(2T7)TbHK2HA by addition of tetracycline (1 mg/ml). Fusion protein harboring an HA tag was detected in immunofluorescence using commercially available affinity purified anti-hemagglutinin (HA) epitope tag rabbit antibody (Rockland Immunochemicals, Gilbertsville, PA).

Results

Initial studies on the organization of glycolytic enzymes in *T. brucei* revealed that most TbHK activity was associated with the peroxisome-like organelles, the glycosomes

(Misset et al., 1986). Following completion of genome sequencing, it was recognized that *T. brucei* harbors two 98% identical HKs (TbHK1 and TbHK2) that have putative N-terminal peroxisomal targeting sequences (PTS2). These sequences can direct proteins to peroxisomes and glycosomes (Blattner et al., 1995). Indeed, proteomic analysis of glycosomes has confirmed that both polypeptides are components of the organelle in PF and BSF parasites (Colasante et al., 2006).

Fractionation studies suggest additional extra-glycosomal TbHK localization – The functions of TbHK1 and TbHK2 remain a mystery. Notably, recombinant TbHK1 is active as an HK *in vitro*, while recombinant TbHK2 lacks detectable HK activity and is only active when oligomerized with TbHK1 (Morris et al., 2006).

The presence of a second TbHK, TbHK2, which is inactive *in vitro*, suggests that earlier fractionation studies that followed TbHK activity might have described only the compartmentalization of TbHK1. To further explore TbHK distribution, parasite cellular components were fractionated and then analyzed by western blotting using antibodies to glycosomal-resident proteins. These include an antibody that detects both TbHK1 and 2 (Fig. 1). While glycerol kinase (GK), a known glycosome-resident protein, is released from both BSF and PF parasites at a similar digitonin concentration (~0.5 mg digitonin/mg protein), other glycolytic enzymes including TbHK release under different conditions in BSF and PF cells. In BSF parasites, TbHK and pyruvate kinase (PK) are found in the supernatant at ~0.01 mg digitonin/mg protein, co-fractionating with the cytosolic enolase (ENO) protein (Fig. 1A) (Hannaert et al., 2003). PF parasites release

HK and GK at a similar digitonin concentration, while cytosolic ENO is still released very early.

Unanticipated distribution of TbHKs has also been observed by proteomic analysis of cell fractions (Personal communication, Dr. Philippe Bastin, Pasteur Institute). TbHK2 peptides were identified in both a cell body fraction and also a flagellar fraction. While most glycosomal enzymes were under-represented in the flagella fraction, TbHK2 was modestly enriched (~2-fold), versus a ~6-fold enrichment for described flagellar-resident proteins.

Immunofluorescence studies of TbHK2 localization suggest multiple localizations –

Using an affinity purified polyclonal antibodies generated to the proximal C-terminal tail of TbHK2 yielded prominent labeling of the both BSF and PF flagellum, while labeling of glycosomes was more diffuse (Fig. 2A). To assess the impact of sample preparation on these observations, cells were blocked with either 20% FBS or 1% BSA supplemented with 0.25% Tween-20, which resulted in similar stain distribution (data not shown). To confirm that the signal was not due to a contaminating host antibody, anti-sera was generated in mice using the same antigen, again yielding primarily flagellar signal with diffuse glycosomal staining (Fig. 2A, lower image). While flagellar staining is clear, glycosomal staining is not as readily obvious, though a single image from a Z stack (Fig. 2B, upper image) layer reveals punctate staining reminiscent of glycosomal staining (Fig. 2B, lower image).

Additional experimental controls were pursued to reduce the likelihood of artifact. First, excess peptide antigen was included during primary antibody incubation, which eliminated flagellar signal (not shown). Additionally, RNAi of TbHK2 reduced the flagellar signal, though we are hesitant to over-interpret these results due to the pleiotropic (and toxic) effect of silencing TbHK2 in BSF parasites (Albert et al., 2005; Chambers et al., 2008a).

Cytoskeletal association of TbHKs – The association of signal with the flagellum led us to consider whether the staining would be preserved in cytoskeletal fractions. Upon detergent extraction of PF cells, TbHK2 signal localization was found in foci proximal to the kinetoplast DNA (Fig. 3A). Additional faint signal was detectable associated with both the flagellum and the nucleus. The weak flagellar signal, likely due to washing out of much of the antigen, suggests TbHK2 is not tightly associated with flagellar components while nuclear localization may be an artifact of the detergent extraction that allows TbHK2, which has a pI of ~9.1, to bind to DNA. Co-staining with antibodies to the axoneme [MAB 25, (Pradel et al., 2006)] suggests that TbHK2 labeling occurs primarily at the terminus of the axoneme (Fig. 3A). This structure is likely the basal body, as anti-basal body antibodies [MAB 22, (Bonhivers et al., 2008)] co-localize with anti-TbHK2 signal (Fig. 2B). Closer inspection (Fig. 3B, inset) indicates that TbHK2 co-localizes primarily with one of the two basal bodies that flank the kDNA. Similar results were observed using an alternative cytoskeletal preparation method that employs Triton X-100 in place of the NP-40 (Robinson et al., 1991). Western blotting of fractions

generated during cytoskeletal preparation supports the microscope-based finding of antigen in the cytoskeletal fraction (Fig. 3D).

To rule out the possibility that the affinity-purified polyclonal anti-TbHK2 antibodies (both rabbit and mouse) were cross-reacting with a cellular epitope that shares features with the C-terminus of TbHK2, we employed reporter epitopes fused to TbHK2 expressed from an ectopic vector (Fig. 3A). The inducible expression vector pLew111, harboring TbHK2 containing an HA epitope fused to the TbHK2 C-terminus (PTSTbHK2HA) was stably transformed into PF parasites and expression scored by IF using an antibody to HA. This epitope tagged TbHK2 also localizes in punctate foci (Fig. 3C). Last, western blotting of cell fractions using anti-TbHK2 antibodies indicates a significant portion of cross reacting signal in the cytoskeletal fraction (Fig. 3D, CS), though signal is found in the soluble fraction of the cell lysate (Fig 3D, S and longer exposure in OS), consistent with enzyme that would be released from glycosomes during the cytoskeletal preparations.

Flagellar targeting sequence analysis – How is TbHK2 targeted to the flagellum?

Comparison of the sequences of several known and predicted flagellar proteins with the sequences of TbHK1 and TbHK2 revealed a shared hexameric sequence (RAVLAK in the TbHKs) (Fig. 4A). This sequence overlaps a flagellar targeting motif found in the PFRA protein that shares high homology to a region in the dynein b heavy chain of the outer arm of *Chlamydomonas* flagellum (Bastin et al., 1999). While both *T. brucei* and *T. gambiense* HKs harbor the hexameric sequence, human glucokinase and the *S. cerevisiae*

HKs lack this sequence, which lies between the HK VI and VII domains common to all characterized HKs. Using a model of the structure of TbHK2 (Morris et al., 2006), the hexamer is positioned on an external face of the protein between the large and small HK subunits and proximal to the active site (Fig. 4B).

The putative flagellar targeting sequence alters GFP localization - To explore the role of the hexameric putative FTS sequence in targeting TbHK2 to the flagellum, we have generated GFP fusions with the sequence in live parasites (Fig. 5). These experiments have employed both transient and stable transfection of parasites with the constitutively expressed pXSGFP vector. Expression of GFP alone yielded cytosolic signal (Fig. 5, panel A), while expression of an N-terminal PTS-2 (residues 1-12 of *T. brucei* aldolase)-bearing GFP led to focusing of the fluorescence into punctate bodies that are consistent with glycosomal localization [Fig. 5, panel B, and (Parker et al., 1995)]. Co-localization was confirmed using fixed cells probed with anti-GFP and anti-glycosomal antibodies (Parker et al., 1995) (data not shown). When the terminal 34 residues of TbHK2 (starting ten amino acids upstream of the RAVLAK and extending to the end of the TbHK2 ORF) were fused to the C-termini of the PTS2-bearing GFP (to yield pXSPTSGFPHKC-terminus), signal was found distributed throughout the cell, but partially localized proximal to the flagellum (Fig. 5, panel C, indicated by the arrows). This localization is not as clear as that provided with the TbHK2 antibody, perhaps because the construct contains only a portion of the TbHK2 sequence (the overall context in which the RAVLAK is presented possibly influences targeting). Notably, altering the

RAVLAK sequence (to RAGGGK) changes the over-all localization (Fig. 5, panel D), with signal limited to glycosomes. However, altering the RAVLAK sequence to RAGGGK does not impact the catalytic properties of recombinant TbHK1 (not shown), suggesting that *in vitro* folding is not dramatically altered in the RAGGGK variant.

The FTS from characterized and presumptive flagellar proteins, including TbPFR-A, is not a C-terminal extension, but rather is an internal signal sequence (Fig. 4A). Fusion of the putative TbHK FTS hexamer to the C-termini of PTS2-bearing GFP indicates that this rule holds true for the TbHKs, as fluorescence from this construct is limited to glycosomes (not shown). This observation suggests that the environment in which the RAVLAK is situated is important for imparting flagellar localization.

Discussion

The association of glycolytic proteins with flagellum is not without precedence, as enzymes involved in glucose metabolism have been found in the flagellum from a range of organisms, including green algae and mammals (Mitchell et al., 2005; Travis et al., 1998). The role of these proteins has primarily been postulated to be in the production of energy for the flagellum. Is TbHK2 serving a similar role in the trypanosome flagellum? TbHK2 is competent for HK activity when organized with TbHK1 into oligomers (Chambers et al., 2008b), although it is not known if TbHK1 is also found in the parasite flagellum in a position to interact with TbHK2. Notably, the polyclonal antibody raised against the C-terminal tail of TbHK2, while specific to the denatured TbHK2 antigen (as determined by western blotting, (Morris et al., 2006)), may cross-react with both native

TbHK1 and TbHK2. The native C-terminal epitope is predicted to form an α -helix with one face of the helix being identical in both TbHK1 and 2, suggesting that the polyclonal antibody may recognize that common feature in native proteins. This suggestion is supported by cross-reacting flagellar signal detected in cell lacking TbHK2 [TbHK2^{-/-}, (Morris et al., 2006), data not shown] and by the presence of the conserved FTS in TbHK1.

If TbHK2 is indeed oligomerized with TbHK1 in the flagellum, it may be playing some role in the regulation of TbHK activity [as seen *in vitro*, (Chambers et al., 2008b)]. To yield ATP through the activity of TbHKs, this model would require that other components of the glycolytic pathway reside near the flagellum (Fig. 6). Consistent with that, pyruvate kinase (this work, Fig. 1), glycerol-3-phosphate dehydrogenase, and glyceraldehyde-3-phosphate dehydrogenase (Oberholzer et al., 2007) have all been found associated with the trypanosome flagellum. Alternatively, flagellar TbHK2 may participate in the metabolism of sugar nucleotides to generate ATP – an activity that has been demonstrated *in vitro* with other HKs (Gamble and Najjar, 1955), but which remains undetected with recombinant TbHKs.

TbHK2 may not be limited to a metabolic function in the flagellum, but rather the protein may play a role in glucose sensing in the flagellum. Glucokinases and HKs from other systems, including yeast, plants, and animals, have all been shown to be central in conveying information to the cell regarding environmental glucose availability that allow the cell to respond (Rolland et al., 2001). In other kinetoplastids, hexose transporters have been found associated with the flagellum (Snapp and Landfear, 1999), suggesting

that uptake of glucose may occur proximal to the flagellar positioning of TbHK2, positioning it to serve in an environmental glucose sensing role. In *T. brucei*, signaling enzymes associated with the flagellum is not without precedence, as an adenylate cyclase (ESAG4) has been found proximal to the flagellum in both PF and BSF parasites (Paindavoine et al., 1992).

Cell fractionation studies suggest that extra-glycosomal localization of TbHK2 (and PK) is limited to the BSF lifecycle stage (Fig. 1). This data appears to contradict the IFA data of PF parasites stained with the TbHK2 polyclonal antibody, which yields both glycosomal and flagellar signal (Fig. 2). Differences in the relative abundance of the protein in the two compartments between the two lifecycles may explain this, as the intensity of glycosomal staining is greater in PF parasites than BSF parasites. This suggests that the total distribution of TbHK2 is different between the two lifecycle stages, with the protein being predominantly flagellar in BSF parasites while being mostly glycosomal in PF parasites.

Previously, we found that TbHK2 expressed in PF parasites with a GFP C-terminal fusion was glycosomally localized (Morris et al., 2006). While the bulky GFP reporter likely interferes with the C-terminal FTS (see Fig. 4 for positioning of the FTS), this observation raises the possibility that TbHK2 flagellar localization requires an obligate transit step through the glycosome. PTS2 deficient HKs tagged with fluorescent proteins are cytosolic (data not shown), supporting this suggestion. Potentially adding to the complexity of targeting to the flagellum, the unusual hexamerization of TbHKs,

which is dynamic and subject to environmental cues (Chambers et al., 2008b), may influence localization.

Acknowledgements

The authors would like to thank Philippe Bastin for thoughtful contribution to this work.

References

Absalon, S., Kohl, L., Branche, C., Blisnick, T., Toutirais, G., Rusconi, F., Cosson, J., Bonhivers, M., Robinson, D. and Bastin, P. (2007). Basal body positioning is controlled by flagellum formation in *Trypanosoma brucei*. *PLoS ONE* **2**, e437.

Albert, M. A., Haanstra, J. R., Hannaert, V., Van Roy, J., Opperdoes, F. R., Bakker, B. M. and Michels, P. A. (2005). Experimental and *in silico* analyses of glycolytic flux control in bloodstream form *Trypanosoma brucei*. *J Biol Chem* **280**, 28306-15.

Bastin, P., MacRae, T. H., Francis, S. B., Matthews, K. R. and Gull, K. (1999). Flagellar morphogenesis: protein targeting and assembly in the paraflagellar rod of trypanosomes. *Mol Cell Biol* **19**, 8191-200.

Biebinger, S., Wirtz, L. E., Lorenz, P. and Clayton, C. (1997). Vectors for inducible expression of toxic gene products in bloodstream and procyclic *Trypanosoma brucei*. *Mol Biochem Parasitol* **85**, 99-112.

Blattner, J., Dorsam, H. and Clayton, C. E. (1995). Function of N-terminal import signals in trypanosome microbodies. *FEBS Lett* **360**, 310-4.

Bonhivers, M., Landrein, N., Decossas, M. and Robinson, D. R. (2008). A monoclonal antibody marker for the exclusion-zone filaments of *Trypanosoma brucei*. *Parasit Vectors* **1**, 21.

Brun, R. and Shonenberger, M. (1979). Cultivation and *in vitro* cloning of procyclic culture forms of *Trypanosoma brucei* in a semi-defined medium. *Acta Tropica* **36**, 289-292.

Chambers, J. W., Fowler, M. L., Morris, M. T. and Morris, J. C. (2008a). The anti-trypanosomal agent lonidamine inhibits *Trypanosoma brucei* hexokinase 1. *Mol Biochem Parasitol* **158**, 202-7.

Chambers, J. W., Kearns, M. T., Morris, M. T. and Morris, J. C. (2008b). Assembly of heterohexameric trypanosome hexokinases reveals that hexokinase 2 is a regulable enzyme. *J Biol Chem* **283**, 14963-70.

Chambers, J. W., Morris, M. T., Smith, K. S. and Morris, J. C. (2008c). Residues in an ATP binding domain influence sugar binding in a trypanosome hexokinase. *Biochem Biophys Res Commun* **365**, 420-5.

- Colasante, C., Ellis, M., Ruppert, T. and Voncken, F.** (2006). Comparative proteomics of glycosomes from bloodstream form and procyclic culture form *Trypanosoma brucei brucei*. *Proteomics* **6**, 3275-93.
- Field, M. C., Allen, C. L., Dhir, V., Goulding, D., Hall, B. S., Morgan, G. W., Veazey, P. and Engstler, M.** (2004). New approaches to the microscopic imaging of *Trypanosoma brucei*. *Microsc Microanal* **10**, 621-36.
- Fleige, T., Fischer, K., Ferguson, D. J., Gross, U. and Bohne, W.** (2007). Carbohydrate metabolism in the *Toxoplasma gondii* apicoplast: localization of three glycolytic isoenzymes, the single pyruvate dehydrogenase complex, and a plastid phosphate translocator. *Eukaryot Cell* **6**, 984-96.
- Gamble, J. L. and Najjar, V. A.** (1955). Studies of the kinetics of the reverse reaction of yeast hexokinase. *J Biol Chem* **217**, 595-601.
- Ginger, M. L., Ngazoa, E. S., Pereira, C. A., Pullen, T. J., Kabiri, M., Becker, K., Gull, K. and Steverding, D.** (2005). Intracellular positioning of isoforms explains an unusually large adenylate kinase gene family in the parasite *Trypanosoma brucei*. *J Biol Chem* **280**, 11781-9.
- Haanstra, J. R., van Tuijl, A., Kessler, P., Reijnders, W., Michels, P. A., Westerhoff, H. V., Parsons, M. and Bakker, B. M.** (2008). Compartmentation prevents a lethal turbo-explosion of glycolysis in trypanosomes. *Proc Natl Acad Sci U S A* **105**, 17718-23.
- Hannaert, V., Albert, M. A., Rigden, D. J., da Silva Giotto, M. T., Thiemann, O., Garratt, R. C., Van Roy, J., Opperdoes, F. R. and Michels, P. A.** (2003). Kinetic characterization, structure modelling studies and crystallization of *Trypanosoma brucei* enolase. *Eur J Biochem* **270**, 3205-13.
- Krishnamurthy, G., Vikram, R., Singh, S. B., Patel, N., Agarwal, S., Mukhopadhyay, G., Basu, S. K. and Mukhopadhyay, A.** (2005). Hemoglobin receptor in Leishmania is a hexokinase located in the flagellar pocket. *J Biol Chem* **280**, 5884-91.
- Marchetti, M. A., Tschudi, C., Kwon, H., Wolin, S. L. and Ullu, E.** (2000). Import of proteins into the trypanosome nucleus and their distribution at karyokinesis. *J Cell Sci.* **113** (Pt 5), 899-906.
- Miki, K., Qu, W., Goulding, E. H., Willis, W. D., Bunch, D. O., Strader, L. F., Perreault, S. D., Eddy, E. M. and O'Brien, D. A.** (2004). Glyceraldehyde 3-phosphate dehydrogenase-S, a sperm-specific glycolytic enzyme, is required for sperm motility and male fertility. *Proc Natl Acad Sci U S A* **101**, 16501-6.
- Misset, O., Bos, O. J. and Opperdoes, F. R.** (1986). Glycolytic enzymes of *Trypanosoma brucei*. Simultaneous purification, intraglycosomal concentrations and physical properties. *Eur. J. Biochem.* **157**, 441-53.
- Mitchell, B. F., Pedersen, L. B., Feely, M., Rosenbaum, J. L. and Mitchell, D. R.** (2005). ATP production in *Chlamydomonas reinhardtii* flagella by glycolytic enzymes. *Mol Biol Cell* **16**, 4509-18.
- Morris, M. T., DeBruin, C., Yang, Z., Chambers, J. W., Smith, K. S. and Morris, J. C.** (2006). Activity of a second *Trypanosoma brucei* hexokinase is controlled by an 18-amino-acid C-terminal tail. *Eukaryot Cell* **5**, 2014-23.

- Nakamura, N., Shibata, H., O'Brien, D. A., Mori, C. and Eddy, E. M.** (2008). Spermatogenic cell-specific type 1 hexokinase is the predominant hexokinase in sperm. *Mol Reprod Dev* **75**, 632-40.
- Oberholzer, M., Bregy, P., Marti, G., Minca, M., Peier, M. and Seebeck, T.** (2007). Trypanosomes and mammalian sperm: one of a kind? *Trends Parasitol* **23**, 71-7.
- Oppendoes, F. R. and Borst, P.** (1977). Localization of nine glycolytic enzymes in a microbody-like organelle in *Trypanosoma brucei*: the glycosome. *FEBS Lett.* **80**, 360-4.
- Paindavoine, P., Rolin, S., Van Assel, S., Geuskens, M., Jauniaux, J. C., Dinsart, C., Huet, G. and Pays, E.** (1992). A gene from the variant surface glycoprotein expression site encodes one of several transmembrane adenylate cyclases located on the flagellum of *Trypanosoma brucei*. *Mol Cell Biol* **12**, 1218-25.
- Parker, H. L., Hill, T., Alexander, K., Murphy, N. B., Fish, W. R. and Parsons, M.** (1995). Three genes and two isozymes: gene conversion and the compartmentalization and expression of the phosphoglycerate kinases of *Trypanosoma (Nannomonas) congolense*. *Mol. Biochem. Parasitol.* **69**, 269-79.
- Pradel, L. C., Bonhivers, M., Landrein, N. and Robinson, D. R.** (2006). NIMA-related kinase TbNRKC is involved in basal body separation in *Trypanosoma brucei*. *J Cell Sci* **119**, 1852-63.
- Robinson, D., Beattie, P., Sherwin, T. and Gull, K.** (1991). Microtubules, tubulin, and microtubule-associated proteins of trypanosomes. *Methods Enzymol* **196**, 285-99.
- Rolland, F., Winderickx, J. and Thevelein, J. M.** (2001). Glucose-sensing mechanisms in eukaryotic cells. *Trends Biochem Sci* **26**, 310-7.
- Snapp, E. L. and Landfear, S. M.** (1999). Characterization of a targeting motif for a flagellar membrane protein in *Leishmania enriettii*. *J Biol Chem* **274**, 29543-8.
- Travis, A. J., Foster, J. A., Rosenbaum, N. A., Visconti, P. E., Gerton, G. L., Kopf, G. S. and Moss, S. B.** (1998). Targeting of a germ cell-specific type 1 hexokinase lacking a porin-binding domain to the mitochondria as well as to the head and fibrous sheath of murine spermatozoa. *Mol Biol Cell* **9**, 263-76.
- Wang, Z., Morris, J. C., Drew, M. E. and Englund, P. T.** (2000). Inhibition of *Trypanosoma brucei* gene expression by RNA interference using an integratable vector with opposing T7 promoters. *J. Biol. Chem.* **275**, 40174-9.
- Xu, K. Y. and Becker, L. C.** (1998). Ultrastructural localization of glycolytic enzymes on sarcoplasmic reticulum vesticles. *J Histochem Cytochem* **46**, 419-27.

Figure Legends

Figure 1. Subcellular distribution of glycolytic enzymes analyzed by digitonin-dependent cell fractionation. Intact bloodstream and procyclic-form trypanosomes were incubated for 4 min with increasing concentrations of digitonin indicated as described in the Materials and Methods. Release of enolase (ENO), glycerol kinase (GK), hexokinase (HK), and pyruvate kinase (PYK) from BSF (A.) or PF (B.) cells were assayed after centrifugation of treated cell suspensions and preparation of western blots of the supernatants. Total release (T.R.) lanes correspond to cells incubated with 0.5% Triton X-100 to solubilize all membranes.

Figure 2. Flagellar localization of TbHK2 in BSF and PF parasites. (A) Immunofluorescence using affinity-pure polyclonal sera from mouse (top) or rabbit (bottom) that had been immunized using the C-termini of TbHK2 as antigen. BSF 90-13 or PF 29-13 were fixed, permeabilized, and stained with primary antibodies (1:1), which were detected with FITC (green)-conjugated goat anti-mouse or mouse anti-rabbit antibodies, respectively. DAPI (blue) was added with anti-fade reagent to stain the nucleus and kDNA. (B) A Z-stack of TbHK2 stained BSF 90-13 cells was captured and an extended focus image was produced to show the signal throughout the parasite (top). To illustrate glycosome-like bodies (arrows), which are lost when an extended focus image is produced from the Z-stack layers, a single Z-stack layer (bottom) is included. Scale bar = 10 mm.

Figure 3. Immunofluorescence of PF cytoskeleton preparations reveal TbHK2 association with the basal body. (A) PF cytoskeletons were stained with affinity-purified rabbit antibodies against TbHK2 (red) and a mouse monoclonal antibody to the axoneme (MAB 25, green (Absalon et al., 2007)), and texas red or FITC-conjugated species-specific secondary antibodies used to visualize localization. (B) Dual immunofluorescence of PF cytoskeleton preparations using the affinity-purified rabbit TbHK2 antibodies (red) and Mab22 (a monoclonal antibody raised against the tripartite attachment complex, which lies near the basal bodies, green (Bonhivers et al., 2008)). The boxed region was enlarged in the image below each figure to more readily view basal body and TbHK2 co-localization. The overall signal is reduced for the anti-TbHK2 staining, in part due to the alteration to fix and block schemes required for Mab22 localization. (C) Immunofluorescence of cytoskeletons from PF29-13 parasites induced to over-express TbHK2 with a C-terminal HA tag from pLew111(2T7)TbHK2HA. The HA tag was detected using an affinity purified anti-hemagglutinin (HA) epitope tag rabbit antibody (Rockland Immunochemicals, Gilbertsville, PA) diluted 1:1000 in block (1% BSA, 0.25% Tween in 1 x PBS) The scale bar = 10 mm throughout this figure. (D) Western blot of PF cytoskeleton preparation. The lanes are as follows: CS – cytoskeleton fraction, S – supernatant of cytoskeleton preparation, WC – whole cells, rTbHK2 – recombinant TbHK2 protein, and OS – over-exposure of the supernatant lane.

Figure 4. TbHKs harbor a sequence that is conserved in other known and predicted flagellar proteins. (A.) Alignment of TbHK1 and TbHK2 FTS with known and

hypothetical flagellar proteins using Clustal W1.8 from MyHits SIB (Swiss Institute of Bioinformatics). (B) The TbHK2 model (based on the yeast crystal structure (Chambers et al., 2008c), with the peroxisomal targeting 2 sequence (PTS2), putative FTS, and 18 residue carboxy terminus noted.

Figure 5. The putative FTS directs GFP to extraglycosomal localizations, including the flagellum. (A) PF2913 parasites harboring pXSGFP express GFP from a constitutively active transgene. (B) Expression of GFP with the PTS2 sequence from *T. brucei* aldolase (pXSAldoPTSGFP). (C) GFP harboring an N-terminal aldolase PTS2 fusion and a C-terminal fusion to the terminal 34 residues of TbHK2 (TbHK2pXSAldoPTSGFPHKC-terminus). The flagellum is indicated by the white arrow. (D) A variant GFP harboring the N-terminal PTS2 and a mutated version of the terminal 34 residues of TbHK2 (VLA to GGG), expressed from pXSAldoPTSGFPHKC-term mut. The scaled bar = 10 μ m.

Figure 6. Schematic illustrating possible functions of TbHK2 while proximal to the flagellum in *T. brucei*.

Fig 1.

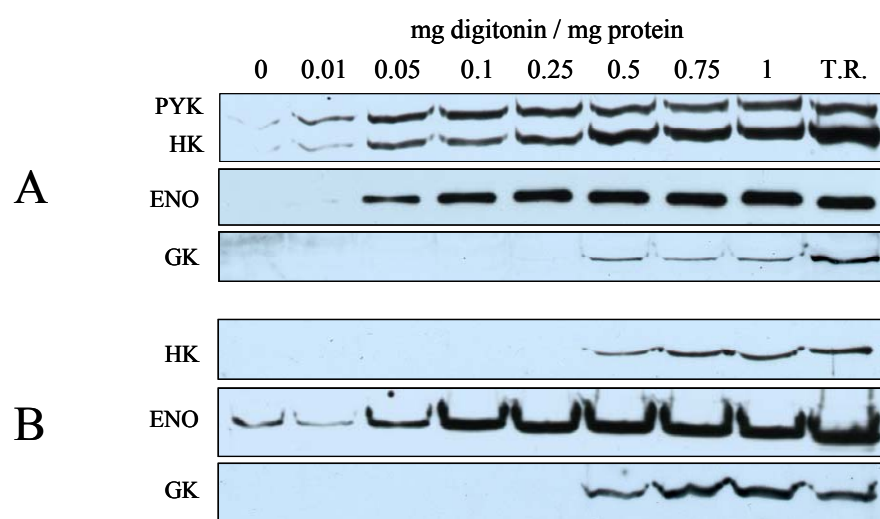


Fig 2.

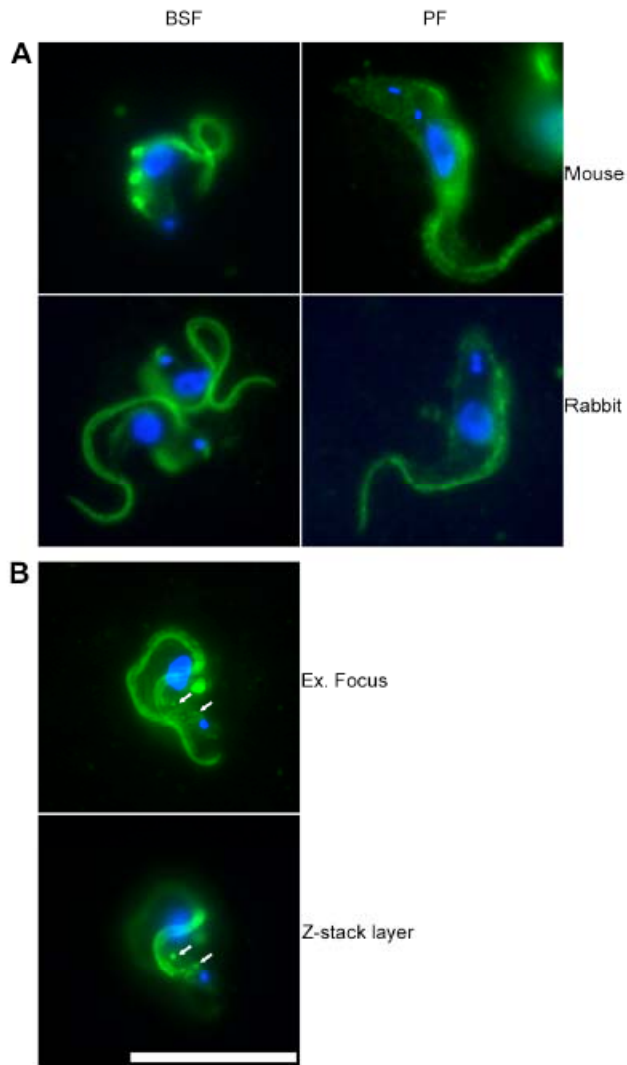


Fig 3.

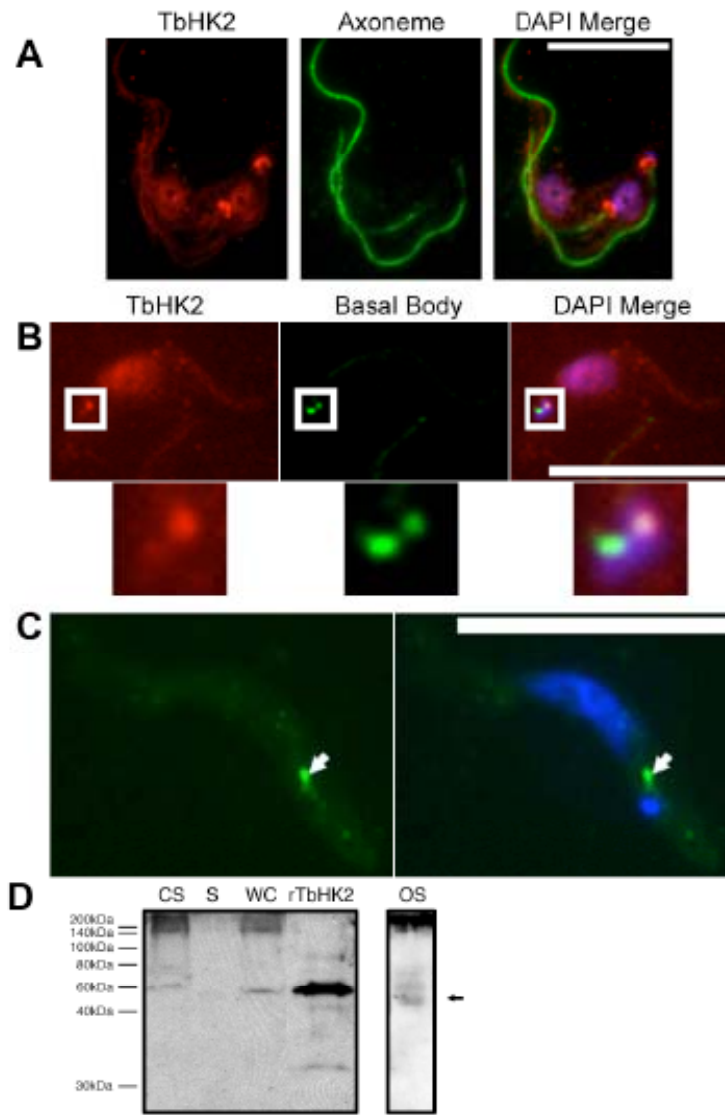


Fig 4.

A

TbHK1	443	PECDVRAVLAKDGSGI
TbHK2	443	PECDVRAVLAKGGSGV
TbPFR-A	556	KMVEYRAHLAKQEEVK
TbPAR4	511	REMEVREQLALETETQ
TbDIGIT	1167	EIASQRAELARLNEIA
TbPutROD	552	VEDEERKVLKKSIVLE
TbPIFTB2	603	CFLALAMHLAKHMVVL
TbTRYPARP	405	AGTSMFPHLAVSRQEY

*

B

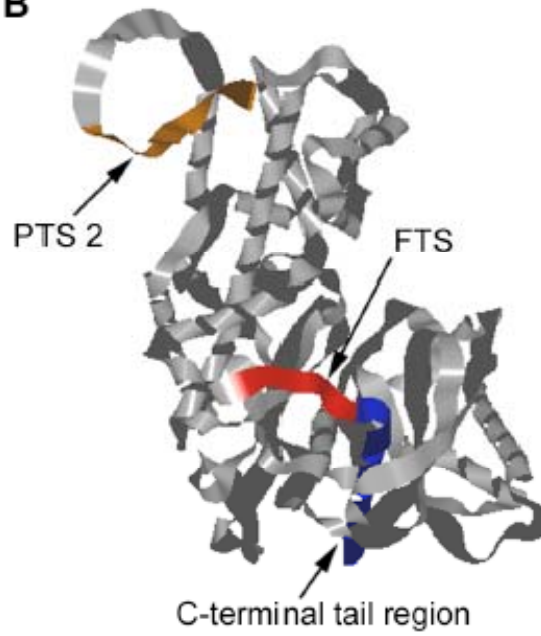


Fig 5.

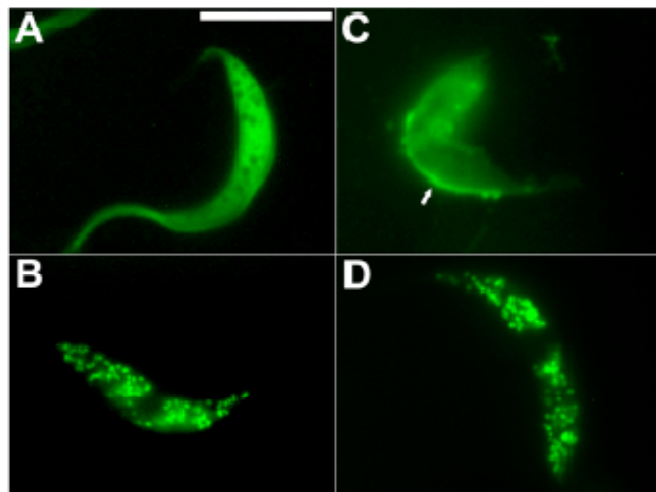
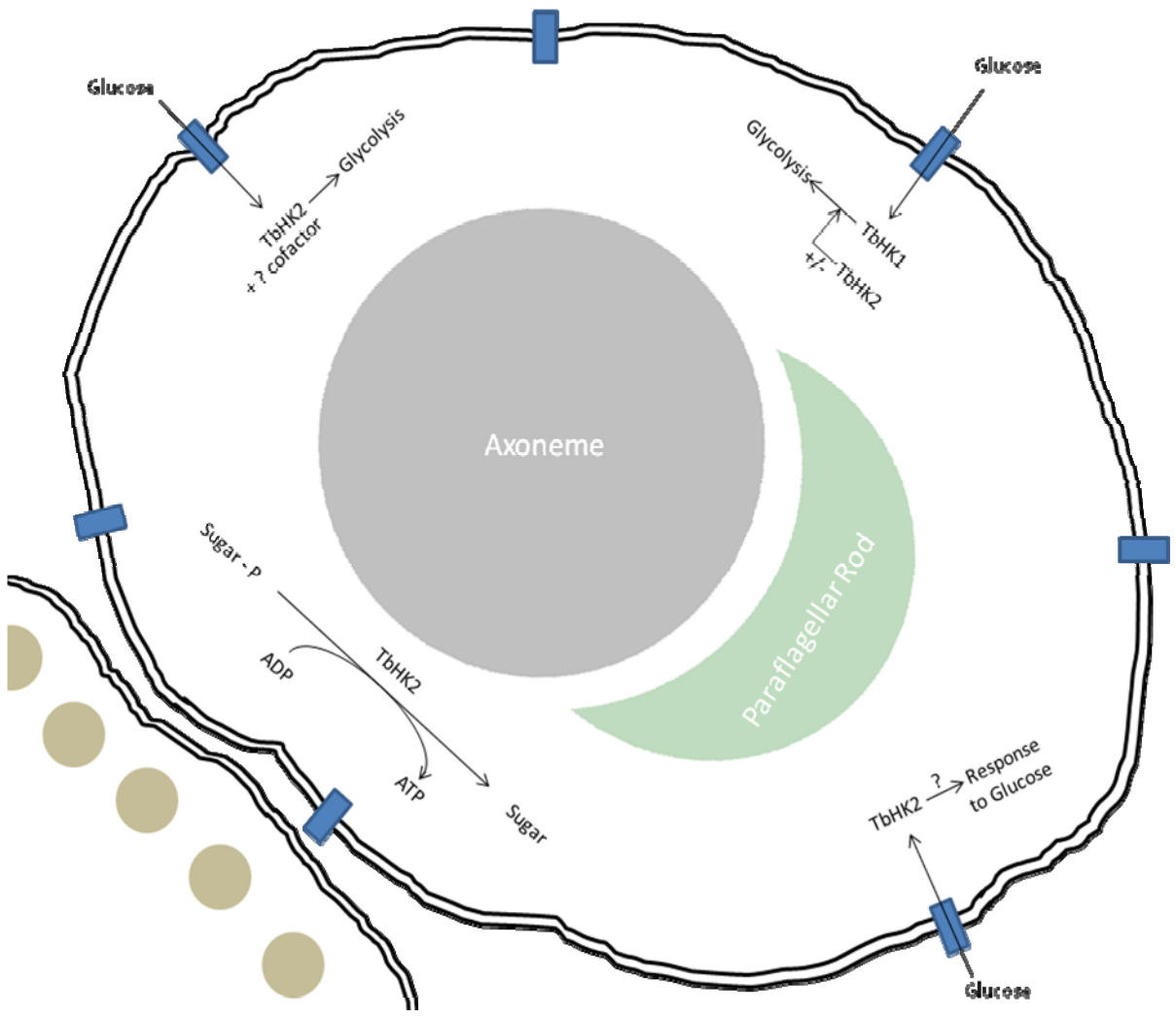


Fig 6.



CHAPTER FIVE

CONCLUSION CHAPTER

The use of TbHK inhibitors as drug therapies for HAT is still under development. However, great strides in target-driven drug development have been accomplished. The efficacy of TbHK inhibitors against HAT has been demonstrated against *in vitro* parasite culture, but more work including *in vivo* parasite experiments will need to be completed to confirm the value of these compounds as therapeutic leads. The ability of a compound to kill parasites in culture does not directly correlate with the same compound's ability to kill parasites found within a mammalian host. Problems including delivery difficulties as a consequence of solubility and toxic side-effects can arise when *in vivo* studies are performed.

There are many unusual questions that arise from the finding of TbHK2 in the flagellum. These include: How does TbHK2 localize to the flagellum? The putative flagellar targeting sequence found on TbHK1 and TbHK2 may be involved in flagellar localization but the route to the flagellum is still unknown. What role does TbHK2 play in the flagellum? TbHK2 could act as a functional hexokinase, TbHK2 could work in the reverse reaction to generate ATP or TbHK2 could be an environmental glucose sensor in the flagellum. Does TbHK2 have a different role in the flagellum than its role in the rest of the cell bodies? TbHK2 may act differently in the glycosome, cytoplasm, and flagellum.

The future is promising for finding a role of TbHK2. TbHK2 may be a vital target for HAT therapies just as TbHK1 has shown very promising results. A therapy for HAT may prove most effective when both TbHK1 and TbHK2 activities are disrupted.

If I was to continue my work at Clemson University, I would attempt to observe the localization of TbHK1. I find it intriguing that both TbHKs have a PTS2 and a FTS. The localization of TbHK1 may elucidate the role of TbHKs in the flagellum even further. Also, I would take the HTS to the next step, mice. The ability of the compounds to kill parasites may be different when observing cell death in culture versus within a mammalian host. And if a compound is found to be promising then pharmacology work would need to be conducted to be able to treat HAT patients.

Overall, the parasite *T. brucei* is an exciting organism to perform research into the realm of biology but the true focus of the research should never be forgotten. The people of sub-Saharan Africa are still influenced by the occurrence of *T. brucei*. In time there will be a solution to the problem. Unfortunately the work is not fast enough. People are dying today. All that is left is the burning question: Will the future ever hold a day when HAT is considered a nuisance instead of a fatal disease?

APPENDICES

Published in Experimental Parasitology 2009 Aug 6 [Epub ahead of print]

PMID: 19647733

Appendix A

TRYPANOSOMA BRUCEI AMP-ACTIVATED KINASE SUBUNIT HOMOLOGS
INFLUENCE SURFACE MOLECULE EXPRESSION

Clarice S. Clemmens^a, Meredith T. Morris^a, Todd A. Lyda^a, Alvaro Acosta-Serrano^{b,1},
and James C. Morris^{a*}

^a*Department of Genetics and Biochemistry, Clemson University, Clemson South Carolina
29634*

^b*Wellcome Centre for Molecular Parasitology, University of Glasgow, Glasgow G12
8TA, UK*

*Corresponding Author:

214 Biosystems Research Complex

51 New Cherry Street, Clemson SC 29634

Tel. (864) 656-0293; FAX (864) 656-0393, E-Mail: jmorri2@clemson.edu

¹Current Address: Liverpool School of Tropical Medicine, Liverpool L3 5QA, UK

FOOTNOTES¹

Abbreviations used: AMPK, AMP-activated kinase; Con A, concanavalin A; aq. HF, aqueous hydrofluoric acid; MALDI-TOF MS, matrix-assisted laser desorption ionization-time of flight mass spectrometry; PF, procyclic form trypanosome; RNAi, RNA interference; TbAMPK β , *T. brucei* homolog of AMP-dependent kinase β subunit; TbAMPK γ , *T. brucei* homolog of AMP-dependent kinase γ subunit; tet, tetracycline;

ABSTRACT

The African trypanosome, *Trypanosoma brucei*, can gauge its environment by sensing nutrient availability. For example, procyclic form (PF) trypanosomes monitor changes in glucose levels to regulate surface molecule expression, which is important for survival in the tsetse fly vector. The molecular connection between glycolysis and surface molecule expression is unknown. Here we partially characterize *T. brucei* homologs of the β and γ subunits of the AMP-activated protein kinase (AMPK), and determine their roles in regulating surface molecule expression. Using flow cytometry and mass spectrometry, we found that TbAMPK β or TbAMPK γ -deficient parasites express both of the major surface molecules, EP- and GPEET-procyclicin, with the latter being a form that is expressed when glucose is low such as in the tsetse fly. Last, we have found that the putative scaffold component of the complex, TbAMPK β , fractionates with organellar components and colocalizes in part with a glycosomal marker as well as the flagellum of PF parasites.

Key Words. *Trypanosoma brucei*, African trypanosome, nutrient sensing, procyclins, mass spectrometry.

INTRODUCTION

Trypanosoma brucei, the protozoan parasite that causes African sleeping sickness, is a hemoflagellate that is transmitted to its mammalian host by the bite of an infected tsetse fly. In the mammalian infection, trypanosomes proliferate within the blood as long slender forms and can differentiate into short stumpy forms that are pre-adapted for life in the insect. When the insect ingests short stumpy trypanosomes during a blood meal, the parasites differentiate into procyclic form parasites (PF¹) in the fly midgut (Vickerman, 1985). After about 3 weeks, they are found in the salivary glands where they develop into metacyclic forms that are infectious to mammals.

The PF parasites are covered by a coat consisting of members of the procyclin family of glycoproteins (Matthews and Gull, 1994, Roditi, et al., 1989, Ziegelbauer, et al., 1990). The GPI-anchored procyclins, EP-procyclins and GPEET-procyclin, have at their C-terminus 22-30 Glu-Pro repeats (EP-procyclin) or five or six Gly-Pro-Glu-Glu-Thr repeats followed by three EP repeats (GPEET-procyclin) (Mowatt and Clayton, 1987, Mowatt, et al., 1989, Richardson, et al., 1988, Roditi, et al., 1987). The different isoforms of procyclins have different features. For example, EP1-1, EP1-2, and EP3 are *N*-glycosylated with a homogeneous Man₅GlcNAc₂ while EP2 is unglycosylated (Acosta-Serrano, et al., 1999, Hwa, et al., 1999, Treumann, et al., 1997). GPEET is unglycosylated but is phosphorylated at the threonine residues (Butikofer, et al., 1999, Mehlert, et al., 1999). Expression of procyclins can be influenced by culture conditions *in vitro*. Glycerol in the culture medium triggers GPEET expression, as can growth in glucose-depleted (~ 0.03 mM) medium (Butikofer, et al., 1997, Morris, et al., 2002,

Treumann, et al., 1997). Early in the *in vitro* differentiation of bloodstream forms to PFs, both types of procyclins are expressed (Vassella, et al., 2001). GPEET expression increases in the first 24 hours, to be replaced by glycosylated EP-procyclins later in development (Vassella, et al., 2001). A similar program of expression has been observed in parasites isolated from tsetse fly infections, though insufficient parasites were available for analysis prior to day 3 of the infection (Acosta-Serrano, et al., 2001, Vassella, et al., 2000). Although the function of the different procyclin isoforms remains to be determined (Vassella, et al., 2009), it is suggested that its polyionic nature may help the parasite to resist attack by tsetse midgut proteases (Acosta-Serrano, et al., 2001).

Previously, we screened an RNAi-based genomic library for cells resistant to the lectin concanavalin A (Con A), which binds the *N*-glycan on EP-procyclins and induces cell death (Hwa, et al., 1999, Pearson, et al., 2000, Welburn, et al., 1996). We found that glycolysis (or the rate of glycolytic flux) was a regulator of procyclin expression. Under conditions in which the rate of glycolysis was reduced, EP-procyclin expression was repressed, while GPEET-procyclin expression was upregulated.

Complicating the connection between glucose metabolism and surface molecule expression is the compartmentalization of a majority of glycolysis in peroxisome-like organelles, the glycosomes. This compartmentalization suggests that some extra-glycosomal metabolic sensor may be involved in the transmission of information about glycolysis to the nucleus. To resolve the components that connect glucose metabolism and surface molecule expression, we have used reverse genetics to characterize genes that were predicted to be involved in glucose sensing based on observations from other

systems. In other organisms, AMP-activated kinase (AMPK), a heterotrimeric enzyme complex consisting of α , β , and γ subunits, is a key regulator in nutrient sensing (reviewed in (Carling, 2004)). The α subunit contains a kinase domain as well as a regulatory domain that inhibits the enzyme in the absence of AMP (Crute, et al., 1998). The β subunit acts as a scaffold for the other components, while the γ subunit is thought to be involved in AMP binding (Cheung, et al., 2000).

AMPK is a member of the AMPK/SNF1 family, which has been described in many eukaryotes (Hardie, et al., 1998, Hardie and Hawley, 2001, Kemp, et al., 1999) and acts in nutrient sensing pathways in yeast and mammals. Under conditions that reduce glycolysis, the yeast SNF1 complex (a homolog of AMPK (Carlson, 1999)) is activated. This kinase modulates the cellular response to decreased glycolysis by phosphorylating (and activating) metabolic enzymes, including glycolytic enzymes such as hexokinase. Similarly, low glucose conditions activate mammalian AMPK (Salt, et al., 1998), which triggers changes in gene expression, including increase in expression of metabolic genes involved in glycolysis (reviewed in (Hardie and Hawley, 2001)).

While the α subunit remains elusive, we have identified homologous genes for the β and γ subunits (TbAMPKb and TbAMPKg, respectively) of the heterotrimeric components (α , β , and γ) of AMPK in *T. brucei* and have explored the role of these genes in the regulation of surface molecule expression in response to glucose levels. Silencing these genes triggers changes in surface molecule expression, while localization of the scaffold (β) subunit suggests positioning in the cell consistent with a role as an intermediary between surface molecule expression and glycolysis.

MATERIALS AND METHODS

Trypanosome growth and RNAi. PF 29-13 *T. brucei*, a 427 strain that expresses T7 RNA polymerase and the tetracycline repressor, were grown in SDM-79 as described (Wang, et al., 2000, Wirtz, et al., 1999). Low glucose SDM-79 was prepared with glucose-free RPMI 1640 replacing the liquid MEM. Also, additional glucose and glucosamine (normally present in SDM-79 at 1 mg/ml and 50 ng/ml, respectively) were omitted. This mixture was supplemented with normal FBS (10%), resulting in a final glucose concentration of ~ 0.5 mM.

RNAi constructs were generated by ligation of *TbAMPK β* (276 bp, from nt 436 to 711 of the open reading frame) or *TbAMPK γ* (461 bp, from nt 895 to 1356) PCR products amplified from *T. brucei* strain 427 genomic DNA into *XhoI/HindIII* cut pZJM (Wang, et al., 2000). Parasites (1×10^8) were transformed with 10 mg *NotI* linearized pZJM(AMPKb) or pZJM(AMPKg) and stable integrants selected with phleomycin (2.5 mg/ml) as described (Wang, et al., 2000). RNAi was induced by the addition of tetracycline (tet, 1 mg/ml) to cultures.

Flow cytometry and surface glycoprotein labeling. Parasites were labeled with fluorescein-conjugated Con A as described (Morris, et al., 2002). Briefly, cells (1×10^6) were resuspended in 1 ml cytomix supplemented with 1 mM $MnCl_2$ (cytoM (van den Hoff, et al., 1992)) containing 10 mg/ml FITC-labeled Con A (Sigma, St. Louis, MO). After 15 min at room temperature, trypanosomes were applied to a FACScan flow

cytometer (Becton Dickinson Biosciences, Franklin Lakes, NJ) and 10,000 cells analyzed per sample. Antibody labeling of surface molecules was performed using 5×10^6 parasites that were washed in PBS, fixed in 4% paraformaldehyde/0.1% glutaraldehyde (12 hr, 4°C), and washed in 1% BSA in PBS (blocking solution). Antibodies to EP-procycalin (monoclonal antibody TBRP1/247, Cedarlane Laboratories, Ontario Canada (Richardson, et al., 1988, Richardson, et al., 1986)) or GPEET-procycalin (monoclonal 5H3 (Butikofer, et al., 1999)), which was a generous gift from Dr. Terry Pearson (University of British Columbia) were diluted (1:100) and incubated with cells (1hr, 4°C) in blocking solution. Parasites were washed, incubated in FITC-conjugated goat anti-mouse antibody (1 hr, 4°C in blocking solution), and then resuspended in sheath fluid for flow cytometry.

MALDI-TOF-MS analysis of procyclins. For mass-spectrometry analysis, procyclins were purified from freeze-dried parasites (1×10^8) by sequential extraction with organic solvents (Acosta-Serrano, et al., 1999). To remove GPI anchors from polypeptides, dry butanolic extracts were dephosphorylated with 25 μ l of 48% aqueous hydrofluoric acid (aq. HF) for 20 h at 0 °C. After treatment, samples were dried in a Speed-Vac and resuspended in 20 μ l of 0.1% TFA. An aliquot ($\sim 0.5 \mu$ l; $\sim 5 \times 10^6$ parasite equivalents) was co-crystallized with 0.5 μ l 10 mg/ml sinapinnic acid in 70 % acetonitrile, 0.1 % TFA and analyzed by positive-ion mode. Data collection was in linear mode on a PerSeptive Biosystems Voyager-DE mass spectrometer (located at the Sir Henry Wellcome Functional Genomics Facility, Glasgow University). The accelerating

voltage was 2500 V and the grid voltage was set at 91 % with an extraction time delay of 100 nsec. Data were collected manually at 200 shots per spectrum, with laser intensity set at 2800. To confirm assignments, HF-treated samples ($\sim 5 \times 10^7$ parasite equivalents) were submitted to mild acid hydrolysis with 40 mM TFA for 20 min at 100 °C, and an aliquot analyzed by MALDI-TOF-MS as described above (Acosta-Serrano, et al., 1999).

Digitonin fractionation and Hexokinase assays. Digitonin fractionation was performed using a method adapted from (Lorenz, et al., 1998). Parasites (1×10^7) were washed in cold PBS, followed by a wash in STE buffer (250 mM sucrose, 25 mM Tris, pH 7.4, 1 mM EDTA). Cells were resuspended in STE+N (150 mM NaCl) with 0.1 M PMSF, pelleted, and resuspended in STE+N with digitonin (0.2 mg/ml). The mixture was vortexed for 5 min and then incubated at 25°C for 4 min. Lysates were centrifuged (2 min, 15,000 x g, 4°C) and pellets resuspended in 0.1 M TEA, pH 7.5 (5×10^5 cell equivalents/ml).

Hexokinase assays were performed in a coupled assay as previously described on equal volumes of the resulting supernatant and pellet from the digitonin fractionation (Misset and Opperdoes, 1984, Morris, et al., 2002). Assays were performed in triplicate in 96-well microtiter plate format using a GENios spectrophotometer (Phenix Research Products, Hayward, CA).

Localization of TbAMPK β subunit. To localize TbAMPK β , PF parasites expressing eYFP fused to the *T. brucei* aldolase peroxisomal targeting sequence 2

(PTS2, which targets proteins to glycosomes) were harvested by centrifugation at 800 x g, washed with Voorheis's modified PBS (vPBS; 137 mM NaCl, 3 mM KCl, 16 mM Na₂HPO₄, 3 mM KH₂PO₄, 46 mM sucrose, 10 mM glucose, pH 7.6) and fixed in an equal volume of 6% paraformaldehyde and vPBS for 1 hr on ice. Cells were washed with vPBS and then allowed to settle on poly-lysine coated slides prior to permeabilization with 0.1% Triton X-100 in PBS (10 min, RT) and then washed in excess PBS three times before the addition of block (1% BSA and 0.25% Tween in PBS, 1 hr, RT). Primary affinity purified rabbit polyclonal antibodies for TbAMPK β , which was purified using an antigen coupled AminoLink Coupling Resin (Thermo Scientific, Rockford IL) following the manufacture's instructions, and a mouse monoclonal against GFP (3E6, Molecular Probes, Eugene, OR) were applied at a dilution of 1:10 and 1:100, respectively, for 1 hour. The slides were washed 3 times in excess PBS before the addition of the secondary antibodies (TexasRed-conjugated goat anti-rabbit and FITC-conjugated goat anti-mouse; Rockland, Gilbertsville, PA, both at 1:100). Slides were then washed 3 times in excess PBS and prepared for visualization by addition of Vectashield mounting media with DAPI. Images were taken on a Zeiss Axiovert 200M using Axiovision software version 4.6.3 for image analysis.

To express TbAMPK β with a C-terminal fusion to GFP in live parasites the *TbAMPK β* open reading frame was cloned into pLew111(2T7)GFP β (the generous gift of Drs. Shawn Motyka and Paul Englund, Johns Hopkins School of Medicine). PF 29-13 strain trypanosomes were transformed with linearized DNA and selected as described

above. Recombinant TbAMPK β GFP expression was induced for 4 days by addition of tet (1 mg/ml) and GFP expression monitored by microscopy.

RESULTS

Identification and silencing of AMPK subunit homologs in *T. brucei*. We have identified candidate single copy homologous genes for the β and γ subunits components of the heterotrimeric enzyme AMPK in the *T. brucei* genome database. The putative *T. brucei* AMPK β subunit (TbAMPK β systematic name Tb927.8.2450) is similar to the rat AMPK β 1 protein (E value = 2.8×10^{-10}), sharing 33% amino acid identity. TbAMPK β is predicted to be a 34.4 kDa protein that contains a 5' AMP-activated protein kinase β -subunit complex interacting region (α/γ interaction domain, residues 195-303) found in the β subunit of mammalian AMPK and yeast homologs of AMPK (Thornton, et al., 1998) (Fig. 1A). In other systems, this domain allows interaction with the kinase (α) subunit and is characteristic of β subunits. TbAMPK β also shares with the rat AMPK β 1 protein a conserved putative N-myristoylation signal (Fig. 1A) and two (of four) conserved Ser (at residue 119 and 126) (Carling, 2004).

The putative *T. brucei* AMPK γ subunit (TbAMPK γ , systematic name Tb10.70.3670) is predicted to be a 55.2 kDa protein that is most similar to human AMPK γ 3 (E value = 1.1×10^{-11} , 27% identical at the amino acid level). The trypanosome protein is predicted to have 4 cystathionine-b-synthase (CBS) domains (residues 80-134, 187-244, 361-414, 430-484), which have been found in other γ subunits

(but are not limited to AMPK γ subunits) (Fig. 1A). The CBS domains have been implicated to function in AMP binding (Cheung, et al., 2000, Daniel and Carling, 2002).

To initiate analysis of the function of TbAMPK subunits, we silenced the putative subunits using the pZJM RNAi vector. The impact of RNAi of either subunit on cell viability was minimal, causing ~2-fold increase in doubling time (not shown). Induction of RNAi for 40 hours led to a dramatic decrease in *TbAMPK β* and *TbAMPK γ* transcript abundance (Fig. 1B) (Wang, et al., 2000). Due to low transcript abundance, the northern blots of TbAMPK β were particularly difficult to assess. Since RNAi ultimately leads to protein depletion, we used western blotting to confirm the *TbAMPK β* knock down using polyclonal antibodies to recombinant TbAMPK β protein after RNAi (Fig. 1C). The ~ 34 kDa polypeptide was detectable by western blot from 1 x 10⁶ parental 29-13 cell equivalents, while silencing *TbAMPK β* led to a ~5-fold reduction in detectable protein with 5 x 10⁶ cell equivalents (Fig. 1C, lanes 3 and 4).

Bioinformatics-based approaches suggested there were 14 active members of the CAMK group of kinases in the *T. brucei* genome, which include the AMPK α subunit (Parsons, et al., 2005). Of these potential α subunits, a candidate *T. brucei* gene that clustered closely with yeast SNF1 and human AMPK α 1, Tb10.70.1760. RNAi of Tb10.70.1760 failed to yield a discernable Con A binding phenotype (see below), suggesting that we had either identified and tested the incorrect homolog, or that functional redundancy was obscuring the resolution of the α subunit. For these reasons, we have focused on the single-copy subunits for the remainder of this manuscript.

RNAi of *TbAMPKβ* or *TbAMPKγ* impacts surface molecule expression.

Previously, we found through an RNAi-based genomic library screen that glycolysis modulated surface glycoprotein expression in PF parasites (Morris, et al., 2002).

Therefore, we reasoned that knockdown of proteins that play a role in the connection of glycolysis to surface molecule expression may yield cells with similar dis-regulation of surface molecule expression.

To determine if *TbAMPK* subunit silencing leads to this phenotype, we first stained *TbAMPKβ* and *TbAMPKγ*-deficient cells with the lectin Con A, which predominantly binds to glycosylated EP-procyclics but not to GPEET on PF trypanosomes (Pearson, et al., 2000) (Fig. 2). We have used this approach to previously characterize the impact of silencing glycolytic enzymes on surface molecule expression (Morris, et al., 2002). The impact of silencing *TbAMPKβ* and *TbAMPKγ* on Con A binding was assessed in cells grown in standard SDM-79 medium or in reduced glucose (~ 0.5 mM) medium for 7 days. While growth in reduced glucose medium did not alter parental PF 29-13 cell Con A-FITC binding (Fig. 2A, light gray line compared to dark grey line, and (Morris, et al., 2002)), culturing of *TbAMPKβ* or *TbAMPKγ*-deficient cells in normal medium caused a subtle reduction in Con A binding while growth in low glucose medium for 7 days caused a dramatic reduction in Con A binding (Fig. 2B and 2C, black line compared to grey line).

To further characterize the nature of the surface molecule change, we used antibodies to the major surface glycoproteins to assess expression by flow cytometry. We found that cells deficient in either *TbAMPKβ* or *TbAMPKγ* have a similar glucose-

dependent RNAi phenotype that is not observed in the parental cell line. Parental 29-13 PF trypanosomes predominantly expressed EP-procycalin (Fig. 3A, left panel) with little detectable GPEET-procycalin (Fig. 3A, right panel). These findings are in agreement with the procycalin repertoire that has been described from PF 29-13 parasites (Acosta-Serrano, et al., 1999, Morris, et al., 2002).

Like parental PF 29-13 cells, *TbAMPK β* -deficient parasites expressed EP-procycalin (Fig. 3B, left panel) and expressed very little GPEET-procycalin (Fig. 3B, right panel). However, if parasites deficient in *TbAMPK β* were grown under reduced glucose (~ 0.5 mM) conditions, a greater proportion expressed GPEET-procycalin (Fig. 3B, right panel, +tet, -glc). These cells continued to express EP-procycalin (Fig. 3B, left panel).

Cells with *TbAMPK γ* silenced also expressed EP-procycalin (Fig. 3C, left panel) and demonstrated a subtle increase in the surface expression of GPEET-procycalin (Fig. 3C, right panel). Under reduced glucose (~ 0.5 mM) conditions, a greater proportion expressed GPEET-procycalin (Fig. 3C, right panel, +tet, -glc). Again, these cells continued to express EP-procycalin (Fig. 3C, left panel), with both procyclins expressed for the duration of these experiments (~14 days). Addition of glucose to these cells blocked the increased expression of GPEET-procycalin (Fig. 3C, right panel, +tet – glc/+glc).

MALDI-TOF mass spectrometry confirms that normally glycosylated EP-procycalin, in addition to GPEET-procycalin, is expressed after RNAi of *TbAMPK β* or *TbAMPK γ* . Silencing either *TbAMPK β* or *TbAMPK γ* subunits triggered a loss of Con A

binding, while antibody staining and flow cytometry analysis of these cells indicated that EP-procycalin was expressed on the surface. These observations seem to conflict, as Con A binds to the *N*-glycan of EP-procycalin. How is there a reduction in Con A binding while the protein to which Con A binds is still expressed? These data suggested that GPEET-procycalin could be masking the *N*-glycan of EP-procycalin. Alternatively, EP-procycalins may not be properly *N*-glycosylated in the TbAMPK β or TbAMPK γ -deficient cells, or EP-2 (a naturally occurring unglycosylated EP-procycalin) could be the dominant EP-procycalin in these cells. To resolve these possibilities, we performed MALDI-TOF mass spectrometry on partially purified procycalins from parental PF 29-13, TbAMPK β -deficient, or TbAMPK γ -deficient trypanosomes grown in low glucose medium (Fig. 4).

Expression of GPEET was confirmed by positive-ion MALDI-TOF-MS on HF-treated procycalin polypeptides. Parental PF 29-13 expressed only glycosylated EP-procycalin species (*i.e.* EP1-1, EP1-2 and EP3) (Fig. 4A). Ions representing GPEET (m/z 6141) or EP2-procycalin (m/z 8345; the only naturally unglycosylated procycalin) were not detected, consistent with the Con A and antibody binding observed by flow cytometry. In contrast, silencing of either TbAMPK β or TbAMPK γ yielded a reduction (but not complete ablation) of glycosylated EP-procycalins with a concurrent increase in expression of GPEET-procycalin. GPEET-procycalin expression is characterized by expression of full length polypeptides (m/z 6,141) and the presence of a truncated form lacking the N-terminus sequence VIVK (marked as "GPEET-4", Fig 4B and 4C) (Acosta-Serrano, et al., 2000). Assignments of the procycalins species present in all samples were confirmed by negative ion MALDI-TOF-MS analyses of the C-terminus after mild acid

hydrolysis (not shown). Since the EP-species have the expected masses of polypeptides bearing the parental oligomannose *N*-glycan, the reduction in Con A binding observed in TbAMPK β or TbAMPK γ -deficient cells is not likely due to alteration in *N*-glycosylation but rather is possibly due to masking of the glycan by GPEET-procyclicin.

Localization of the TbAMPK β subunit homolog. In mammals, the AMPK β -1 subunit localizes to extranuclear particulate structures that are neither mitochondria nor endoplasmic reticulum (Warden, et al., 2001). The localization and activity of the AMPK complex are altered if the AMPK β -1 subunit N-myristoylation site is mutated, suggesting that this component of the complex directs the subcellular localization of the complex. To explore the localization of TbAMPK β , affinity-purified antibodies were generated against recombinant TbAMPK β . These antibodies recognized a single polypeptide (that does not react with pre-immune sera) in western blots of whole trypanosomal lysates (Fig. 5A and data not shown).

Digitonin fractionation of trypanosomes was used to separate soluble cytoplasmic proteins from organellar components. When this fraction was analyzed by western blot, TbAMPK β was detected exclusively in the particulate fraction (Fig. 5B, P). As a control, the hexokinase activity of each of the fractions was determined and ~90% of the hexokinase activity was found associated with the particulate fraction (which should include intact glycosomes). Not all proteins fractionated with the particulate matter, as a putative cyclophilin-like protein (Tbcyp22) was found with near-equal distribution in both fractions (Fig. 5B).

Immunofluorescence of parasites expressing yellow fluorescent protein (YFP) targeted to glycosomes (as a result of fusion with an N-terminal PTS2) was used to further assess the cellular localization of TbAMPK β . These parasites had a TbAMPK β distribution that overlapped with the glycosomal YFP marker but was not exclusively glycosomal (Fig. 6A). For example, signal was also detected in or near the flagellum. Similarly, live parasites expressing a fusion of TbAMPK β with GFP yielded punctate fluorescence consistent with glycosomes, as well as faint flagellar signal (Fig. 6B). YFP bearing an N-terminal PTS2 (for glycosome targeting, Fig. 6B, left panel) localizes primarily in points in live cells, while expression of GFP without a targeting sequence yielded signal throughout the parasite (Fig. 5B, right panel).

DISCUSSION

The African trypanosome inhabits two very different environments, requiring adaptation to conditions found in these different hosts. In the mammalian bloodstream, the parasite is bathed in its primary carbon source, glucose, while in the tsetse fly glucose is rapidly depleted during bloodmeal digestion. In the fly, the parasites persist by metabolism of amino acids, taking advantage of the abundance of proline produced by the fly to power its flight muscles.

Both PF and bloodstream parasites monitor glucose abundance to make developmental decisions. During differentiation from BSF to PF, parasites switch surface coats from VSG to procyclin in a process that can be triggered *in vitro* by growth in low glucose medium (Milne, et al., 1998). In the fly, PF parasites respond to changes

in glucose concentrations by altering surface molecule expression. PF parasites very early in the differentiation progression express both EP- and GPEET- procyclins, but switch to express predominantly GPEET-procycloin shortly after initiation of the infection (Acosta-Serrano, et al., 2001, Vassella, et al., 2001, Vassella, et al., 2000). This switch is coincident with the fall of glucose levels during digestion of the bloodmeal. This progression can be recapitulated by growing parasites in very low (0.03 mM) glucose conditions or by using RNAi to silence glycolytic enzymes (Morris, et al., 2002). These observations suggest that glucose levels, presumably reflected in the rate of glycolysis, are being monitored to regulate GPEET-procycloin expression.

The molecular mechanisms that govern the expression of the procyclins likely differ, as both *cis*- and *trans*- factors have been identified (Vassella, et al., 2000, Walrad, et al., 2009). The 3' UTR of GPEET-procycloin contain a glucose response element required for the upregulation of GPEET-procycloin expression in response to low glucose medium and during its development in the fly (Vassella, et al., 2004). EP-procycloin expression is likely not regulated by glucose, as culturing parasites in low glucose does not ablate EP-procycloin expression (Morris, et al., 2002). Furthermore, deletion of the *TbGale* gene, which encodes an epimerase that interconverts UDP-Glc and UDP-Gal in glycosomes, leads to a 10-fold increase in the expression of EP- but not GPEET-procycloin, suggesting that Gal metabolism is also involved in controlling the expression and copy numbers of the procycloin molecules (Roper, et al., 2005).

We have demonstrated here that TbAMPK β and γ play a role in surface molecule expression, as silencing of the genes leads to upregulation of GPEET-procycloin

expression. The change in procyclin expression is only detectable when RNAi cells were grown in low glucose media, suggesting that the incomplete penetrance of the RNAi of the AMPK subunits was not alone sufficient to trigger GPEET expression.

The physical connection between glucose and surface molecule expression is problematic, as the majority of glucose metabolism is compartmentalized in the glycosome – how is a signal transmitted from the glycosome to the rest of the cell? In other eukaryotes, AMPK plays a key role in responding to cellular glucose metabolism, being activated to trigger changes throughout the cell in response to changes in glycolysis (Hardie, 2008). AMP generated as a result of glucose metabolism could activate a *T. brucei* complex that is homologous to mammalian AMPK (Fig. 7). Hexokinase and phosphofructokinase both consume ATP, which may be regenerated by a glycosomal adenylate kinase (ADKD) (Ginger, et al., 2005). In other systems, this enzyme synthesizes ATP from ADP with the concomitant production of AMP and the cells use the ATP:AMP ratio as a marker for the status of energy levels (Hardie, 2008).

Immunolocalization of TbAMPKb indicates a widespread distribution, which could reflect the role of the subunit as part of a signaling complex. Although TbAMPKb lacks a C-terminal tripeptide peroxisomal targeting sequence (PTS1) (Opperdoes, 1987) or a PTS2-type targeting sequence, the subunit partially co-localizes with glycosomes (Fig. 5A), where its activity may be influenced by ADKD (Ginger, et al., 2005). Additionally, the b subunit localizes to the flagellum, where it is positioned to interact with a previously described flagellar AK (Pullen, et al., 2004). TbAMPK β subunit localization (and function) may be dependent on the protein's myristoylated state, akin to

mammalian AMPK- β 1 (Resh, 1999, Warden, et al., 2001). It is also possible that the as of yet unidentified a subunit provides cellular targeting information to the complex. The partial localization of TbAMPK β with glycosomes positions the complex to potentially monitor the status of glycolysis in the cell, which has been previously demonstrated to play a central role in the modulation of surface molecule regulation.

ACKNOWLEDGMENTS

This work was supported by US National Institutes of Health 1R15AI075326 to JCM. CSC was partially supported by a research grants from the Calhoun Honors College, Clemson University and from the HHMI/SCLIFE Undergraduate Research Program. AAS was supported by a Wellcome Trust Research Career Development Fellowship.

LITERATURE CITED

1. Acosta-Serrano, A., Cole, R. N., and Englund, P. T., 2000. Killing of *Trypanosoma brucei* by concanavalin A: structural basis of resistance in glycosylation mutants. *Journal of Molecular Biology* 304, 633-644.
2. Acosta-Serrano, A., Cole, R. N., Mehlert, A., Lee, M. G., Ferguson, M. A., and Englund, P. T., 1999. The procyclin repertoire of *Trypanosoma brucei*. Identification and structural characterization of the Glu-Pro-rich polypeptides. *Journal of Biological Chemistry* 274, 29763-29771.
3. Acosta-Serrano, A., Vassella, E., Liniger, M., Kunz Renggli, C., Brun, R., Roditi, I., and Englund, P. T., 2001. The surface coat of procyclic *Trypanosoma brucei*: programmed expression and proteolytic cleavage of procyclin in the tsetse fly. *Proceedings of the National Acadamey of Sciences U.S.A.* 98, 1513-1518.
4. Butikofer, P., Ruepp, S., Boschung, M., and Roditi, I., 1997. 'GPEET' procyclin is the major surface protein of procyclic culture forms of *Trypanosoma brucei brucei* strain 427. *Biochemical Journal* 326, 415-423.
5. Butikofer, P., Vassella, E., Ruepp, S., Boschung, M., Civenni, G., Seebeck, T., Hemphill, A., Mookherjee, N., Pearson, T. W., and Roditi, I., 1999. Phosphorylation of a major GPI-anchored surface protein of *Trypanosoma brucei*

- during transport to the plasma membrane. *Journal of Cell Science* 112 (Pt 11), 1785-1795.
6. Carling, D., 2004. The AMP-activated protein kinase cascade--a unifying system for energy control. *Trends in Biochemical Sciences* 29, 18-24.
 7. Carlson, M., 1999. Glucose repression in yeast. *Current Opinions in Microbiology* 2, 202-207.
 8. Cheung, P. C., Salt, I. P., Davies, S. P., Hardie, D. G., and Carling, D., 2000. Characterization of AMP-activated protein kinase gamma-subunit isoforms and their role in AMP binding. *Biochemical Journal* 346 Pt 3, 659-669.
 9. Crute, B. E., Seefeld, K., Gamble, J., Kemp, B. E., and Witters, L. A., 1998. Functional domains of the alpha1 catalytic subunit of the AMP-activated protein kinase. *Journal of Biological Chemistry* 273, 35347-35354.
 10. Daniel, T., and Carling, D., 2002. Functional analysis of mutations in the gamma 2 subunit of AMP-activated protein kinase associated with cardiac hypertrophy and Wolff-Parkinson-White syndrome. *Journal of Biological Chemistry* 277, 51017-51024.
 11. Ginger, M. L., Ngazoa, E. S., Pereira, C. A., Pullen, T. J., Kabiri, M., Becker, K., Gull, K., and Steverding, D., 2005. Intracellular positioning of isoforms explains an unusually large adenylate kinase gene family in the parasite *Trypanosoma brucei*. *Journal of Biological Chemistry* 280, 11781-11789.
 12. Hardie, D. G., 2008. Role of AMP-activated protein kinase in the metabolic syndrome and in heart disease. *FEBS Letters* 582, 81-89.
 13. Hardie, D. G., Carling, D., and Carlson, M., 1998. The AMP-activated/SNF1 protein kinase subfamily: metabolic sensors of the eukaryotic cell? *Annual Review of Biochemistry* 67, 821-855.
 14. Hardie, D. G., and Hawley, S. A., 2001. AMP-activated protein kinase: the energy charge hypothesis revisited. *Bioessays* 23, 1112-1119.
 15. Hwa, K. Y., Acosta-Serrano, A., Khoo, K. H., Pearson, T., and Englund, P. T., 1999. Protein glycosylation mutants of procyclic *Trypanosoma brucei*: defects in the asparagine-glycosylation pathway. *Glycobiology* 9, 181-190.
 16. Kemp, B. E., Mitchelhill, K. I., Stapleton, D., Michell, B. J., Chen, Z. P., and Witters, L. A., 1999. Dealing with energy demand: the AMP-activated protein kinase. *Trends in Biochemical Sciences*. 24, 22-25.
 17. Lorenz, P., Maier, A. G., Baumgart, E., Erdmann, R., and Clayton, C., 1998. Elongation and clustering of glycosomes in *Trypanosoma brucei* overexpressing the glycosomal Pex11p. *The EMBO Journal* 17, 3542-3555.
 18. Matthews, K. R., and Gull, K., 1994. Evidence for an interplay between cell cycle progression and the initiation of differentiation between life cycle forms of African trypanosomes. *Journal of Cell Biology* 125, 1147-1156.
 19. Mehler, A., Treumann, A., and Ferguson, M. A., 1999. *Trypanosoma brucei* GPEET-PARP is phosphorylated on six out of seven threonine residues. *Molecular and Biochemical Parasitology* 98, 291-296.
 20. Milne, K. G., Prescott, A. R., and Ferguson, M. A., 1998. Transformation of monomorphic *Trypanosoma brucei* bloodstream form trypomastigotes into

- procyclic forms at 37 degrees C by removing glucose from the culture medium. *Molecular and Biochemical Parasitology* 94, 99-112.
21. Misset, O., and Opperdoes, F. R., 1984. Simultaneous purification of hexokinase, class-I fructose-bisphosphate aldolase, triosephosphate isomerase and phosphoglycerate kinase from *Trypanosoma brucei*. *European Journal of Biochemistry* 144, 475-483.
 22. Morris, J. C., Wang, Z., Drew, M. E., and Englund, P. T., 2002. Glycolysis modulates trypanosome glycoprotein expression as revealed by an RNAi library. *The EMBO Journal*. 21, 4429-4438.
 23. Mowatt, M. R., and Clayton, C. E., 1987. Developmental regulation of a novel repetitive protein of *Trypanosoma brucei*. *Molecular and Cellular Biology* 7, 2838-2844.
 24. Mowatt, M. R., Wisdom, G. S., and Clayton, C. E., 1989. Variation of tandem repeats in the developmentally regulated procyclic acidic repetitive proteins of *Trypanosoma brucei*. *Molecular and Cellular Biology* 9, 1332-1335.
 25. Opperdoes, F. R., 1987. Compartmentation of carbohydrate metabolism in trypanosomes. *Annual Review of Microbiology* 41, 127-151.
 26. Parsons, M., Worthey, E. A., Ward, P. N., and Mottram, J. C., 2005. Comparative analysis of the kinomes of three pathogenic trypanosomatids: *Leishmania major*, *Trypanosoma brucei* and *Trypanosoma cruzi*. *BMC Genomics* 6, 127.
 27. Pearson, T. W., Beecroft, R. P., Welburn, S. C., Ruepp, S., Roditi, I., Hwa, K. Y., Englund, P. T., Wells, C. W., and Murphy, N. B., 2000. The major cell surface glycoprotein procyclin is a receptor for induction of a novel form of cell death in African trypanosomes *in vitro*. *Molecular and Biochemical Parasitology* 111, 333-349.
 28. Pullen, T. J., Ginger, M. L., Gaskell, S. J., and Gull, K., 2004. Protein targeting of an unusual, evolutionarily conserved adenylate kinase to a eukaryotic flagellum. *Molecular Biology of the Cell* 15, 3257-3265.
 29. Resh, M. D., 1999. Fatty acylation of proteins: new insights into membrane targeting of myristoylated and palmitoylated proteins. *Biochimica et Biophysica Acta* 1451, 1-16.
 30. Richardson, J. P., Beecroft, R. P., Tolson, D. L., Liu, M. K., and Pearson, T. W., 1988. Procyclin: An unusual immunodominant glycoprotein surface antigen from the procyclic stage of African trypanosomes. *Molecular and Biochemical Parasitology* 31, 203-216.
 31. Richardson, J. P., Jenni, L., Beecroft, R. P., and Pearson, T. W., 1986. Procyclic tsetse fly midgut forms and culture forms of African trypanosomes share stage- and species-specific surface antigens identified by monoclonal antibodies. *Journal of Immunology* 136, 2259-2264.
 32. Roditi, I., Carrington, M., and Turner, M., 1987. Expression of a polypeptide containing a dipeptide repeat is confined to the insect stage of *Trypanosoma brucei*. *Nature* 325, 272-274.
 33. Roditi, I., Schwarz, H., Pearson, T. W., Beecroft, R. P., Liu, M. K., Richardson, J. P., Buhning, H. J., Pleiss, J., Bulow, R., Williams, R. O., and Overath, P., 1989.

- Procyclin gene expression and loss of the variant surface glycoprotein during differentiation of *Trypanosoma brucei*. *Journal of Cell Biology* 108, 737-746.
34. Roper, J. R., Guther, M. L., Macrae, J. I., Prescott, A. R., Hallyburton, I., Acosta-Serrano, A., and Ferguson, M. A., 2005. The suppression of galactose metabolism in procyclic form *Trypanosoma brucei* causes cessation of cell growth and alters procyclin glycoprotein structure and copy number. *Journal of Biological Chemistry* 280, 19728-19736.
 35. Salt, I. P., Johnson, G., Ashcroft, S. J., and Hardie, D. G., 1998. AMP-activated protein kinase is activated by low glucose in cell lines derived from pancreatic beta cells, and may regulate insulin release. *Biochemical Journal* 335 (Pt 3), 533-539.
 36. Thornton, C., Snowden, M. A., and Carling, D., 1998. Identification of a novel AMP-activated protein kinase beta subunit isoform that is highly expressed in skeletal muscle. *Journal of Biological Chemistry* 273, 12443-12450.
 37. Treumann, A., Zitzmann, N., Hulsmeier, A., Prescott, A. R., Almond, A., Sheehan, J., and Ferguson, M. A., 1997. Structural characterisation of two forms of procyclic acidic repetitive protein expressed by procyclic forms of *Trypanosoma brucei*. *Journal of Molecular Biology* 269, 529-547.
 38. van den Hoff, M. J., Moorman, A. F., and Lamers, W. H., 1992. Electroporation in 'intracellular' buffer increases cell survival. *Nucleic Acids Research* 20, 2902.
 39. Vassella, E., Acosta-Serrano, A., Studer, E., Lee, S. H., Englund, P. T., and Roditi, I., 2001. Multiple procyclin isoforms are expressed differentially during the development of insect forms of *Trypanosoma brucei*. *Journal of Molecular Biology* 312, 597-607.
 40. Vassella, E., Den Abbeele, J. V., Butikofer, P., Renggli, C. K., Furger, A., Brun, R., and Roditi, I., 2000. A major surface glycoprotein of *Trypanosoma brucei* is expressed transiently during development and can be regulated post-transcriptionally by glycerol or hypoxia. *Genes and Development* 14, 615-626.
 41. Vassella, E., Oberle, M., Urwyler, S., Renggli, C. K., Studer, E., Hemphill, A., Fragoso, C., Butikofer, P., Brun, R., and Roditi, I., 2009. Major surface glycoproteins of insect forms of *Trypanosoma brucei* are not essential for cyclical transmission by tsetse. *PLoS ONE* 4, e4493.
 42. Vassella, E., Probst, M., Schneider, A., Studer, E., Renggli, C. K., and Roditi, I., 2004. Expression of a major surface protein of *Trypanosoma brucei* insect forms is controlled by the activity of mitochondrial enzymes. *Molecular Biology of the Cell* 15, 3986-3993.
 43. Vickerman, K., 1985. Developmental cycles and biology of pathogenic trypanosomes. *British Medical Bulletin* 41, 105-114.
 44. Walrad, P., Paterou, A., Acosta-Serrano, A., and Matthews, K. R., 2009. Differential trypanosome surface coat regulation by a CCCH protein that co-associates with procyclin mRNA cis-elements. *PLoS Pathogens* 5, e1000317.
 45. Wang, Z., Morris, J. C., Drew, M. E., and Englund, P. T., 2000. Inhibition of *Trypanosoma brucei* gene expression by RNA interference using an integratable

- vector with opposing T7 promoters. *Journal of Biological Chemistry* 275, 40174-40179.
46. Warden, S. M., Richardson, C., O'Donnell, J., Jr., Stapleton, D., Kemp, B. E., and Witters, L. A., 2001. Post-translational modifications of the beta-1 subunit of AMP-activated protein kinase affect enzyme activity and cellular localization. *Biochemical Journal* 354, 275-283.
 47. Welburn, S. C., Dale, C., Ellis, D., Beecroft, R., and Pearson, T. W., 1996. Apoptosis in procyclic *Trypanosoma brucei rhodesiense* in vitro. *Cell Death and Differentiation* 3, 229-236.
 48. Wirtz, E., Leal, S., Ochatt, C., and Cross, G. A., 1999. A tightly regulated inducible expression system for conditional gene knock-outs and dominant-negative genetics in *Trypanosoma brucei*. *Molecular and Biochemical Parasitology* 99, 89-101.
 49. Ziegelbauer, K., Quinten, M., Schwarz, H., Pearson, T. W., and Overath, P., 1990. Synchronous differentiation of *Trypanosoma brucei* from bloodstream to procyclic forms *in vitro*. *European Journal of Biochemistry* 192, 373-378.

FIGURE LEGENDS

Fig. 1. Targeting TbAMPK β and TbAMPK γ by RNAi impacts transcript and protein levels. (A) TbAMPK β and γ diagram. TbAMPK β contains a putative N-myristoylation sequence (MGNTSAE), two conserved Ser residues (corresponding to Ser101 and Ser108 from rat AMPK β 1), and a α/γ interaction domain. TbAMPK γ contains 4 CBS domains that have been implicated in AMP binding (Cheung, et al., 2000, Daniel and Carling, 2002). (B) Analysis of RNAi of TbAMPK β and TbAMPK γ by northern blot. Total RNA from parental (-) and tetracycline induced (+) (for 40 h) cells containing the construct pZJM(TbAMPK β) or pZJM(TbAMPK γ) was purified from 5×10^7 parasites and electrophoresed on a formaldehyde 1.5% agarose gel. Ribosomal RNA levels were estimated by ethidium bromide staining to ensure equal loading of RNA. (C.) Western blot performed on 5×10^6 or 1×10^6 cell equivalents of PF 29-13 (lanes 1-2) or cells induced 4 days to silence TbAMPK β with pZJMAMPK β (lanes 3-4) were resolved by SDS-PAGE, transferred to nitrocellulose and probed with affinity purified TbAMPK β antibodies. The bottom panel is a Ponceau S-stained band used to estimate loading.

Fig. 2. Silencing TbAMPK β or γ causes a change in surface molecule expression that is enhanced by growth in reduced glucose medium. (A.) Living PF 29-13 trypanosomes were cultured for two weeks in normal SDM-79 (parental, light grey line) or reduced glucose medium (-Glc, dark grey line) and then incubated with 10 mg/ml fluorescein-conjugated Con A for 15 min at room temperature in cytoM. Parasites were then analyzed by flow cytometry (10,000 cells/assay). (B.) Cell line PF 29-13 (parental, light

grey line), cells induced to silence TbAMPK β for 7 days (+tet, black line) and cells induced to silence TbAMPK β for 7 days grown in reduced glucose medium for 7 days (+tet -Glc, grey line) were analyzed after Con A-FITC staining. Laser intensity was adjusted to yield autofluorescence from unstained cells (purple shade) of ~3 fluorescence intensity units. (C.) Cells in which TbAMPK γ was silenced for 7 days (+tet, black line), trypanosomes induced to silence TbAMPK γ for 7 days grown in reduced glucose medium (+tet, -Glc, grey line), and cells induced to silence TbAMPK γ for 7 days grown in reduced glucose with glucose supplemented (5 mM) (+ tet, -Glc/+Glc, grey line) for 7 days were analyzed.

Fig. 3. Trypanosomes deficient in either TbAMPK β or TbAMPK γ express GPEET-procycalin. Parasites were grown in normal SDM-79 (light grey line) or reduced glucose medium (-Glc, dark grey line), and cells induced to silence TbAMPK subunits for 7 days (+tet). Induced cells were also grown in reduced glucose medium (+tet -Glc), or in media with glucose supplemented (5 mM) (+ tet, -Glc/+Glc). Parasites (5×10^6) were fixed and stained with antibodies to EP-procycalin (TBRP1/247) or GPEET-procycalin (monoclonal 5H3). Primary antibodies were detected with FITC-conjugated anti-mouse secondary antibody and cells (10,000) analyzed by flow cytometry.

Fig. 4. Mass spectrometry analysis of procyclins. Butanol extracts of (A) PF 29-13, (B) TbAMPK β , and (C) TbAMPK γ silenced cells grown in low glucose medium were

dephosphorylated with aqueous HF and aliquots analyzed by MALDI-TOF-MS in positive mode. Some of the unlabelled ions in B and C correspond to fragments of EP-procyclins that lack 10 amino acids from the N-terminus (Acosta-Serrano, et al., 2000). Asterisks represent a contaminant that has been previously assigned as KMP-11 (Acosta-Serrano, et al., 1999).

Fig. 5. TbAMPK β has an organellar digitonin fractionation. (A.) Affinity-purified antibodies raised against TbAMPK β recognize a single polypeptide in total *T. brucei* cell lysates. (B.) TbAMPK β partitions with the particulate fraction of digitonin permeabilized cells. Following fractionation, equal volumes of supernatant and resuspended pellet (1 x 10⁶ cell equivalents/lane) were resolved by SDS-PAGE, transferred to nitrocellulose, and probed with antibodies to either TbAMPK β (1:100) or Tbcyp22 (1:100). Primary antibodies were detected with HRP-conjugated goat anti-mouse antibodies (1:10,000). To explore hexokinase activity, fractions were assayed in a coupled hexokinase reaction, with the conversion of NAD to NADH by glyceraldehyde-3-phosphate dehydrogenase monitored by spectrophotometer.

Fig. 6. TbAMPK β is localized to punctate bodies that partially co-localize with glycosomes. (A.) Immunofluorescence using affinity-pure polyclonal sera raised against recombinant TbAMPK β . Transgenic PF 29-13 harboring pXS2(PTS2YFP) were fixed, permeabilized, and stained with a mouse anti-GFP monoclonal antibody (left panel) or affinity-purified polyclonal anti-TbAMPK β antibodies (center panel). Primary antibodies

were detected with FITC-conjugated goat anti-mouse or mouse anti-rabbit antibodies, respectively. Scale bar = 5 mm. (B.) Expression of TbAMPK β fused to GFP in live cell using pLew111(2T7)GFP β (middle panel). Transformed trypanosomes were induced to express the recombinant fusion protein for 4 days by addition of tet (1 mg/ml). For comparison, live cells expressing glycosomally targeted YFP (left panel) or GFP without a targeting sequence (right panel) are included. Cells were washed, resuspended in PBS and spotted on slides after mixing with an equal volume of antifade reagent.

Fig. 7. A schematic representation of the connection of TbAMPK to surface molecule expression. The pathway labeled with a question mark remains to be resolved, as extra-glycosomal AMP may function to activate TbAMPK. ADKD, glycosomal adenylate kinase.

Fig 1

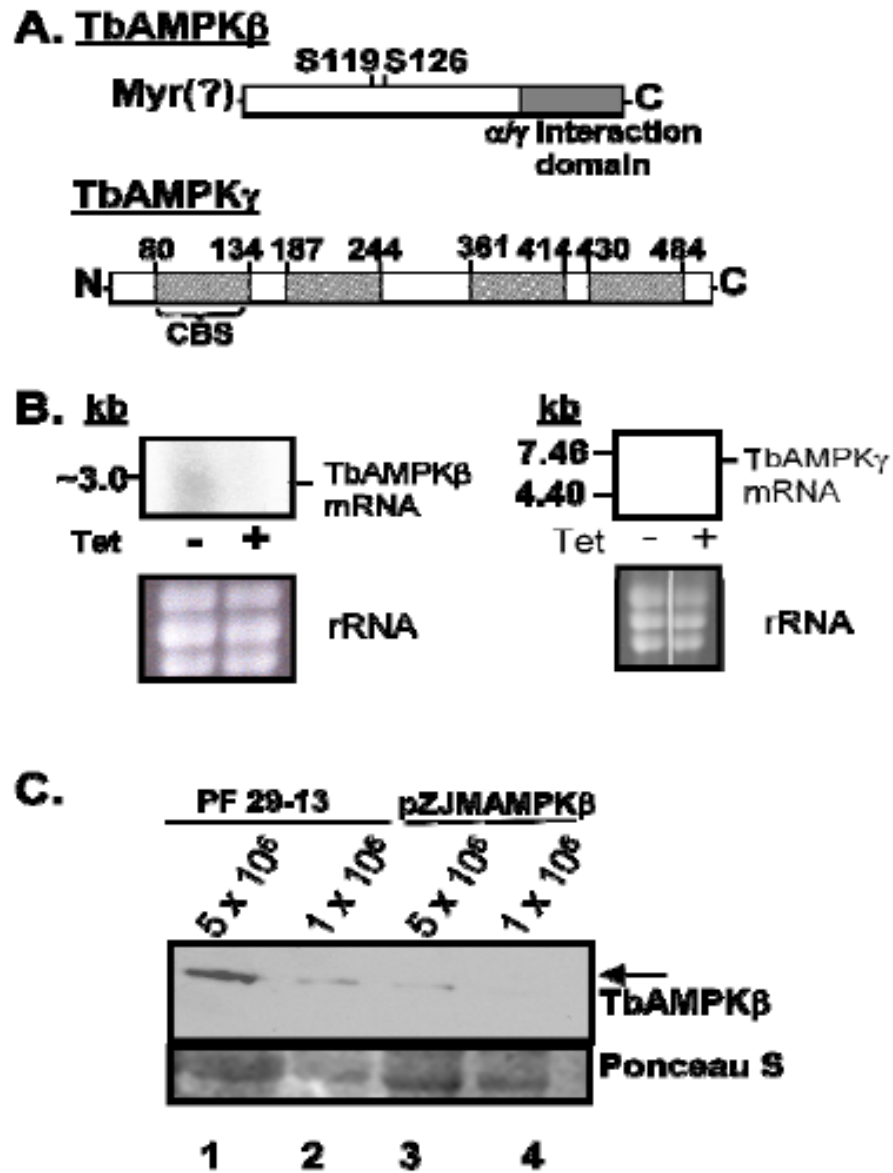


Fig 2.

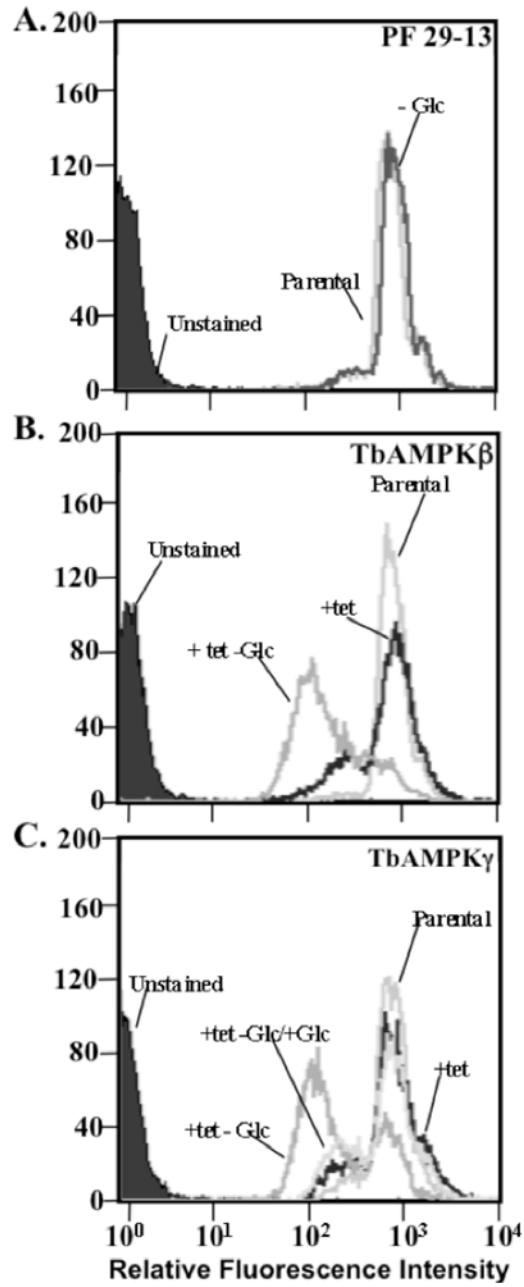


Fig 3.

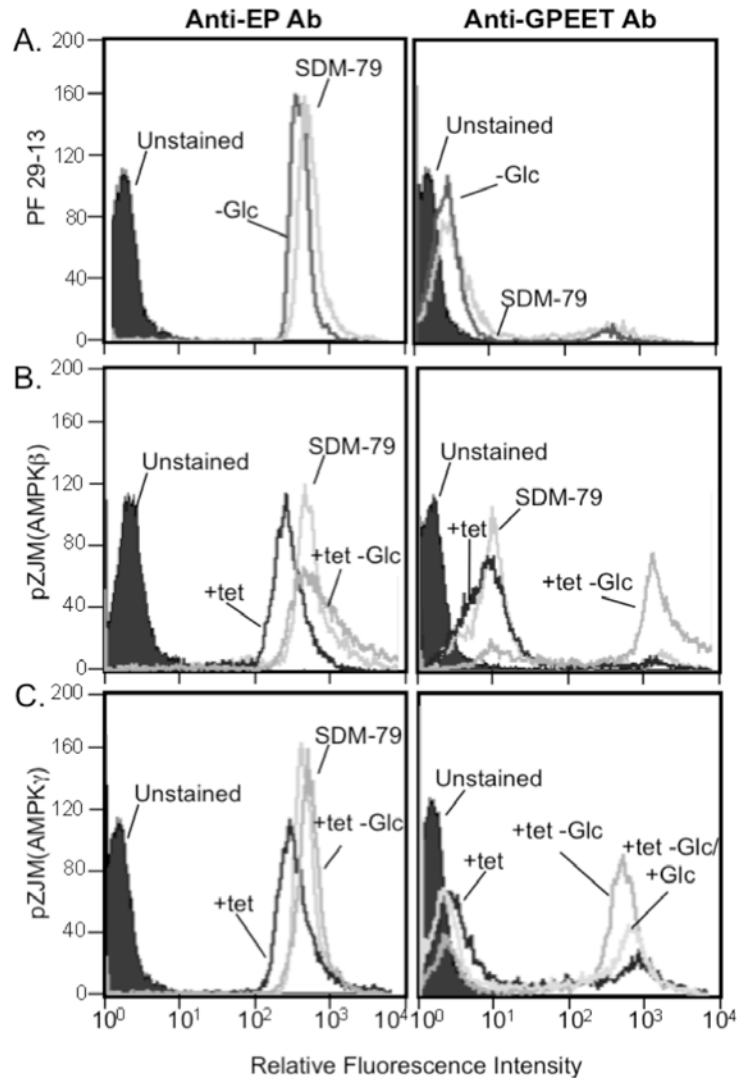


Fig 4.

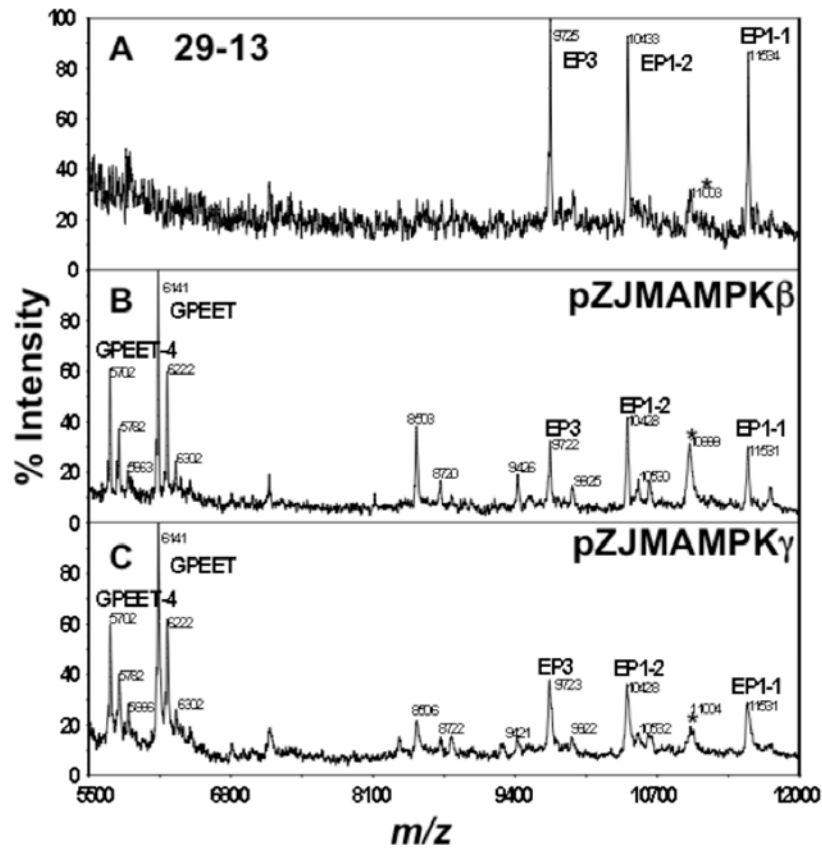


Fig 5.

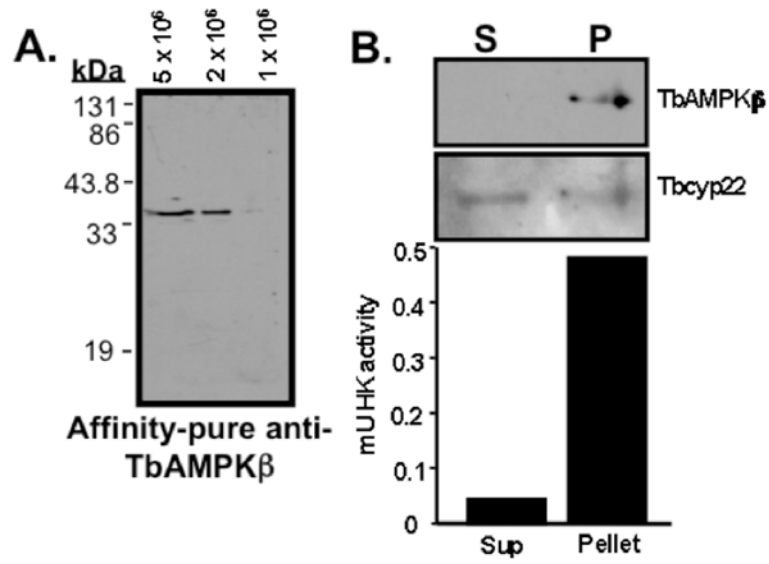


Fig 6

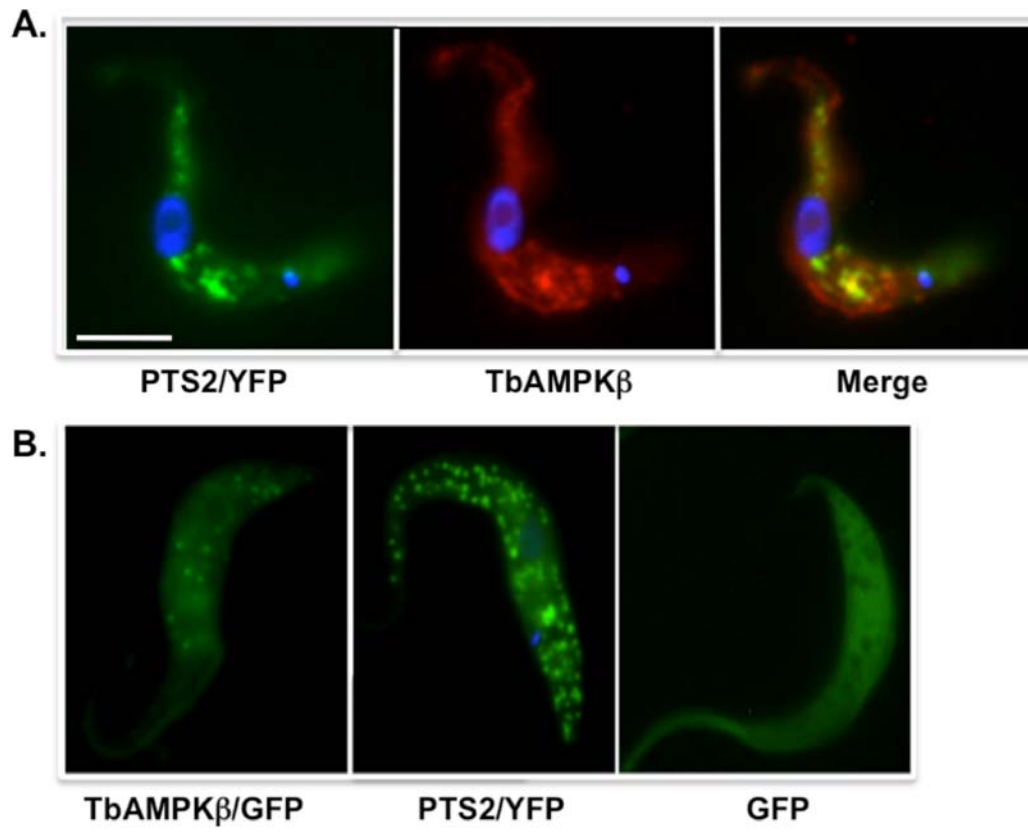
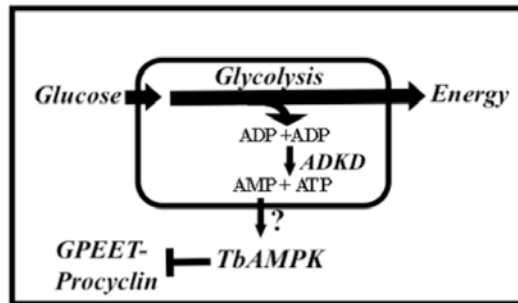


Fig 7.



Appendix B

IMPROVING AN ANTI-TRYPANOSOMAL COMPOUND:
LONIDAMINE ANALOGS INHIBIT *T. BRUCEI* HEXOKINASE ACTIVITY AND
CELL GROWTH

T. A. Lyda¹, J. Chambers¹, M. Morris¹, G. Georg², J. Morris^{1*};

¹Clemson Univ., Clemson, SC

²Univ. of Minnesota, Minneapolis, MN

*Corresponding Author: jmorri2@clemson.edu

Abstract

Through genetic manipulation, glycolysis has been shown to be essential to both the mammalian bloodstream form (BS) and the insect stage of *Trypanosoma brucei*. Disrupting glycolysis with compounds can kill the parasites. One drug, lonidamine (LND, 1-(2,4-dichlorobenzyl)-1H-indazole-3-carboxylic acid), inhibits *T. brucei* hexokinase 1 (TbHK1), the enzyme in the first step of glycolysis. *In vitro* studies have shown that LND is a potent trypanocidal agent [2]. Here we have screened a panel of 108 LND analogs for potency as TbHK1 inhibitors and as anti-trypanosomal compounds. Of the 108 analogs, 12 analogs were equivalent or better inhibitors of TbHK1 than LND. These studies suggest that alteration to the Z₃-position on LND can increase TbHK1 inhibition and toxicity, while changes to the carboxylic acid at the R₁ position appear to be less inhibitory.

Key Words

Hexokinase, lonidamine, *Trypanosoma brucei*, lonidamine analog

Abbreviations

T. brucei (*Trypanosoma brucei*), TbHK1 (*Trypanosoma brucei* hexokinase 1), LND (lonidamine)

Introduction

Trypanosoma brucei is the causative agent of African sleeping sickness in humans and nagana in cattle. The effects of *T. brucei* on the people of Africa are detrimental to the health of individuals as well as the economy of the continent. The infected regions of sub-Saharan Africa are also termed “Green Deserts” because of the inability to use these regions for agricultural means. An estimated \$4.5 billion is lost annually in the green desert [1]. Current treatments for *T. brucei* are quite noxious to the host, killing between 3% and 10% of patients [1]. Therefore, alternative drugs that kill *T. brucei* but not the host should be considered.

Bloodstream form parasites use glycolysis exclusively for energy production. Therefore, compounds that inhibit glycolysis may be potential anti-trypanosomal compounds. One such inhibitor of glycolysis, specifically targeting hexokinases, is lonidamine (LND, 1-(2,4-dichlorobenzyl)-1H-indazol-3-carboxylic acid). LND is currently used as an anti-cancer agent and male contraceptive [3- 4]. It has been approved for use in Europe for cancer and is still undergoing trials for use as a male contraceptive. Interestingly, LND has been shown to not only inhibit *T. brucei* hexokinase 1 (TbHK1) but to also inhibit cell growth and ultimately kill the bloodstream parasites in culture [5]. The reported IC₅₀ and LD₅₀ in bloodstream form parasites for LND are 850 μM and 50 μM respectively.

In an attempt to improve the lethality of LND to *T. brucei*, analogs have been generated and their ability to inhibit TbHK1 and kill bloodstream form parasites has been

tested. The following paper describes the use of LND analogs on TbHK1 enzyme assays and parasite culture growth.

Materials and Methods

Reagents

Lonidamine (LND, 1-(2,4-dichlorobenzyl)-1H-indazol-3-carboxylic acid) was purchased from Sigma-Aldrich (St. Louis, MO). The lonidamine analogs were produced by the laboratory of Dr. Gunda I. Georg at the University of Minnesota (Twin Cities).

Trypanosome cell culture

Bloodstream form 90-13 cells (a 427 strain) were grown in HMI-9 media containing 10% fetal bovine serum and 10% Serum Plus (Sigma-Aldrich).

rTbHK1 inhibition assays using LND analogs

Recombinant TbHK1 was produced using previously described techniques [6]. Hexokinase assays contained glucose-6-phosphate dehydrogenase (1 unit/assay, EMD Biosciences, Inc., San Diego, CA) as a coupling enzyme which reduces NADP⁺ to NADPH when G6-P is oxidized to 6-phosphogluconic acid. The assay was performed in final concentrations of 0.1 M TEA, pH7.9 containing 1.0 mM ATP, 33 mM MgCl₂, 20 mM glucose, and 0.75 mM NAD⁺. Levels of NADPH were measured using a GENios spectrophotometer (Phenix Research Products, Hayward, CA) in a 96-well microtiter

plate. LND analogs were used at a final concentration of 1 mM for the initial screens. The top 12 best inhibiting analogs determined from the initial 1 mM screen were used for IC₅₀ analysis at concentrations of 1 mM, 500 μM, 100 μM, 50 μM, and 0 μM (DMSO control)

Lethal Dose Assays using LND analogs

Bloodstream form parasites were grown in 24 well culture plates at a volume of 1mL HMI-9 culture media. LND analogs were added to the 1 mL cultures at final concentrations of 100 μM, 50 μM, 25 μM , 5 μM and 0 μM (DMSO control). Cell numbers were determined daily using a Becton-Dickinson FACScan flow cytometer.

Results

Initial LND analog screen

In an attempt to minimize the number of IC₅₀ assays preformed, a hexokinase assay was used for each analog to determine if the analog is an inhibitor. Many LND analogs lost their ability to inhibit rTBHK1 after modification (data not shown). However, twelve of the 108 LND analogs tested inhibited rTBHK1 to the same extent or better than LND. These 12 analogs share similar modifications at positions R₁ and R₂ as shown in Table 1.

LND analogs reduce IC₅₀

Previously, the IC₅₀ for LND on rTBHK1 activity was found to be 850 μM [5]. Here we find that analogs of LND can improve the IC₅₀ to 250 μM (See Table 1).

However, two of the 12 LND analogs, RC-MC-223 and JWS-1-232, were less inhibitory even though they were eliminated during the initial screen. RC-MC-223 and JWS-1-232 exhibited IC₅₀ concentrations of 971.2 μM and 2134.3 μM, respectively.

LND analogs reduce LD₅₀

To determine if modified LND analogs could kill *T. brucei* we grew bloodstream form parasites in the presence of the drug. To date the lowest observed LD₅₀ for an LND analog is 3.5 μM when using RC-MC-223 which is an order of magnitude lower than the LD₅₀ for LND (50 μM, Chambers et al.). Surprisingly, the most potent rTBHK1 enzyme inhibitor RC-MC-217 was not the most potent anti-trypanocidal compound with an LD₅₀ of 80 μM. The LD₅₀ results are summarized in Table 1.

Discussion

Trypanosoma brucei accounts for a tremendous loss in both human lives and economic success for the sub-Saharan region of Africa. Finding safe treatments for *T. brucei* infection should be explored further. The current treatments may lead to encephalopathy or death. The LND analog inhibition assay discovered a total of 12 LND analogs of interest. These analogs had equivalent or better inhibition of TbHK1 at 1 μM final concentration of inhibitor in the assay than the parental LND. A basic trend in the side chain alteration was noticed. Many of the effective analogs have an addition of a trifluoromethyl group to the Z₃ carbon. Also the carboxylic acid was altered by the addition of 2 to 3 carbons on the R₁ side chain location. These two changes seem to be

enhancers of inhibition for LND. Both the IC_{50} and LD_{50} suggest that Z_3 and R_1 positions are crucial to the inhibitory nature of LND analogs. Interestingly, many of the non-inhibitory LND analogs had major changes to these two locations (data not shown).

Surprisingly, the best inhibitor of TbHK1 enzyme activity, RC-MC-217, with an IC_{50} of 247.2 μM , was not the most potent inhibitor of cell growth, LD_{50} of 87.6 μM . This may be due to a delivery problem within the cell. Potentially, the analog may not localize to the glycosome where hexokinase is located. However, another reason for this decrease in IC_{50} but increase in LD_{50} may be that the analog targets other pathways besides just glycolysis in which cell growth could be activated instead of shut down. In either case, the best LND analog for killing bloodstream form parasites is RC-MC-223 with an LD_{50} of 3.5 μM . The low concentration of 3.5 μM is theoretically achievable because in a rat model system, LND was observed to be at a blood serum level of 3-37.3 μM after 48 hours when 100mg/kg of LND was given orally [7] and in humans plasma levels were 14-105 μM after 30 days treatment with 450mg per day given orally [8].

Future experiments include testing the most potent LND analogs such as RC-MC-223 in a mouse model and observing the effects on both the host and the parasite. It will be important to determine if the increase in effectiveness of the LND analogs as anti-trypanosomal compounds also increases the toxicity to the host.

Acknowledgements

The authors would like to thank Heidi Dodson, Marcia Wilson, Drew Sayce, Jarrod Smith and Eric Knapp for their intellectual conversations which took place during the experimental procedures.

References

- [1] Enserink M. Welcome to Ethiopia's Fly Factory. *Science* 2007;317:310-3.
- [2] Pepin J, Milord F. African trypanosomiasis and drug-induced encephalopathy: risk factors and pathogenesis. *Trans R Soc Trop Med Hyg* 1991;85:222-4.
- [3] Silvestrini B, Burberi S, Catanese B, et al. Antispermatic activity of 1-*p*-chlorobenzyl-1H-indazol-3-carboxylic acid (AF 1312/TS) in rats. I. Trials of single and short-term administrations with study of pharmacologic and toxicologic effects. *Exp Mol Pathol* 1975;23:288-307.
- [4] Floridi A, Lehninger AL. Action of the antitumor and antispermatic agent lonidamine on electron transport in *Ehrlich ascites* tumor mitochondria. *Arch Biochem Biophys* 1983;226:73-83.
- [5] Chambers JW, Fowler ML, Morris MT, Morris JC. The anti-trypanosomal agent lonidamine inhibits *Trypanosoma brucei* hexokinase 1. *Molecular & Biochemical Parasitology* 2008;158:202-207.
- [6] Morris MT, DeBruin C, Yang Z, Chambers JW, Smith KS, Morris JC. Activity of second *Trypanosoma brucei hexokinase* is controlled by an 18-amino-acid C-terminal tail. *Eukaryot Cell* 2006;5:2014-23.
- [7] Grippa E, Gatto MT, Leone MG, et al. Analysis of lonidamine in rat serum and testis by high performance liquid chromatography. *Biomed Chromatogr* 2001;15:1-8.
- [8] Newell DR, Mansi J, Hardy J, et al. The pharmacokinetics of oral lonidamine in breast and lung cancer patients. *Semin Oncol* 1991;18:11-7.

Figure

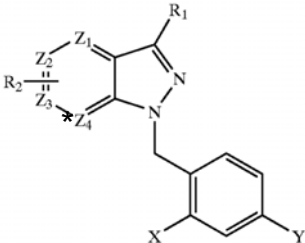
Table 1. LND Analog Changes and IC ₅₀ /LD ₅₀ Data			
		<p><u>Lonidamine</u> R₁ = Carboxylic Acid Z₁-Z₄ = Carbon X = Chlorine Y = Chlorine IC₅₀ = 850 μM LD₅₀ = 50 μM</p>	
Name	Changes from Lonidamine ^A	IC ₅₀ μM ^B	LD ₅₀ μM ^C
RC-MC-223	R ₁ = 1-propene(3)ol R ₂ = trifluoromethyl (Z ₃ Carbon)	971.2	3.5
RC-MC-294-1	R ₁ = isobutyric acid R ₂ = trifluoromethyl (Z ₃ Carbon)	271.8	4.8
RC-MC-241	R ₁ = cis-acrylic acid R ₂ = trifluoromethyl (Z ₃ Carbon)	274.9	11.0
JWS-2-224	R ₁ = trans-acrylic acid R ₂ = trifluoromethyl (Z ₃ Carbon) X = methyl	410.5	15.4
JWS-2-232-1	R ₁ = trans-acrylic acid R ₂ = trifluoromethoxyl (Z ₃ Carbon) X = methyl	256.9	17.69
RC-MC-217	R ₁ = 2-methyl acrylic acid R ₂ = trifluoromethyl (Z ₃ Carbon)	247.2	87.6
<p>^A Changes from Lonidamine: Analogs are the same as LND except where noted in the table ^B Amount (μM) of analog necessary to inhibit TbHK1 activity by 50% ^C Amount (μM) of analog necessary to kill 50% of 90-13 bloodstream form parasites by day 2</p>			

Figure Legend

Table 1. LND Analog Changes and IC₅₀/LD₅₀ Data. The LND analogs are described along with the corresponding concentration to achieve 50% inhibition and 50% lethal dose for each. The locations for changes in the LND molecule are described in the chemical drawing as R₁, R₂, Z₁, Z₂, Z₃, Z₄, X, and Y.

Appendix C

CELL TITRE BLUE ASSAY DEVELOPMENT FOR TRYPANOSOMA BRUCEI
VIABILITY TESTS USING HIGH THROUGHPUT SCREENING TECHNIQUES

Trypanosoma brucei (*T. brucei*), the protozoan parasite that causes African sleeping sickness in man, annually infects ~500,000 people in sub-Saharan Africa, leading to 50,000-70,000 deaths per year. The Special Programme for Research and Training in Tropical Diseases (TDR) currently considers the disease a category 1 (emerging or uncontrolled) disease (WHO, www.who.int). Current therapies for African sleeping sickness are inefficacious and toxic (Barrett *et al.*, 2003). The lack of affordable, safe, and effective therapies for those infected with the African trypanosome makes the identification of new therapeutic leads a priority in our effort to reduce disease in the world today.

Here, we have developed methods to identify small molecules via high throughput screening (HTS) with differences in toxicity of toward the bloodstream form (BSF) parasite, the stage that infects mammals and the procyclic form (PF) parasites, which infect the tsetse fly vector. To identify these differences in drug susceptibility, the two life cycle stages will be grown in culture and then subjected to a validated HTS assay format to identify anti-trypanosomal compounds. Impact on parasite growth and viability will be determined using an alamar blue-based assay that we have developed here is simple, reproducible, and well-suited for HTS implementation. We will then systematically confirm the growth inhibitory activity of primary hits using a series of

standardized secondary confirmation assays (IC₅₀ determinations for cherry-picked compounds, assessment of toxicity toward a mammalian cell line).

BACKGROUND AND SIGNIFICANCE

African sleeping sickness conjures images of the past - of disease-induced fatal slumber striking down men, women, and children while the malady decimates villages of colonial Africa. Unfortunately, people living in many countries of sub-Saharan Africa today know that African sleeping sickness is not a disease of history but rather is a much-neglected disease of the present, particularly in areas that suffer the additional burdens of war, famine, and other infectious agents. A survey conducted by the W.H.O. indicated that major outbreaks of African sleeping sickness occurred in 2005 in Angola, the Democratic Republic of Congo and Sudan. At the same time, the disease was a major public health burden in Central African Republic, Chad, Congo, Côte d'Ivoire, Guinea, Malawi, Uganda and United Republic of Tanzania. While these outbreaks went essentially unnoticed in the rest of the world, tens of thousands were infected and untold numbers succumbed to the disease.

The African trypanosome, *T. brucei* is the protozoan parasite that causes African sleeping sickness and nagana, a disease of animals. The parasite lives in the bloodstream of the infected mammal as a BSF parasite, consuming host glucose to generate energy through glycolysis. When parasites are taken up by a blood feeding tsetse fly, they

differentiate into PF parasites, a form that has adaptations for life in the fly that include an active mitochondria that allows for amino acid metabolism.

Current treatments are expensive, dangerous, and difficult to administer. Most of the drugs used in the treatment of African sleeping sickness are antiquated, with only two compounds (eflornithine and DB289) being developed since 1950. Pentamidine, melarsoprol, suramin and eflornithine are all difficult and expensive to administer, requiring intravenous or intramuscular injections delivered over extended periods of time. In addition, most of these drugs are extremely toxic. For example, melarsoprol, a derivative of arsenic, causes brain injuries in 5-10% of patients (50% of which are fatal) (Pepin *et al.*, 1991).

Due to its lower toxicity, eflornithine (DFMO) is currently the first choice for treatment of late stage African sleeping sickness. However, this drug has drawbacks. First, a total of nearly one-half of a kilogram of drug must be delivered over 14 days by I.V. injection with treatments every six hours (per the Mayo Clinic recommendations). Second, the availability of this drug in the future is in question. In 1990, Aventis discontinued the production of eflornithine for the treatment of African sleeping sickness, but did continue its production for use in over-the-counter depilatory creams. Negotiations with MSF and the WHO have ensured its production until 2011. It is unknown if the drug will be available after that date.

The most recent therapeutic hope, DB289 (pafuramidine) reached clinical trials but has recently been discontinued due to liver and kidney abnormalities in volunteers treated with the drug (Immtech Pharmaceutical press release, December 26, 2007).

HTS approaches to identify compounds with anti-kinetoplastid activity – HTS technology has been used previously to identify compounds with activity against *T. brucei* and the related kinetoplastid parasite, Leishmania. Using an ATP-bioluminescence assay, Mackey and colleagues screened a library of 2160 drugs that had been developed for other uses for anti-*T. brucei* activity. This effort yielded 35 compounds with trypanocidal activity (Mackey *et al.*, 2006). More recently, a HTS has been initiated at the UPDDI for small molecules that are growth inhibitory to Leishmania major promastigotes (Sharlow *et al.*, In Press). This screen employs Alamar blue to assess cell viability, and when implemented against a library of 196,146 compounds resulted in Z-factors 0.9 ± 0.1 .

In addition to “whole cell” HTS, there have been a number of HTS to identify probes for important enzymes from the kinetoplastids. These include screens for activators and inhibitors of *T. brucei* hexokinase 1 (collaboration between the PI and UPDDI), screens for activators and inhibitors of *L. mexicana* pyruvate kinase (Malcom Walkinshaw, Hugh Morgan and Linda Gilmore, University of Edinburgh, Edinburgh, UK and the National Institutes of Health Chemical Genomics Center (NCGC)), a screen for inhibitors of trypanothione reductase (Martyn *et al.*, 2006), and a screen for inhibitors of

cruzain from *T. cruzi* (Brian Shoichet, University of California, San Francisco and NCGC).

Significance: This work is part of our overall research effort focusing on the elucidation of the mechanisms involved with growth and viability of BSF and PF *T. brucei* life cycle forms. The primary goal of this effort is to discovery novel, potent and specific inhibitors of the growth/viability of *T. brucei*. High throughput methodologies, used in conjunction with available open source datamining tools (e.g. PubChem) as well as genetic tools such as RNA interference-based libraries, can rapidly identify potential molecular targets and signaling pathways critical for *T. brucei* growth and viability. Moreover, these efforts can also rapidly identify novel chemotypes that may serve as the basis for novel drug discovery. This is particularly relevant since drugs for the treatment of African sleeping sickness are ineffective and toxic; and, there is a desperate need for new safe and effective drugs (Barrett *et al.*, 2003). While HTS approaches to identify anti-trypanosomal compounds have been used by others [(Mackey *et al.*, 2006) for example] the need for additional chemotypes to provide the basis for diversification of the arsenal of anti-parasitic drugs is clear, as parasitic protozoa have a well-documented propensity for the development of resistance to therapeutics. Resistance to suramin [both laboratory generated resistance (Scott *et al.*, 1996) and in veterinary applications against a related parasite (El Rayah *et al.*, 1999)] and resistance to eflornithine (Bacchi *et al.*, 1993) raise concerns that these compounds will eventually be less useful as anti-trypanosomal drugs.

Here, we have developed two closely related alamar blue-based HTS assays for

the identification of trypanocidal compounds through collaboration with the UPDDI that could lead to the development of much-needed new therapies. Further, the compounds identified here will become chemical probes to allow for comparative analysis of the biology of different lifecycle stages of the African trypanosome (i.e. BSF versus PF life cycle forms) as well as with *Leishmania*, a related genus.

Rationale for screening for anti-trypanosomal small molecules.

A. Probe for differences in the biology of BSF and PF parasites– Some compounds will likely be more toxic (or exclusively toxic) to BSF parasites. For example, probes that inhibit glycolysis may be more toxic to the BSF parasite than PF parasites, as BSF rely exclusively on glycolysis for energy production, while PF also metabolizes amino acids and can grow under glucose depleted conditions. Once an inhibitor has been identified we can use gene knockouts, transgene expression and RNAi to characterize the molecular targets of these inhibitors.

B. Identify desperately needed anti-trypanosomal lead compounds – Therapies currently used to treat infections are unsatisfactory due primarily to toxicity (Barrett *et al.*, 2003), so the development of new anti-parasitic compounds is essential. According to Médecins Sans Frontières, the group responsible for the majority of primary care for afflicted individuals, “... the greatest obstacle to fighting the disease is the lack of new, better diagnostic tools and medicines,” (<http://www.doctorswithoutborders.org/news/issue.cfm?id=2401>).

C. Reveal differences between *T. brucei* and Leishmania – Recently a HTS has been performed at the UPDDI to identify probes that are toxic to *Leishmania major* promastigotes and intracellular amastigotes. While *T. brucei* and *Leishmania* are both in the order Kinetoplastida, their distinct biology (BSF *T. brucei* is exclusively extracellular, while *Leishmania* can infect host cells, for example) suggests that probes to unique biology will be identified.

3. RESEARCH DESIGN AND METHODS

T. brucei viability is a promising focus for HTS for the following reasons:

- A. Current therapies for African trypanosomiasis are not suitable.
- B. Many molecular tools have been developed in the *T. brucei* system for understanding gene function – these will work collaboratively with the probes identified here.
- C. A simple and reproducible assay has successfully been modified for use in a 96-well format.

3.A. Assay Development

The primary assay used is an adaptation of an alamar blue-based cell viability assay (using Cell-Titer Blue) to a 96-well format (Fig. 1). We have experience with this assay

format, which measures the reduction of resazurin to resorufin by cellular processes and is well-suited for HTS development and implementation (Fig. 2).

In vitro growth conditions for BSF and PF parasites – *Trypanosoma brucei brucei* PF parasites (strain 29-13) and BSF parasites (strain 90-13) were grown as described (Wirtz *et al.*, 1999; Morris *et al.*, 2002; Morris *et al.*, 2001). This subspecies of parasite infects cattle and rats and is routinely used as a model African trypanosome, in part because tools for molecular genetics (including RNAi vectors, over-expression cassettes, and gene knockout approaches) have been developed using this line (Wirtz *et al.*, 1994; Biebinger *et al.*, 1997; Wirtz *et al.*, 1999).

Alamar blue-based assessment of parasite population health.

BSF parasites. To establish parameters for the preliminary assay described below, parasites were seeded at 5×10^3 , 5×10^4 , 5×10^5 cells/well into 96-well clear bottomed polystyrene plates in 100 μ l of growth medium (HMI-9, see below). Cells were then grown in 5% CO₂ at 37°C and then alamar blue (commercially available as CellTiter Blue reagent from Promega, Madison, Wisconsin) was added to a final concentration of 16% (v/v). Plates were then incubated under standard culture conditions for 1, 2, or 4 hours and fluorescence of samples characterized by excitation at 546nm with scoring of fluorescence emission at 585nm (Fig. 2, top). After an initial lag in growth (a phenomena seen when BSF parasites are transferred from growth in flasks to microtiter plates), BSF

growth is linear. As BSF trypanosomes typically double every 8-12 hours, the fluorescence (within standard deviation) is a reasonable reflection of the doubling rate of the trypanosomes. Please note that the population continues to grow until the population reaches $\sim 1 \times 10^7$ /ml, at which point the parasites die.

PF parasites. Parasites seeded at 5×10^3 , 5×10^4 , 5×10^5 cells/well into 96-well clear bottomed polystyrene plates were cultured in 100 ml of growth medium (SDM-79, see below). While PF doubling time is density dependent, PF cultures between $5 \times 10^5 - 1 \times 10^7$ /ml typically double every 16-18 hours. PF parasites are less sensitive than BSF to overgrowth, reaching a stationary phase (at $> 1.5 \times 10^7$ cells/ml) that can persist for several days before the culture begins to die (Fig. 2, bottom).

Thus, we have determined that both *T. brucei* life cycle forms can effectively metabolize the alamar blue reagent, setting the stage for development of the HTS assay format.

Initial assessment for suitability of assay format for HTS development

Bloodstream Form Trypanosomes. Briefly, 5×10^3 parasites were seeded into 96-well clear-bottomed polystyrene plates in growth medium (see below for specific differences for BSF and PF parasites). For background signal, cells were grown in the presence of the trypanotoxic compound quercetin dihydrate (100 μ M) (Mamani-Matsuda *et al.*,

2004). Cells were then grown for 3 days in 5% CO₂ at 37C and then CellTiter Blue was added to a final concentration of 16% (v/v). Plates were then incubated for 3 hours under standard culture conditions. Fluorescence of samples was then characterized by excitation at 546nm with scoring fluorescence emission at 585nm. Preliminary results indicate that DMSO is well tolerated by BSF parasites and has minimal impact on the assay described here, with 1% DMSO (f.c.) causing a 16% reduction in cell number at the end of the three day assay.

In the 96 well format, 96 wells of parasites grown in the presence of carrier (1% DMSO) generated a mean fluorescence intensity of 27052 (+/- 3431) compared to quercetin killed parasites, which yielded fluorescence of 3697 (+/- 163). These values generated a Z factor value of 0.62 (Fig. 3). The maximum background well value was 5.8-fold lower than the well with the lowest value that contained cells (3676 compared to 21184).

Dose-dependence of the alamar blue-based assay. To assess the dose dependence of the assay using an anti-parasitic compound, BSF parasites were incubated with varying amounts of an experimental trypanocidal compound (PubChem SID 371557) and cell viability determined using CellTitre Blue (Promega) as described above. Increasing levels of the compound was toxic to *T. brucei* (Fig. 4), and the percentages of remaining viable cells were in good agreement with the values determined by microscope and hemacytometer. While we cannot differentiate between cytostatic and cytotoxic compounds using the CellTitre Blue-based assay, both types of probes would be useful

leads, as trypanosomes must divide to establish successful infections by avoiding the host immune response as a result of antigenic variation (the replacement of one surface-coat bearing population with another).

Procyclic Form Trypanosomes. Parasites (5×10^4 /well) were grown in 96-well clear bottomed polystyrene plates (with background cells treated with quercetin, as described above) in growth medium for 2 days in 5% CO₂ at 25C and then CellTiter Blue was added to a final concentration of 16%. Plates were then incubated for 1 hour under standard culture conditions. Fluorescence of samples was then characterized as above. As with the BSF, DMSO has minimal impact on the PF assays when included in assays at 1% (f.c.) for the 2 day assay.

In the 96 well format, vehicle treated parasites yielded a mean fluorescence intensity of 14768 (+/- 1185) compared to the quercetin-killed cells, which had a mean fluorescence of 2804 (+/- 62.3). These values yielded a Z factor value of 0.69 for the entire plate (Fig. 3). The maximum background well value was 4.1-fold lower than the well with the lowest value that contained cells (2983 compared to 12363).

For both *T. brucei* life cycle forms, these results suggest that the assay format will be amenable to HTS assay development and implementation procedures. Thus, studies will focus on: (a) generating a *T. brucei* parasite bank; (b) confirming growth characteristics of the life cycle forms to ensure harvesting each *T. brucei* lifecycle form in

exponential growth phase; (c) determining optimal seeding densities, culturing conditions and timing of the assay; (d) capturing data within the linearity range of signal readout; and (e) confirming the developed assay parameters with known *T. brucei* growth inhibitors. Moreover, in the 384-well HT screens for both cell types, assay plates will include maximum (DMSO vehicle), minimum (quercetin inhibited signal) and IC₅₀ controls (Sharlow *et al.*, 2008).

3.B. Configuration of Assays for HTS

To configure the assay format to an HTS amenable format additional studies will be conducted to (a) define the DMSO tolerance of each life cycle form; (b) identify the maximum and minimum assay controls from which the HTS Z-factor statistic will be derived; (c) conduct a three-day variability assessment to determine predicted plate-to-plate and day-to-day variability as well as coefficient of variance and signal to background; and (d) validate the optimized HTS assay conditions using the LOPAC set to determine hit criteria and screening concentration as well as identify initial differences in chemosensitivities between the BSF and PF life cycle forms (Sharlow *et al.*, 2007).

Evaluate Significance of active compounds – Primary hits identified from the validated HTS assays will progress through a series of secondary confirmation assays. To confirm the activity of the primary hits (and thus eliminate false positives), 10 point IC₅₀ determinations will be conducted (in duplicate) with the hit compounds using the optimized HTS assay parameters. To be considered as a *T. brucei* growth inhibitor,

compounds must confirm in each 10 point IC₅₀ determination run. Based on previous experience with the *L. major* promastigote assay where we identified nanomolar as well as picomolar inhibitors of *L. major* promastigote growth, it may be necessary to run 20 point concentration determinations. Thus the starting concentration of the concentration response assessment will be determined by the final screening concentration (e.g. 1 or 5 μM) of the LOPAC library. Additionally, confirmed actives from the screened library will be purchased (or otherwise obtained) and retested to confirm growth inhibitory activity. This will control for lot-to-lot compound variability as well as for inhibitory activity that may be the result of compound degradation within the compound library. It is also possible that some of the natural compounds that will be screened will fluoresce around 585nm, thus other cell viability assays, including those that measure ATP production using luciferase, would be considered if the interfering signal routinely causes problems as well as to confirm the inhibitory activity of the compound in another assay format.

Plans to develop counter-screens (selectivity and potential toxicity)

Counter-screening against mammalian cells. Confirmed trypanosome growth inhibitors will be screened against mammalian cells to initially assess selectivity as well as potential toxicity to the host, with IC₅₀ values determined using the CellTiter Blue reagent. These counter-screening assays are available at the UPDDI and include HTS validated cancer cell line assay panel (e.g. A549, DU-145, HeLa, cells).

Additional analysis. During a *T. brucei* infection, parasites evade the host immune system by a process known as antigenic variation. In this process, the majority of the infectious population harbors a given surface coat antigen. After 10-14 days, it is eliminated by the host immune system, only to be replaced by a new population that expresses an antigenically distinct coat. The new population grows until it too is eliminated and replaced. This suggests that compounds that are cytostatic would prevent parasite growth (and therefore population replacement) and therefore antigenic variation. Growth curve analysis (and microscopic examination) can be employed to determine whether confirmed actives are growth inhibitory or cytotoxic (Chambers *et al.*, 2008).

Additionally, confirmed *T. brucei* growth inhibitors will be screened using a validated *Leishmania major* promastigote HTS assay (Sharlow *et al.*, In Press), in order to explore the species selectivity of small molecule probes.

This proposal seeks to identify probes that are toxic to BSF and PF parasite life stages. These stages occupy distinct niches, and as a result, harbor a remarkable number of different biochemical pathways. Stage-specific anti-parasitic compounds would therefore provide insight into biochemical differences between the PF and BSF parasites. For example, PF parasites decorate the GPI anchors of their major surface glycoprotein with a variety of fatty acids, while BSF parasites include myristate exclusively in their mature

GPIs. A compound that specifically targets the myristate incorporation pathway may therefore be toxic to only the BSF parasite.

Recommendations for test concentrations and concentration cutoff – The screening of the LOPAC library will be performed at two concentrations, 1 and 10 μM and the hit rates (based on 50% inhibition of signal readout) will be determined for each of the tested concentrations. Thus, the screening concentration of subsequent libraries will be determined by the hit rate as predicted by the LOPAC library. Ideally the hit rate for the LOPAC set would be 1% or lower to ensure that there will be a reasonable number (not an excessive quantity) of primary hits that would be cherry-picked for secondary screening procedures. This is especially important when screening larger compound libraries. Structure activity relationships can be developed for promising lead compounds (those with IC_{50} s in the nM range).

Reagent sources and costs - The reagents and consumables required for the primary HTS assay are commercially available except for the two life stages of the trypanosome and potential inhibitors.

a. Bloodstream Form Trypanosomes – BSF strain 90-13 express the T7 RNA polymerase and the tetracycline repressor (Wirtz *et al.*, 1999). The T7 RNA polymerase and the tetracycline repressor are maintained by culturing the parasites in the presence of 2.5 $\mu\text{g}/\text{ml}$ G418 and 5 $\mu\text{g}/\text{ml}$ hygromycin. (These are dispensable here, so drug selection

is not required for the HTS. This strain and the corresponding PF strain will be essential to future studies using molecular genetics, hence our interest in using it during the HT screen.) The parasites are grown in HMI-9 supplemented with 10% fetal bovine serum and 10% Serum Plus (JRH Biosciences, Lenexa, KS) (HMI-9/FBS10) (Hirumi *et al.*, 1989), with cell densities maintained between 1×10^4 - 1×10^6 cell/ml. Maintaining the cultures between these densities is essential, as overgrowth is lethal to the BSF parasites. Prior to adding parasites, the medium is warmed to 37C and equilibrated to 5% CO₂ for 1 h in the growth incubator. (Please note that clonal populations are routinely generated by limiting dilution into 96 well plates, so parasites are amenable to growth in plates.)

HMI-9 for BSF growth (Hirumi *et al.*, 1989) - For 1 liter, mix the following dry ingredients: Hypoxanthine (136 mg), bathocuproine sulfonate (28 mg), cysteine (182 mg), pyruvic acid (110 mg), thymidine (39 mg)

Add the dry ingredients to the following liquids: 2-mercaptoethanol (14 ml), Iscove's Modified Dulbeccos's Medium with L-glutamine and HEPES (730 ml), penicillin/streptomycin solution 100X (10 ml).

Adjust volume to 800 ml, filter sterilize and add heat-inactivated fetal bovine serum (100 ml) and Serum Plus Medium Supplement (100 ml) (from JRH Biosciences). Store at 4C for up to 6 months.

Cost (per liter): \$27.75 + 10% serum (\$52.60) + 10% Serum Plus (\$50.00) = \$130.35/L

b. Procyclic Form Trypanosomes – PF strain 29-13 (Wirtz *et al.*, 1999), which harbors integrated genes for T7 RNA polymerase and the tetracycline repressor, are grown in SDM-79 supplemented with 10% FBS (SDM-79/FBS10) (see below).

SDM-79 for PF trypanosome growth [slightly modified from (Brun *et al.*, 1979)] - For 1 liter, mix the following dry ingredients: Grace's Insect Cell Culture Media with L-glutamine and without sodium bicarbonate (2.0 g), glucose (1.0 g), HEPES (8.0 g), MOPS (5.0 g), NaHCO₃ (2.0 g), pyruvic acid (100 mg), L-alanine (200 mg), L-arginine (100 mg), L-glutamine (300 mg), L-methionine (70 mg), L-phenylalanine (80 mg), L-proline (600 mg), L-serine (60 mg), L-aurine (160 mg), L-threonine (350 mg), L-tyrosine (100 mg), adenosine (10 mg), guanosine (10 mg), D-glucosamine-HCl (50 mg), folic acid (4 mg), p-aminobenzoic acid (2 mg), biotin (0.2 mg).

Dissolve the dry solids (20.2 g) in the following: Minimum Essential Medium (MEM) with L-glutamine (600 ml), MEM amino acid solution 50X without L-glutamine (8 ml), MEM non-essential amino acids 100X (6 ml), bovine hemin (2 mg/ml in 50 mM NaOH) (3.75 ml), Basal Medium Eagle vitamin solution 100X (10 ml), penicillin/streptomycin solution 100X (10 ml).

Adjust the pH to 7.3 with 10 N NaOH, and increase the volume to 850 ml with H₂O. Filter sterilize with a 0.22 µm filter. Add heat-inactivated (56°C, 30 min) fetal bovine serum (150 ml) to the filtered solution – do not filter the serum. Store at 4°C for up to 6 months.

Cost (per liter): \$27.75 + 15% serum (\$78.90) = \$106.65/L

c. Other Solutions for Parasite Husbandry -

Freezing medium - 50% glycerol in cytomix, filter-sterilized. Once parasite lines have been established, a portion of the culture should be stored for future use. To freeze trypanosomes, freezing medium (0.2 ml of 50% glycerol in cytomix that has been filter-sterilized) is added to 0.8 ml of culture containing $1-5 \times 10^6$ cells/ml in a liquid nitrogen compatible cryotube. The cells are mixed thoroughly by inversion, and then frozen at –80°C overnight in a modified trypanosome freezing carton. This carton is made of two Styrofoam racks (in which 15 ml conical centrifuge tubes are shipped) taped together; samples placed in the carton freeze more slowly than exposed tubes. The cryotube is then transferred the next day to liquid nitrogen. To thaw PF trypanosomes, frozen cryotubes are warmed to room temperature, and the contents of a single tube are transferred to 9 ml SDM-79/FBS15/G/H and grown at 27°C in 5% CO₂. To thaw frozen BSF trypanosomes, cryotubes are warmed to room temperature, and the contents are transferred to 9 ml warmed and equilibrated (37°C/5% CO₂) medium.

d. Other reagents

LOPAC library daughter set - \$1000

Control reagents (known inhibitors) \$ 250

Pilot screening of a library of pharmaceutically active compounds (LOPAC) - Assay development procedures, including tests for required optimization of assay parameters, HTS assay control identification, parasite banking, and three day variability assessment will require ~3-4 months, with an additional month for completion of validation and the LOPAC screen (1280 compounds).

Conclusions and outlooks:

The lack of affordable, safe, and effective therapies for those infected with the African trypanosome makes the identification of new therapeutic targets a priority in our effort to reduce disease in the world today (Barrett *et al.*, 2003). We will identify new lead compounds for anti-trypanosomal therapies and we may, through the genetic and comparative approaches proposed here, identify compounds that target a particular parasite pathway, allowing further elucidation of the function of that pathway in the biology of the organism.

References

1. Barrett, M. P., Burchmore, R. J., Stich, A., Lazzari, J. O., Frasc, A. C., Cazzulo, J. J., and Krishna, S. (2003) *Lancet* **362**, 1469-1480
2. Pepin, J., and Milord, F. (1991) *Trans R Soc Trop Med Hyg* **85**, 222-224
3. Mackey, Z. B., Baca, A. M., Mallari, J. P., Apsel, B., Shelat, A., Hansell, E. J., Chiang, P. K., Wolff, B., Guy, K. R., Williams, J., and McKerrow, J. H. (2006) *Chem Biol Drug Des* **67**, 355-363
4. Martyn, D. C., Jones, D. C., Fairlamb, A. H., and Clardy, J. (2007) *Bioorg Med Chem Lett* **17**, 1280-1283
5. Scott, A. G., Tait, A., and Turner, C. M. (1996) *Acta Trop* **60**, 251-262
6. El Rayah, I. E., Kaminsky, R., Schmid, C., and El Malik, K. H. (1999) *Vet Parasitol* **80**, 281-287
7. Bacchi, C. J., Garofalo, J., Ciminelli, M., Rattendi, D., Goldberg, B., McCann, P. P., and Yarlett, N. (1993) *Biochem Pharmacol* **46**, 471-481
8. Wirtz, E., Leal, S., Ochatt, C., and Cross, G. A. (1999) *Mol. Biochem. Parasitol.* **99**, 89-101
9. Morris, J. C., Wang, Z., Drew, M. E., and Englund, P. T. (2002) *EMBO J.* **21**, 4429-4438
10. Morris, J. C., Wang, Z., Drew, M. E., Paul, K. S., and Englund, P. T. (2001) *Mol. Biochem. Parasitol.* **117**, 111-113.
11. Wirtz, E., Hoek, M., and Cross, G. A. (1998) *Nucleic Acids Res.* **26**, 4626-4634
12. Biebinger, S., Wirtz, L. E., Lorenz, P., and Clayton, C. (1997) *Mol Biochem Parasitol* **85**, 99-112
13. Mamani-Matsuda, M., Rambert, J., Malvy, D., Lejoly-Boisseau, H., Daulouede, S., Thiolat, D., Coves, S., Courtois, P., Vincendeau, P., and Mossalayi, M. D. (2004) *Antimicrob Agents Chemother* **48**, 924-929
14. Sharlow, E. R., Leimgruber, S., Yellow-Duke, A., Barrett, R., Wang, Q. J., and Lazo, J. S. (2008) *Nat Protoc* **3**, 1350-1363
15. Sharlow, E. R., Leimgruber, S., Shun, T. Y., and Lazo, J. S. (2007) *Assay Drug Dev Technol* **5**, 723-735
16. Chambers, J. W., Fowler, M. L., Morris, M. T., and Morris, J. C. (2008) *Mol Biochem Parasitol* **158**, 202-207
17. Drew, M. E., Morris, J. C., Wang, Z., Wells, L., Sanchez, M., Landfear, S. M., and Englund, P. T. (2003) *J. Biol. Chem.* **278**, 46596-46600
18. Sommer, J. M., Hua, S., Li, F., Gottesdiener, K. M., and Wang, C. C. (1996) *Mol. Biochem. Parasitol.* **76**, 83-89
19. Hirumi, H., and Hirumi, K. (1989) *J. Parasitol.* **75**, 985-989
20. Brun, R., and Shonenberger, M. (1979) *Acta Tropica* **36**, 289-292

Figure Legends

Figure 1. Cell-Titer Blue reactions scheme.

Figure 2. Growth curves, as monitored by CellTiter Blue fluorescence. BSF (seeded at 5×10^3 /well) or PF (seeded at 5×10^4 /well) were grown for the indicated days and then incubated with CellTiter Blue for the indicated number of hours and fluorescence monitored as described. Please note that “over flow” signal (saturation) was at 5×10^4 RFU.

Figure 3. Z factor determination for BSF (upper) and PF (lower) parasites (see text for details) grown in carrier (1% DMSO, open symbols). The background signal (filled symbols) was determined using cells were grown in the presence of the trypanotoxic compound quercetin dihydrate ($100 \mu\text{M}$).

Figure 4. Monitoring dose-dependent response to an anti-parasitic compound using CellTiter Blue. BSF parasites (5×10^3) were grown for in the presence of an experimental trypanocidal compound (PubChem SID 371557) for 3 days and then CellTiter Blue was added to the cultures and incubated an additional 3 hours prior to assessing fluorescence emission.

Figure 1

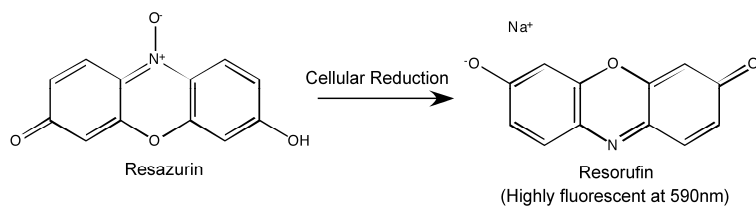


Figure 2

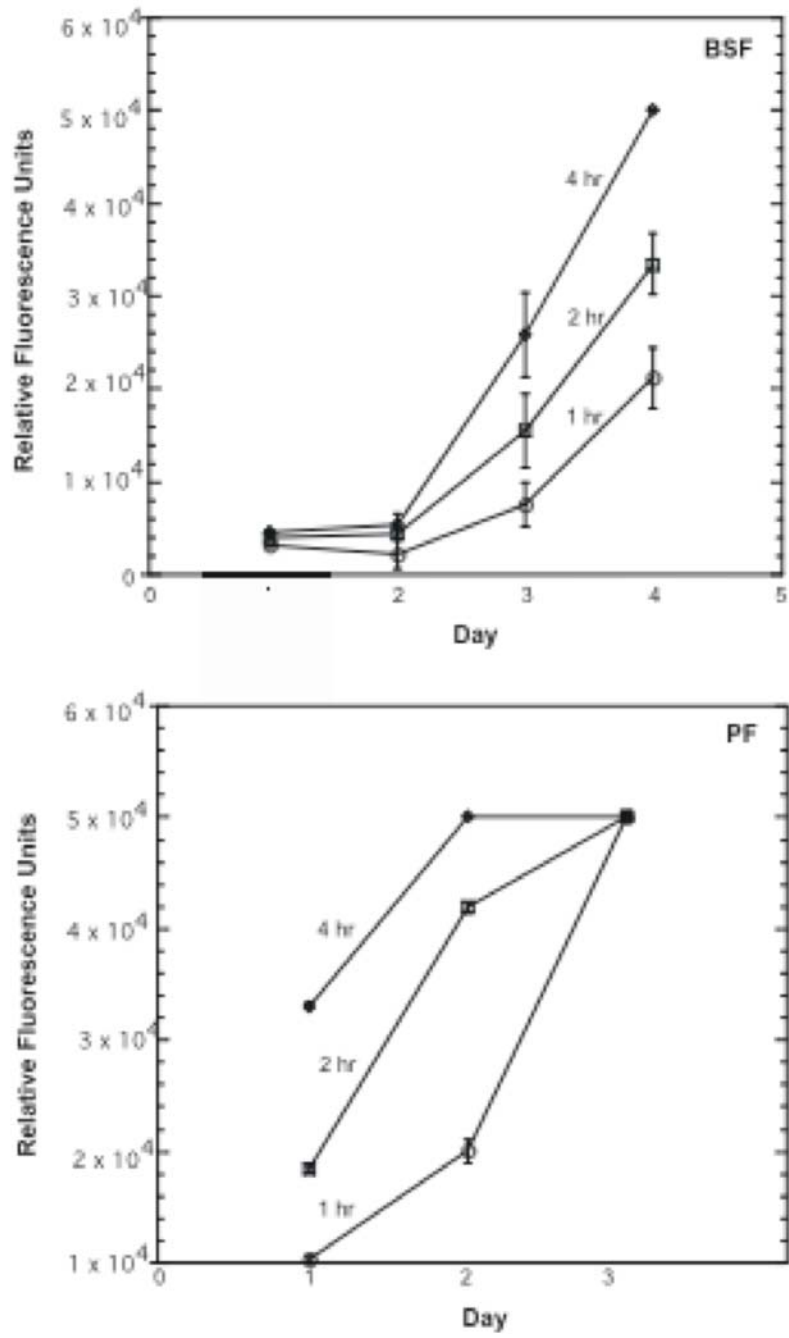


Figure 3

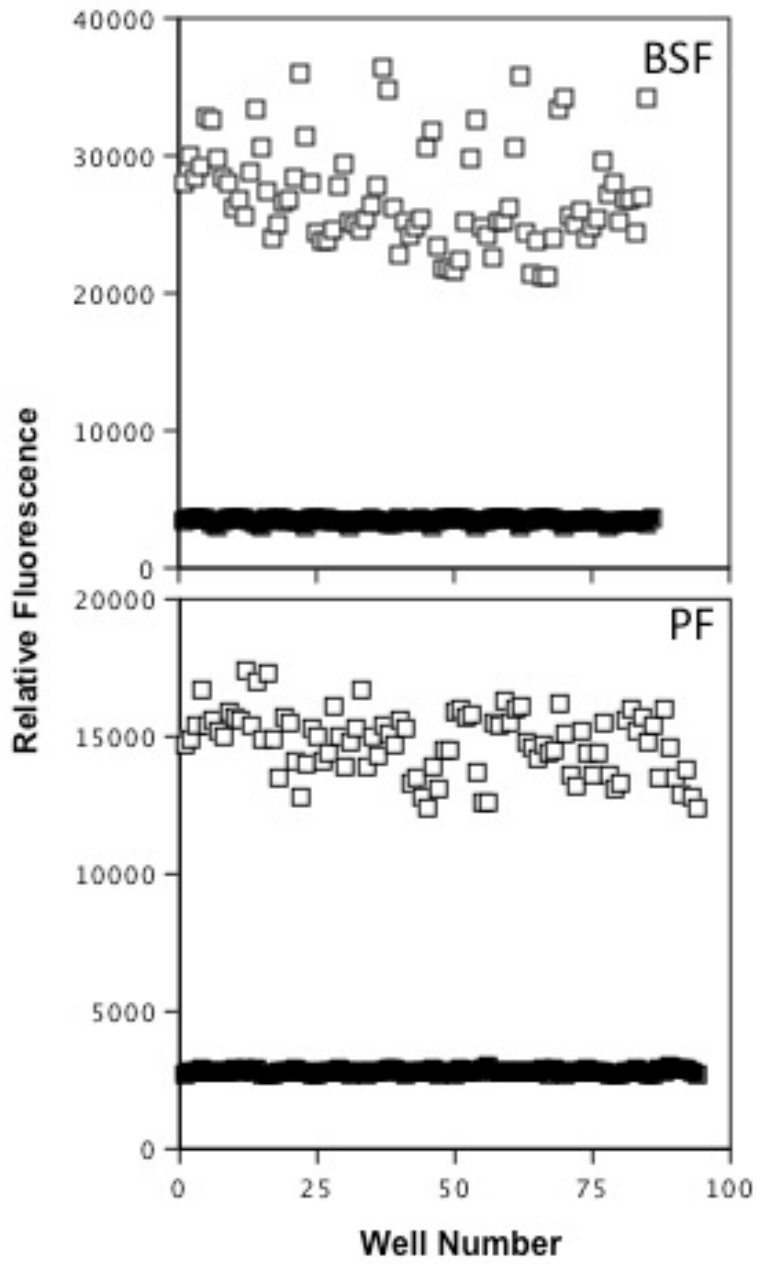


Figure 4

